Luca Ferrari

UNIVERSITÀ DEGLI STUDI DI MILANO

Scuola di Dottorato in Scienze Biologiche e Molecolari

XXV Ciclo

Fas/Fasl pathway is impaired in chordoma and is involved in zebrafish (*Danio rerio*) notochord development and regression

L. Ferrari
PhD Thesis

Scientific tutor: Paola Riva

Academic year: 2011-2012

Luca Ferrari

SSD: BIO/13

Thesis performed at the **Dipartimento di Biotecnologie Mediche e Medicina Traslazionale, Università Degli Studi di Milano, Milano**

Collaborations:

Prof. Franco Cotelli
Dipartimento di Bioscienze, Università Degli Studi di Milano, Milano

Prof. Gianfranco Canti
Dipartimento di Biotecnologie Mediche e Medicina Traslazionale, Università Degli Studi di Milano, Milano

Prof. Pietro Mortini
Dipartimento di Neurochirurgia
IRCCS Ospedale San Raffaele, Milano

Contents

Abstract

Chordoma is a rare malignant tumor characterized by chemoresistance and unforeseeable prognosis, originating from notochord remnants that do not disappear during development. The apoptotic mechanisms are fundamental for notochord cells development and regression, but little is known about the role of specific apoptotic pathways. At this purpose we investigated the possible implication of Fas/Fasl apoptotic pathway in chordoma tumorigenesis. *FASL* expression was absent, while both *FAS* anti- and pro-apoptotic isoforms were detected in most chordomas analyzed and in U-CH1 cells. These findings, besides the prevalent expression of inactive Caspases 8 and 3, suggest that Fas/Fasl pathway is impaired in this tumor. The enhancement of apoptosis in U-CH1 cells by treatment with soluble Fasl indicates that Fas/Fasl pathway can be activated in chordoma, suggesting Fas/Fasl as potential pharmacological targets. We also hypothesized that Fas/Fasl pathway dysregulation may have a role in chordoma onset. To unravel this issue we investigated the function of *fas* and *fasl* homologs in the zebrafish notochord development. We found that these genes were specifically expressed in notochord cells. Morpholino mediated knock-down of *fas* and *fasl* resulted in abnormal phenotypes mainly showing curved tail and altered motility. Notochord multi-cell-layer jumps instead of the typical "stack-of-coins" organization, larger vacuolated cells, defects in the peri-notochordal sheath structure and in vertebral mineralization have been detected in most morphants. In addition, we observed the persistent expression of *ntla* and *col2a1a*, the zebrafish homologs of the human *T* gene and *COL2A1*, which were found to be specifically upregulated in chordoma. In conclusion, our findings indicate that Fas/Fasl pathway activity can be enhanced in chordoma. Moreover, we demonstrated for the first time the involvement of *fas* and *fasl* in notochord development, differentiation and regression in zebrafish suggesting the implication of this pathway in chordoma onset.

Background

CHORDOMA

Definition and epidemiology

Chordoma is a rare malignant tumor arising from embryonic remnants of the notochord that do not disappear during development of vertebral bodies.

The incidence of chordoma is of 0,08 per 100000, with predominance in men and peak incidence between 50–60 years of age (McMaster et al., 2001), while they have very low incidence in patients younger than 40 years, and rarely affect children and adolescents (<5% of all chordoma cases) (Wold and Laws, 1983).

Chordoma can localize with almost equal distribution in the skull base (32%), mobile spine (32,8%), and sacrum (29·2%) (Walcott et al.,2012) and is characterized by local invasiveness, tendency for recurrences, with a potential to metastasize (Higinbotham et al., 1967), but unlike most malignant neoplasms, it is generally slow-growing.

Chordomas lie in the bone, accounting for 1% - 4% of all malignant bone tumors (Bydon et al., 2012), so they initially grow at extradural level with bone destruction, having an osteolytic activity, and secondary extension into the adjacent soft tissues (Oikawa et al., 2001).

Clinical presentation and histopathology

This tumor is often clinically silent until the late stages of disease. The clinical manifestations vary and depend on location. Skull-base chordomas (SBCs) often grow in the clivus and present with cranial-nerve palsies. Depending on their size and involvement of the sella, endocrinopathy can also occur (Stark and Mehdorn, 2003). Chordomas of the mobile spine and sacrum can present with localized deep pain or radiculopathies related to the spinal level at which they occur (Fourney and Gokaslan, 2003). Unfortunately, the non-specific

nature of these symptoms and insidious onset of pain often delays the diagnosis until late in the disease course. Studies show that neurological deficit is more often observed in chordomas of the mobile spine than in chordomas of the sacrococcygeal region (Boriani et al., 1996). Chordomas are midline lesions and often appear radiographically as destructive bone lesions, with an epicentre in the vertebral body and a surrounding soft tissue mass. Unlike osteosarcomas and chondrosarcomas of the vertebral column, chordomas locally invade the intervertebral disc space as they spread to adjacent vertebral bodies (Chambers and Schwinn, 1979).

Microscopically the tumor is characterized by the physalipherous cells, the typical notochordal cells with a nucleus surrounded by large vacuoles. Chordomas manifest as one of three histological variants: classical (conventional), chondroid, or dedifferentiated. Classical chordomas appear as soft, gray-white, lobulated tumors composed of groups of cells separated by fibrous septa. They have round nuclei and an abundant, vacuolated cytoplasm described as physaliferous (having bubbles or vacuoles). Unlike classical chordoma, chondroid chordomas histologically show features of both chordoma and chondrosarcoma, a malignant cartilage-forming tumor.

Classically, chordomas were pathologically identified by their physaliferous features and immuno-reactivity for the protein S-100 and epithelial markers such as epithelial membrane antigen (MUC1) and cytokeratins. However, until recently, distinguishing between chondroid chordomas and chondrosarcomas was challenging because of their shared S-100 immunoreactivity, making it difficult to interpret cytokeratin expression on small biopsies (Henderson et al., 2005). Several groups have postulated that the notochord developmental transcription factor Brachyury could be the novel discriminating biomarker for chordomas. This hypothesis was validated with a tissue-microarray-based analysis that assessed 103 skull-base, head and neck chondroid tumors. In that

study, Oakley and colleagues identified Brachyury as a discriminating biomarker of chordomas, and when combined with cytokeratin staining, sensitivity and specificity for detection of chordoma was 98% and 100%, respectively (Oakley et al., 2008). Brachyury staining to discriminate chordomas from other chondroid lesions has therefore become integral in the pathological work-up during diagnosis (Figure 1). Moreover, also the lack of *IDH1* or *IDH2* mutation in chordoma helps to differentiate it from other cartilaginous tumors, especially in differentiating the skull base chondrosarcoma from chordoma (Szuhai and Hogendoorn, 2012).

In a recent characterization of chordoma tumors and cell lines, other genes were found differentially expressed in this tumor; among them the alpha collagen type II (*COL2A1*) was significantly overexpressed (Bruderlein et al., 2010).

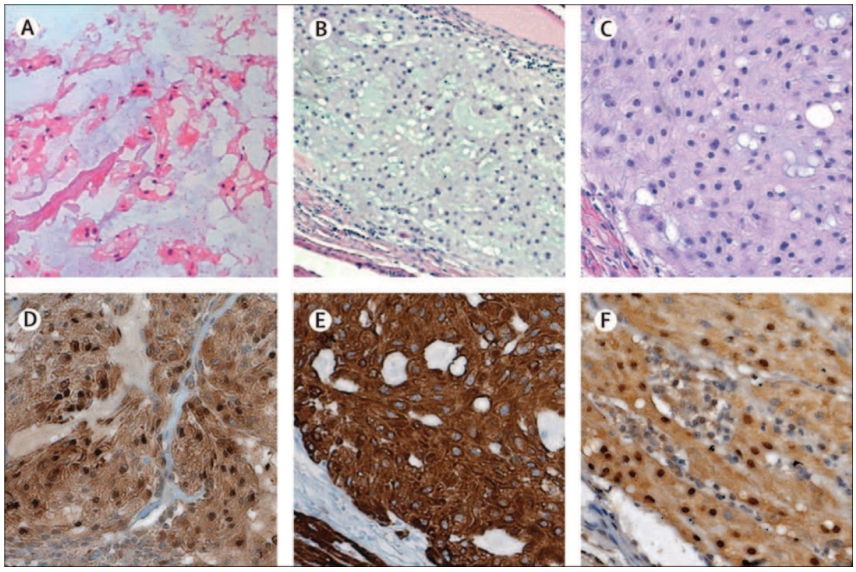

Figure 1. **Immunohistochemical characterisation of human chordoma tissue**
Intraoperatively obtained chordoma tissue with physaliferous phenotype; haematoxylin and eosin (H&E) stained, frozen tissue smear (A,B,C). Intraoperatively obtained chordoma tissue with physaliferous phenotype; H&E stained, formalin-fi xed tissue (D,E,F). Chordoma tissue is positive for S-100β in A, for cytokeratin AE1/AE3 in B, and for brachyury in C; immunohistochemistry with diaminobenzidine chromogen.
Lancet Oncol. 2012 Feb;13(2):e69-76. doi: 10.1016/S1470-2045(11)70337-0

Prognosis

Extent of resection, previous treatment, adjuvant proton beam therapy and the karyotype are thought to influence the prognosis of chordoma (Colli and Al-Mefty, 2001). Despite the possibility of a long progression-free survival after gross total or subtotal resection and radiation therapy, ultimately the majority of patients will experience recurrence and will die of local progression of their disease. It also appears, however, that chordomas that have been resected to the same extent and that received post-operative radiotherapy might exhibit different rates of re-growth (Gagliardi et al., 2012). This result supports the hypothesis that the recurrence rate of chordomas might be dependent on variables other than the extent of resection and the postoperative radiotherapy. Several studies investigated the classic pathological paradigms in relation to the biological and clinical behavior of chordomas. Matsuno et al. studied the immunohistochemical expression of MIB-I, p53, cyclin D1 and identified these markers as important predictors of recurrence (Matsuno et al., 1997). It was also demonstrated that the proliferative potential of chordoma was correlated with the combination of p53 overexpression, anaplasty, high-grade atypia and diffuse proliferation (Naka et al., 2005; Naka et al., 2009; Naka et al., 2008). The expression of telomerase transcriptase mRNA (hTERT) and mutation of p53 were associated with the risk for early recurrence (Pallini et al., 2003). More recently, the occurrence of 1p36 loss of heterozygosty (LOH) was frequently observed in skull base chordomas (75%) and the absence of LOH was associated with a mild prognosis, indicating 1p36 LOH as a potential prognostic marker to be validated in a larger casuistry (Longoni et al., 2008; Miozzo et al., 2000; Riva et al., 2003).

Despite all the observed associations between clinical outcome and molecular features of chordomas, no validated molecular markers are available to monitor the tumor progression. Therefore, there is the need of identifying suitable

prognostic markers to be considered for the clinical approach and the setting-up of targeted treatment protocols.

Treatment

Major role in the treatment of chordomas is played by extensive surgical resection when possible. Goals of surgery are to remove as much neoplastic tissue as possible and to preserve or improve patient's functional status (Gagliardi et al., 2012). An important role in the management of chordomas is played by high-dose radiotherapy, which provides a good tumor control. Chordomas are considered relatively resistant to conventional radiotherapy and the most common delivery methods applied in their treatment include proton beam radiotherapy, high-dose radiotherapy and radiosurgery using Gamma Knife and Cyber- Knife. Radiotherapy provides better local control when administered postoperatively than when delivered after recurrence following surgical resection. Main delivery methods are, radiosurgery and radioactive sources (Gagliardi et al., 2012).

Unfortunately, systematic review of the literature found chordomas to be insensitive to conventional chemotherapies (Walcott et al., 2012). Nevertheless, molecular profiling of chordomas has revealed that they express the Platelet-Derived Growth Factor Receptor (PDGFR)B, PDGFRA, and KIT receptors, in both tumor and stroma cells, and chemotherapy with imatinib mesylate (IM), a PDGFR inhibitor, might represent a therapeutic option in patients with recurrent chordoma not even eligible for surgery or radiotherapy (Gagliardi et al., 2012). The anti-tumor activity of IM was documented by the detection of a decrease in the size of the tumor and/or tumor stabilization with altered tumor density (Casali et al., 2004), notwithstanding the complete remission of the mass tumor was never observed. Furthermore the association of IM with other

chemotherapeutic agents, such as mTOR inhibitor molecules, showed to be effective in the treatment of IM-resistant chordomas (Stacchiotti et al., 2009; Stacchiotti et al., 2013).

As tumor characteristics are further elucidated, additional molecular pathways have been targeted. In a series of 12 patients with chordoma, strong expression of Epidermal Growth Factor Receptor (EGFR) and c-MET was described and it was reported the response to cetuximab, gefitinib and erlotinib, three drugs designed to inhibit the EGFR pathway (Singhal et al., 2009). A recent analysis of 70 chordoma samples showed activation of phosphorylated-Signal-Transducer and Activator of Transcription 3 (STAT3), a transcription factor known to be activated in several human cancers and associated with poor prognosis. The use of STAT3 inhibitors in chordoma cell lines *in vitro* showed strong inhibition of cell growth and proliferation (Yang et al., 2009a).

Despite these preliminary but encouraging data, the evaluation of the reported pharmacological targets or the identification of new ones, represent a challenge for the research in this field, aimed at setting up an effective chemotherapy for the treatment of chordoma.

Brachyury: the pathognomonic marker of chordoma

The maintenance of the notochordal tissue characteristics in chordoma is confirmed by microscopic features, the localization of the tumor along the axial skeleton, and the expression of similar transcription factors. Among them, the most significant is the transcription factor T (encoding for Brachyury), the founder member of the T-box family involved in notochord development (Glickman et al., 2003; Salisbury, 2001; Salisbury et al., 1993) and recently identified as the pathognomonic marker for chordoma (Nelson et al., 2012).

The T-box genes encode a family of transcription factors sharing a characteristic sequence similarity within the DNA-binding domain (T-domain). To date, 18 different mammalian T-box genes have been identified, many of which have orthologous in a wide variety of multicellular organisms (Showell et al., 2004). Brachyury is localized to the nucleus, binds DNA in a sequence-specific manner, and can regulate transcriptional levels of heterologous and downstream target genes in several different contexts (Showell et al., 2004). This protein functions as a transcriptional activator of mesoderm-specific genes, indeed its expression is required for the specification of mesodermal identity, representing one of the key molecules regulating notochord formation (Henderson et al., 2005).

Brachyury was the first molecule identified which specifically links notochord with chordoma. Extensive investigations were performed on various normal tissues, organs and several tumor entities for the expression of Brachyury, including various types of carcinomas, sarcomas, haematological malignancies, germ cell tumors, and benign lesions. Expression of Brachyury was rarely observed in normal testis (> 20%), and a similar frequency was observed in germ cell tumor of testis. A specific and highly prevalent expression of Brachyury was observed, as well as in chordoma, in haemangioblastoma of the central nervous system (CNS) (100% of the cases) (Tirabosco et al., 2008). This tumor is likely derived from a mesodermal sub-population, with differentiation capacity towards both endothelial cells and haematopoietic cells, in line with the role of Brachyury in the development of the posterior mesoderm including haemangioblasts formation (Szuhai and Hogendoorn, 2012). Moreover, the expression of Brachyury has been detected in benign notochord cells tumor of extraosseous origin, which is the benign tumor which leads to malignant chordoma (Deshpande et al., 2007; Yamaguchi et al., 2008).

High-resolution array-CGH profiling of familial chordoma cases revealed duplication of the chromosome 6q27 region, with the smallest duplicated region containing the *T* gene region only (Yang et al., 2009b). In a follow-up study of sporadic chordomas, however, it was shown that duplication or amplification of the *T* locus was present in less than 5% of investigated chordoma cases (Presneau et al., 2011). No mutations of the *T* gene were identified in chordoma specimens (Shalaby et al., 2009; Yang et al., 2009b). These results were in line with the deleterious effect of mutant protein on embryonic differentiation leading to the Brachyury (short tale) phenotype or lethality in cases of homozygous mutation in different animal models.

Diverse pathways have been demonstrated to regulate Brachyury expression during evolution, such as Wnt/β-catenin, TGF-β/Nodal/activin, BMP, and FGF; among them the most relevant is activated by the Fibroblastic Growth Factor Receptors (FGFRs) through RAS/RAF/MEK/ERK and ETS2 in ascidian, *Xenopus* and zebrafish, although little is known about its regulation in mammals. The expression of the members of this pathway was investigated in chordoma samples and most of them expressed at least one of the FGFRs, nevertheless no conclusive association was identified between Brachyury and FGFRs expression in chordoma (Shalaby et al., 2009).

At a functional level, the silencing of Brachyury induced growth arrest in a chordoma cell line (Presneau et al., 2011), while its overexpression, observed in the human pancreatic cell line PANC-1 which does not express it, resulted in enhanced proliferation, motility and invasiveness (Fernando et al., 2010). Moreover, an integrated functional genomics approach showed that the silencing of Brachyury in the U-CH1 chordoma cell line altered the expression of several direct targets and of other targets that indirectly influenced. Interestingly, Brachyury expression was not detected in de-differentiated chordomas, pointing its loss as a form of tumor progression, marking the

evolution from a differentiated chordoma, similar to notochord, to a de-differentiated form of the tumor (Jambhekar et al., 2010).

These findings pinpoint Brachyury as a master regulator of an elaborate oncogenic transcriptional network encompassing diverse signaling pathways including components of the cell cycle, and extracellular matrix components (Nelson et al., 2012). All these evidences taken together, identify Brachyury as the diagnostic marker for chordoma and as a strong potential target for the development of new specific therapies, but the causes at a developmental and at molecular levels of its expression in chordoma are still unclear. In fact, the finding of the *T* gene expression in this tumor might be due to its deregulated expression in notochord cells leading to chordoma, alternatively the defects in notochord regression may maintain proliferating notochord cells which express the *T* gene, or both of these possibilities (Szuhai and Hogendoorn, 2012).

Therefore, studies of *T* gene expression regulation are necessary to clarify chordoma tumorigenesis, but also parallel studies aimed at identifying further mechanisms possibly involved in the biology of this tumor and in the notochord development/regression must be pursued.

NOTOCHORD

Definition

The notochord is an embryonic midline rod-like shaped structure common to all members of the phylum Chordata. Accordingly, it serves as the axial skeleton of the embryo until other elements, such as the vertebrae, form.

In some vertebrate clades, such as the agnathans (lampreys), cephalochordates and in primitive fish, such as sturgeons, the notochord is essential for locomotion and persists throughout life (Stemple, 2005). For the ascidian

(tunicate) invertebrate chordates, the notochord exists during embryonic and larval free-swimming stages, providing the axial structural support necessary for locomotion (Urano et al., 2003).

In higher vertebrates, the notochord exists transiently and becomes ossified in regions of forming vertebrae and persists in the center of the intervertebral discs, in a structure called the nucleus pulposus (Linsenmayer et al., 1986; Smits and Lefebvre, 2003). In these vertebrate clades, it has two important functions. First, the notochord is positioned centrally in the embryo with respect to both the dorsal-ventral (DV) and left-right (LR) axes. This structure produces secreted factors that signal to all surrounding tissues, providing position and fate information and specifying ventral fates in the central nervous system. The notochord also controls aspects of LR asymmetry, inducing pancreatic fates, controlling the arterial versus venous identity of the major axial blood vessels and specifying a variety of cell types in forming somites (Christ et al., 2004; Danos and Yost, 1995; Fouquet et al., 1997; Goldstein and Fishman, 1998; Lohr et al., 1997; Munsterberg and Lassar, 1995; Pourquie et al., 1993; Yamada et al., 1993).

Embryogenesis and functions

In vertebrates, the notochord arises from the dorsal organiser, a region of a vertebrate gastrulae that, when transplanted into prospective lateral or ventral regions of a host embryo, induces the formation of a second embryonic axis, while only contributing to notochord and prechordal mesendoderm (Harland and Gerhart, 1997). In amphibians, this region is the dorsal lip of the blastopore. In other species, homolog structures have been found: the embryonic shield of teleost fish, Hensen's node in the chick and the node of

mouse embryos all possess essentially the same activities as amphibian dorsal organiser (Beddington, 1994).

Leading to notochord formation, the first major transition occurs from dorsal organiser to chordamesoderm. During early gastrula stages, the chordamesoderm, which is the direct antecedent of the notochord, becomes morphologically and molecularly distinct from other mesoderm. Cellular rearrangements involving the mediolateral intercalation and convergence of cells towards the dorsal midline, force the chordamesoderm into an elongated stack of cells. Genetic screens in zebrafish have identified the gene *floating head* (*flh*) and the locus *bozozok* (where the gene *dharma* is mapped– Zebrafish Information Network), as being essential for this transition to occur (Amacher and Kimmel, 1998; Fekany et al., 1999; Solnica-Krezel et al., 1996; Talbot et al., 1995). *bozozok* mutant embryos lack a morphologically distinct shield, and both *bozozok* and *floating head (flh)* mutant embryos fail to form a notochord (Fekany et al., 1999; Talbot et al., 1995). Expression of *flh* mRNA is a good prospective marker of notochord fate (Gritsman et al., 2000). In early gastrula zebrafish embryos, *flh* is expressed superficially within the organiser region. Simultaneously, another homeodomain-encoding gene, *goosecoid* (*gsc*) is expressed in deep organiser tissues. While *gsc* was found to be involved in the induction of the rostral part of the axis, *flh* was found to predominantly regulate the formation of trunk and tail (Saude et al., 2000).

Another mechanism that occurs before to the one just described is the induction of mesoderm. Many of the molecules involved in mesoderm induction are the Nodal pathway- and the Nodal-related pathway- proteins. Importantly, the response of animal cap cells to Nodal is graded, so that different levels of Nodal signalling lead to different mesodermal and axial mesendodermal fates. High levels of Nodal signaling specify the deep *gsc*-expressing cell fates, while lower levels specify *flh*-expressing prospective chordamesoderm (Gritsman et al.,

2000). Therefore, Nodal signalling pathway is required for specification of dorsal mesendodermal fates and for early mesoderm induction. It is not, however, required for dorsal specification or neural induction (Gritsman et al., 2000).

After neurulation the notochord lies beneath the floor plate of the neural tube, above the endoderm, and between the paired somites that extend the length of the trunk and the tail (Cunliffe and Ingham, 1999).

As development proceeds, chordamesoderm cells acquire a thick extracellular sheath and a vacuole. Osmotic pressure within the vacuole acts against the sheath, gives the notochord its characteristic rod-like appearance, and provides mechanical properties that are essential for the proper elongation of embryos and for the locomotion of invertebrate chordates and many vertebrate species (Adams et al., 1990; Koehl, 1999). The transition from chordamesoderm to mature notochord requires a host of genes that have been identified in zebrafish genetic screens (Odenthal et al., 1996; Stemple et al., 1996).

Critical to its function, the notochord expresses transcription factors encoded by the *brachyury, HNF-3b* and *floating head* genes (Smith et al., 1991; Talbot et al., 1995), as well as the secreted factor *sonic hedgehog* (Ingham, 1995).

Studies in the mouse, *Xenopus*, and zebrafish have demonstrated that the trancription factor brachyury is required for differentiation of axial midline mesoderm into notochord as well as for the formation of posterior mesodermal tissues (Cunliffe and Ingham, 1999). It regulates the expression of several genes. These include extracellular matrix proteins, cell adhesion molecules, and cytoplasmic signaling pathway components.

The notochord has several roles in patterning surrounding tissues, and among them also the neural tube. A series of experiments involving both the transplantation and the removal of the notochord during development showed that the notochord can signal the formation of the floor plate, which is the

ventral-most fate of the spinal cord (Placzek et al., 2000; van Straaten et al., 1989). Among the signals secreted by the notochord are the Hedgehog (Hh) proteins. Sonic Hedgehog, in particular, induces a range of ventral spinal cord fates in a graded fashion while simultaneously suppressing the expression of characteristically dorsal genes. Reinforcing and maintaining earlier developmental events, notochord signals are also involved in establishing LR asymmetry (Danos and Yost, 1995; Lohr et al., 1997). In teleosts, notochord-derived Hh signals control the formation of the horizontal myoseptum, as well as specifying slow-twitch muscle fates (Barresi et al., 2000) (Figure 2).

Although the patterning roles of the notochord are essential for normal vertebrate development, the notochord also has an essential structural role. The notochord is the main axial skeletal element of the chordate early embryo; without a fully differentiated notochord, embryos fail to elongate (Stemple, 2005). For many species, this results in the inability to swim properly, to escape predation and to feed (Stemple et al., 1996).

There is some relationship between notochord differentiation and the presence of the basement membrane. This is likely to involve signalling from the basement membrane to chordamesoderm. The state of differentiation can be determined by analysis of gene expression. For example, *echidna hedgehog*, which is a zebrafish homologue of mammalian Indian hedgehog, is normally expressed in chordamesoderm, but when the notochord differentiates and vacuoles inflate, *echidna hedgehog* expression is extinguished (Currie and Ingham, 1996).

Consistent with its structural role in vertebrate development, the notochord shares many features with cartilage. It expresses many genes that are characteristic of cartilage, such as those that encode type II and type IX collagen, aggrecan, Sox9 and chondromodulin (Dietzsch et al., 1999; Sachdev et al., 2001; Zhao et al., 1997). There is, however, one clear difference between

chondrogenesis and notochord formation. Chondrocytes normally secrete a highly hyrdrated extracellular matrix, which gives cartilage its main structural properties (Knudson et al., 2000). By contrast, notochord cells produce a thick basement membrane sheath, and retain hydrated materials in large vacuoles (Parsons et al., 2002). These vacuoles allow notochord cells to exert pressure against the sheath walls, which give the notochord its structural properties (Koehl, 1999). The ultimate fate of the notochord also emphasizes the relatedness of notochord and cartilage. During endochondral bone formation, the type II collagen-rich extracellular matrix of cartilage is deposited with type X collagen, which signals the eventual replacement of cartilage by bone (Aszodi et al., 1998; Linsenmayer et al., 1986). Similarly, during the development of vertebrae, notochord that runs through the middle of each vertebra first expresses type II and type X collagen and is then replaced by bone(Linsenmayer et al., 1986). Between the vertebrae, the notochord does not express type X collagen and is not replaced by bone, but becomes the centre of the intervertebral disc – the nucleus pulposus (Aszodi et al., 1998; Smits and Lefebvre, 2003). Thus, notochord can become ossified in a fashion similar to cartilage. Consistent with this view, in mutant mice that lack type II collagen, the notochord is not replaced by bone, presumably because the type II collagen network is required for proper deposition of type X collagen.

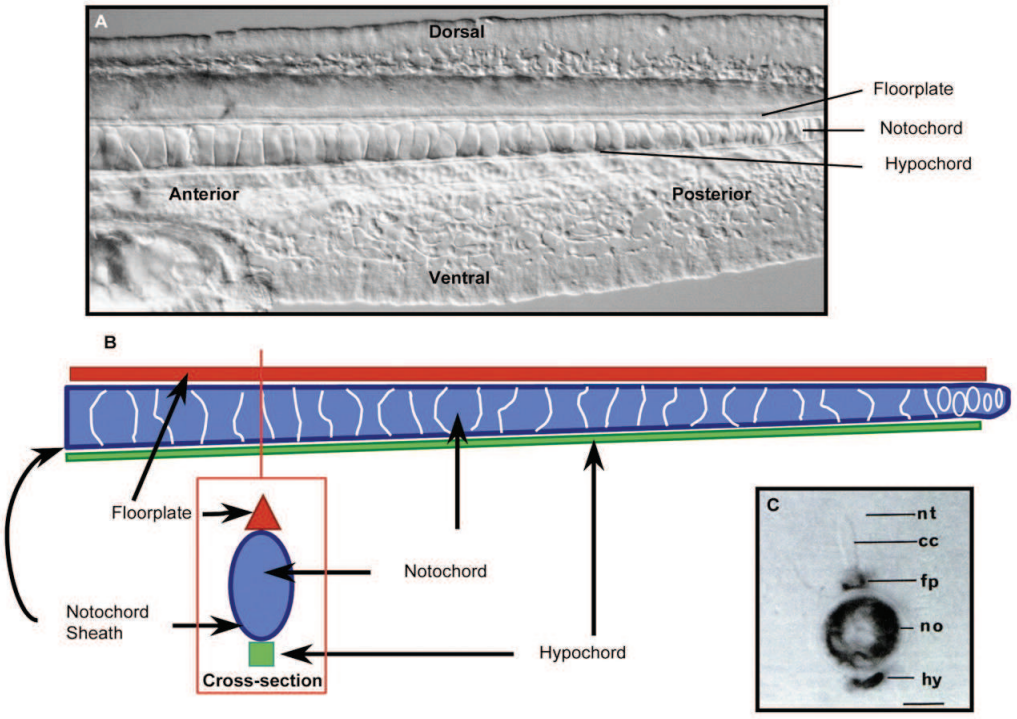

***Figure 2*. Structural aspects of the notochord**. (A) A lateral view of a living zebrafish tail at 24 hpf, showing the main features of the notochord. Dorsal to the notochord is the floor plate, in the ventral-most part of the forming spinal cord. Ventral to the notochord is the hypochord. (B) A schematic diagram of lateral and cross-sections of the notochord, showing the floor plate and hypochord acting as cables running along the top and bottom of the notochord. (C) As well as the notochord, the floor plate and hypochord express type II collagen. cc, central canal; fp, floor plate; hy, hypochord; no, notochord; nt, neural tube.
Development. 2005 Jun;132(11):2503-12

Regression

During the embryonic development, notochord regresses and is replaced by bone.

In teleosts, the development of the vertebral bodies begins with the mineralization of the notochord that presents an Extra Cellular Matrix (ECM) similar to the cartilage, which is rich in proteoglycans and type II collagen, and is covered by a thin layer of elastin. Several evidence suggests that the

notochord cells themselves induce such mineralization (Bensimon-Brito et al., 2010; Grotmol et al., 2006). The mineralized bone tissue is placed in the notochord region only during the second phase of the vertebral bodies formation (Grotmol et al., 2006). In this infraclass of vertebrates, cartilage, unlike higher vertebrates (such as mammals), is not involved in the initial formation of bone tissue (Knopf et al., 2011).

In the intervertebral discs, notochord-like cells have a role in maintaining the integrity of the disk (Erwin and Inman, 2006): these cells are localized in the nucleus pulposus. As a matter of fact, the expression of proteoglycans, the major matrix proteins of the nucleus pulposus of the intervertebral discs, seems to depend on factors secreted by notochordal cells of the intervertebral disks (Aguiar et al., 1999).

The development of the vertebral bodies in zebrafish begins with the formation of the perichordal center (also known as cordacentra), a mineralized structure shaped as a ring surrounding the notochord. The perichordal center is formed by segments in the anterior-posterior direction (Du and Dienhart, 2001; Haga et al., 2009) (Figure 3 A-E). The vertebrae and intervertebral discs are distinguishable at the stage of 15 Days Post Fertilization (dpf), 7 mm, and the notochord cells-like in the intervertebral discs are largely vacuolated and are clearly visible in larvae startign from 15 dpf. Within 21 dpf (9 mm), the size of the disks increases significantly and at the stage of 47 dpf the discs are occupied by two large vacuoles surrounded by a layer of small cells, and separated by two layers of cells in the center. The structure called notochordal center is located in the center of the vertebrae; it is probably the remnant of the notochord and the large vacuoles of the intervertebral disks are connected to this channel (Figure 3 F-I) (Haga et al., 2009).

Differently to the intervertebral discs, the vertebral bodies are formed for the most part from calcified bone tissue.

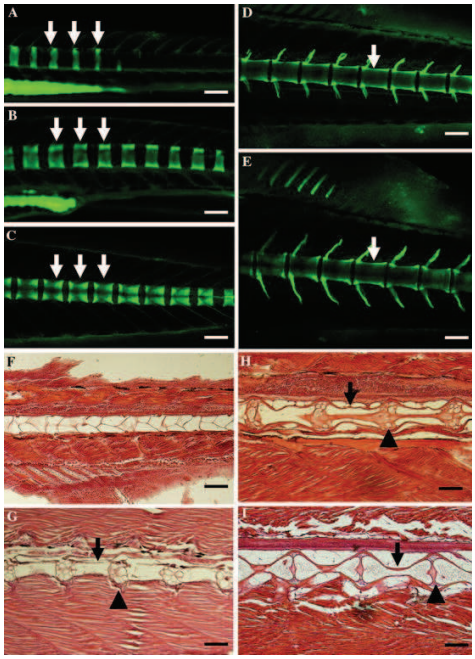

Figure 3. Analyses of notochord segmentation and vertebral formation. Calcein staining shows notochord segmentation by formation of calcified chordacentra from the anterior to the posterior notochord. (A) chordacentra formation (arrows) in the anterior region of the notochord at 11 dpf. (B) chordacentra appears in the posterior region of the notochord by 13 dpf. (C) the width of individual chordacentra expands significantly by 15 dpf. Vertebral bodies (arrows) are clearly developed in zebrafish larvae at 18 (D) and 21 (E) dpf. Histological analyses of H&E staining shows the sagittal views of the vertebral column at 12 (F), 15 (G), 21 (H) and 47 (I) dpf. (F) The vertebral column is primarily occupied by large vacuolated notochord cells at 12 dpf. Intervertebral discs (arrowhead) appear in a segmented manner at 15 (G), 21 (H), and 47 (I) dpf. The intervertebral disc contains large vacuolated notochord-like cells. Arrows indicate a notochordal canal in the center of the vertebral body that connects with the intervertebral discs. Scale bars (A-C) ~75 μm; (D,E) ~100 μm; (F-H) ~50 μm
Transgenic Res. 2009 Oct;18(5):669-83. doi: 10.1007/s11248-009-9259-y

Otherwise, during embryonic development of mammals, sclerotomal cells migrate towards the notochord and are arranged around it forming a continuous perichordal tube. It is initially non-segmented and is not in direct contact with the notochord, but is separated by a fibrous sheath of notochordal origin. This axial mesenchyme subsequently acquires a metameric structure of alternating regions consisting in condensed cells groups and in non-condensed cells groups. The condensed portions give rise to the annulus fibrosus of the

intervertebral discs, while the non-condensed perichordal cells form the cartilage primordia of the vertebral bodies (Theiler, 1988).

During the embryonic development, the inner part of the annulus fibrosus differentiates into hyaline cartilage-like tissue and forms an uninterrupted cartilage column surrounding the notochord together with the vertebral bodies. Concurrently with the chondrification process, the notochord regresses in the areas where vertebral bodies will develop, while it expands between the vertebrae to form the nucleus pulposus (Theiler, 1988).

Many transcription factors, growth factors, and extracellular matrix molecules play a conserved role during evolution in the development of the notochord and intervertebral discs. The transcription factors Sox5 and Sox6 are required for the survival of the notochord and the development of the nucleus pulposus (Smits and Lefebvre, 2003), while the type II collagen, is required for the formation of the intervertebral discs (Aszodi et al., 1998; Barbieri et al., 2003). The Retinoic acid (RA) is another signal molecule involved in the development of the vertebral disc.

In mammals, after birth, the nucleus pulposus of notochordal origin undergoes to a cartilage transition (Rufai et al., 1995). The notochordal cells which are present in the nucleus pulposus are progressively replaced by chondrocytes from cartilage plates (Kim et al., 2003). During this change the notochord cells gradually regress. In humans, this transition may be completed within the second decade (Buckwalter, 1995).

To date, little is known about the molecular mechanisms that lead to the regression of notochord cells: Malikova et al., demonstrated that apoptosis is necessary for the proper morphogenesis of the notochord during the formation of the anterior-posterior axis in embryos of *Xenopus laevis*. They detected apoptotic cells in the notochord starting from the neural groove stage and increasing in number as the embryo developed. The dying cells were distributed

in an anterior to posterior pattern, correlated with notochord extension through vacuolization. The inhibition of apoptosis *in vivo* decreased the length of the notochord which also appeared severely kinked. The notochord progressively lacked any recognizable structure, although notochord markers were expressed in a normal temporal pattern, moreover the somites were severely disorganized (Malikova et al., 2007). Their results indicate that apoptosis is required for normal notochord development during the formation of the anterior posterior axis and possibly for its consequent regression.

Interestingly, *Kim et al.* (*2005*) demonstrated that the apoptotic pathway mediated by *Fas* and *Fasl* is a mechanism through which notochord cells of the adult nucleus pulposus regress in rat. The coexpression of *Fas* and *Fasl* by the same cell has been implicated in the regulation of physiological cell turnover, the maintenance of immune privileged status and the protection of some tissues against potential malignant cells. Thus, *Fas* and *Fasl* coexpression by the notochord cells seems to have similar biological functions in the notochordal nucleus pulposus (Kim et al., 2005). The notochord cell population probably controls its proliferative status through the pathway mediated by fas and fasl through an autocrine or paracrine counterattack (Kim et al., 2005).

Fasl is an important effector molecule of cell mediated cytotoxicity against transformed cells. Therefore, resistance to Fas mediated apoptosis could provide a malignant cell with a selective advantage in its attempt to evade immune surveillance. Indeed, resistance to Fas crosslinking has been reported in a large percentage of cancer cell lines, and appears to be more common in lines originating from high-grade tumors. Several mechanism of resistance to Fas-mediated apoptosis have been suggested, including downregulation of Fas expression, mutations and deletions of Fas gene and the production and release of soluble decoy receptors that binds and inactivate Fasl (Poulaki et al., 2001).

Fas AND Fas ligand

Apoptotic pathway mediated by Fas and Fasl

Fas Ligand (Fasl) is a member of the tumor necrosis factor (*TNF*) superfamily that induces apoptosis in susceptible cells upon cross-linking of its own receptor, Fas (Apo-1/CD95), member of *TNF* receptors (*TNFR*) superfamily. The autocrine–paracrine interaction between Fas and Fasl results in the trimerization and activation of the Fas receptor. Fas intracellular death domain (DD) binds to the Fas-associated DD-containing protein (*FADD*) forming the death-inducing signaling complex (DISC). There are two different pathways downstream of Fas. In so called type I cells, the death signal is propagated by a caspase cascade initiated by the auto-activation of large amounts of caspase 8 recruited by *FADD* and which in turn initiates downstream activation of caspase- 3, -6, and -7. In type II cells, however, very little DISC is formed, so the caspase cascade cannot be propagated directly and has to be amplified via mitochondria. In the mitochondrial pathway, the apoptosome forms when intracellular signals trigger the release of cytochrome-*c*, which triggers the assembly of the Apaf-1/caspase-9 holoenzyme and in turn activates caspase-3 (Fig 4). The effector Caspases, Caspase-3, -6, and -7, cleave several different cellular substrates causing irreversible morphological changes in cells and nuclei associated with apoptosis (Figure 4) (Scaffidi et al., 1998; Scaffidi et al., 1999). Each step in the cascade is tightly controlled by intracellular factors that can inhibit the apoptotic pathway either at the “initiator” or “effector” level (Villa-Morales and Fernandez-Piqueras, 2012).

The Caspases are a family of cysteine proteases that cleave their substrates after aspartic acid residues. So far, 14 members of the caspase family have been identified. The Caspases involved in apoptosis are divided into two subfamilies, the initiator (Caspase 2, 8, 9, and 10) and executioner Caspases (caspase 3, 6,

and 7) (Li et al., 2010). Caspases are constitutively present within cells as latent zymogens or precursors that require proteolysis to achieve their active, heterodimeric configuration (Sharma et al., 2000).

Multiple mechanisms regulate the sensitivity of Fas-expressing cells to Fas-induced apoptosis, including alternative splicing of *FAS* pre-mRNA. The inclusion of *FAS* exon 6 results in the synthesis of the mRNA encoding the proapoptotic form of the *FAS* receptor, while mRNAs lacking exon 6 encode soluble form of the receptor, which, sequestering Fasl, lead to a reduction of Fas signaling, inhibiting apoptosis (Izquierdo, 2011; Izquierdo and Valcarcel, 2007).

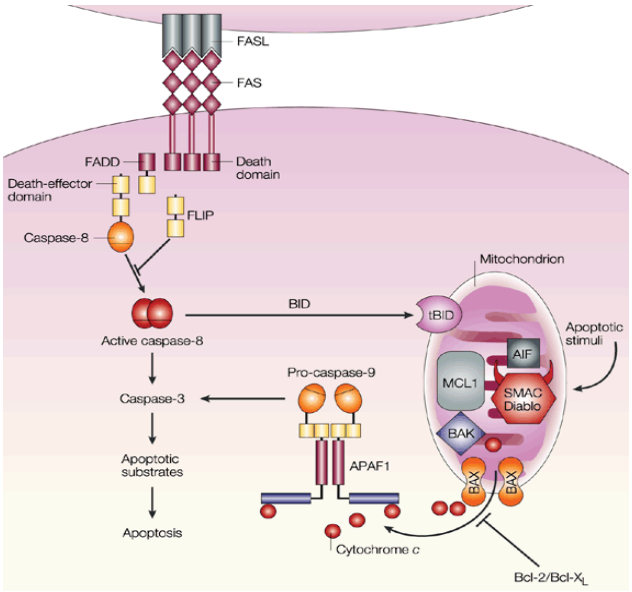

***Figure 4*. Intrinsic and extrinsic Caspase-dependent apoptotic pathways**. The extrinsic pathway is activated by the membrane receptor Fas that, following interaction with its ligand Fasl activates Caspase 8, which in turn activates the effector caspase 3. The intrinsic pathway also involves the mitochondrion, determining the release of cytochrome C, the activation of Capsase 9 and in the downstream the Capsase 3. Both the extrinsic pathway that the intrinsic involve the activation of caspase 3 that cuts activating various substrates that determine irreversible morphological changes in the nucleus and cytosol leading to apoptosis. Apaf1, apoptotic protease activating factor-1, ATP, adenosine triphosphate; FADD, Fas-associated death domain.

http://pi-patologia.blogspot.it/

On the other hand, diverse mechanisms play a role in the control of *FAS* and *FASL* expression. Recently, *FAS* (rs1800682 and rs2234767) and *FASL* (rs763110) functional SNPs have been identified. In different populations specific alleles were demonstrated to be associated with *FAS* and *FASL* dysregulation in several tumors such as breast cancer, squamous cell carcinoma of the larynx and hypopharynx, epithelial ovarian cancer and non-small cell lung cancer (Girnita et al., 2006; Hashemi et al., 2012; Li et al., 2013; Park et al., 2009; Wang et al., 2013; Wu et al., 2013; Xiang et al., 2012). The rs1800682 *FAS* SNP is situated within the Signal Transducers and Activators of Transcription 1 (*STAT1*) binding element, and the G/G genotype reduces the promoter activity (Sibley et al., 2003). The rs2234767 *FAS* SNP is located within the Stimulatory protein 1 (Sp1) Transcription Factor binding site of the *FAS* gene, and the A/A genotype was associated to the diminution of the promoter activity (Huang et al., 1997). The rs763110 *FASL* C/C genotype, located within the binding motif for the transcription factor CAAT/ enhancer binding protein β, is associated with a higher *FASL* expression then the C/T and T/T genotypes (Wu et al., 2003).

Also post-transcriptional mechanisms play a role in the regulation of *FAS* and *FASL* expression. Several microRNA were demonstrated to directly regulate *FAS* expression, and among them miR-20a was shown to be involved in the increase of metastatic potential of osteosarcoma (Huang et al., 2012). miR-196b also regulates *FAS* expression and its upregulation was involved in *FAS* repression in MLL-leukemia (Li et al., 2012). *FASL* is known to be targeted by miR-21, which has been shown to be involved in tumor progression and its up-regulation was correlated with a lower cancer survival rate in different tumors (Frezzetti et al., 2010; Zhu et al., 2012). miR-21 has been shown to be a biomarker for chemoresistance and clinical outcome following adjuvant

therapy, and it could be a potential pharmacological target to be evaluated in cancer (Frezzetti et al., 2010).

Extrinsic apoptotic pathway conservation during evolution

The two distinct signaling mechanisms, the cell-intrinsic and cell-extrinsic pathways, control the activation of the proapoptotic caspase family in mammals (Danial and Korsmeyer, 2004). While components of the intrinsic pathway apparently exist in all metazoans, the extrinsic pathway is a more recent evolutionary development (Eimon et al., 2006). No TNF or TNFR superfamily members have been found to date in *Caenorhabditis elegans*. In Drosophila, a single TNF ligand (Eiger) and its associated receptor (Wengen) induce apoptosis indirectly, by activating the caspase-9 homolog DRONC through the c-Jun N-terminal kinase (JNK) pathway; Drosophila homologs of caspase-8 (DREDD) and FADD do not appear to play a role in the extrinsic apoptotic pathway (Igaki et al., 2002; Kanda et al., 2002). DD-containing TNFRs have been reported exclusively in vertebrates, with examples in teleost (Eimon et al., 2006), avian (Brojatsch et al., 2000), and mammalian species (Locksley et al., 2001). Interestingly, not all DD-containing TNFRs are dedicated activators of the extrinsic apoptosis pathway. For example, mammalian TNFR1 signals through the adaptor TNFR-associated DD (TRADD) and its principal role *in vivo* is NF-kB activation, which inhibits apoptosis (Varfolomeev and Ashkenazi, 2004). Only DR4, DR5, and Fas have DDs that directly bind FADD.

In mammals, the extrinsic pathway plays an important role in regulating the immune system (Varfolomeev et al., 1998). As a matter of fact, the importance of Fas/Fasl mediated apoptosis is emphasized by the effects of the *gld* (generalized lymphoproliferative disease) and *lpr* (lymphoproliferation)

mutations, which are mutations respectively of the murine *Fas ligand* and *Fas* genes (Adachi et al., 1993; Watanabe-Fukunaga et al., 1992). Both of these mutations cause an age-related autoimmune syndrome that is characterized in part by the production of autoantibodies and the peripheral accumulation of large numbers of atypical double-negative (DN) T cells, leading to lymphadenopathy and splenomegaly (Cohen and Eisenberg, 1991). The lack of a functional fas/fasl- mediated pathway of apoptosis is believed to produce this autoimmune syndrome as a result of an impairment in both the clonal deletion of autoreactive lymphocytes in the periphery and the elimination of previously activated lymphocytes (Russell and Wang, 1993). Mice in which the gene for *Fas* has been deleted develop an autoimmune syndrome that is similar to that displayed by the *lpr* and *gld* mice (Adachi et al., 1995; Senju et al., 1996) and humans carrying homozygous mutations in the *FAS* gene also develop an autoimmune lympho- proliferative disorder.

Studies carried on FADD- and Caspase-8- knockout mice suggest that the extrinsic pathway also may be required during embryogenesis. In fact, knockout mice of the extrinsic pathway inhibitor c-FLIP (cellular FLICE inhibitory protein) all die *in utero* between embryonic days 10.5 and 12.5 (Yeh et al., 2000; Yeh et al., 1998). However, other observations seem to indicate that the extrinsic pathway *per se* is not essential for embryonic development but is part of a very complex mechanism that includes the enrollment of several pathways (Eimon et al., 2006). As a matter of fact, mice deficient for Fasl or Apo2L/TRAIL signaling complete embryogenesis(Cretney et al., 2002; Karray et al., 2004).

Eimon and colleagues characterized the extrinsic pathway in zebrafish to determine how it operates in a non-mammalian vertebrate (Eimon et al., 2006). They identified the zebrafish homologs of Fasl and Apo2L/TRAIL, their receptors, and other components of the cell death machinery. Studies with three

Apo2L/TRAIL homologs demonstrated that they bind the receptors *hdr* (previously linked to hematopoiesis) and ovarian TNFR (*otr*). Ectopic expression of these ligands during embryogenesis induced apoptosis in erythroblasts and notochord cells. Inhibition of *hdr*, *otr*, the adaptor *fadd*, or caspase-8-like proteases blocked ligand-induced apoptosis, as did antiapoptotic Bcl-2 family members. Thus, it was demonstrated that the extrinsic apoptosis pathway in zebrafish closely resembles its mammalian counterpart and cooperates with the intrinsic pathway to trigger tissue-specific apoptosis during embryogenesis (Eimon et al., 2006).

The zebrafish *fas* and *fasl* genes are reported in the Ensembl database (http://www.ensembl.org/index.html). The annotation ENSDARG00000043586 refers to *fas*, which is located on chromosome 17 of zebrafish, and the annotation ENSDARG00000011520 is relative to *fasl*, which is located on chromosome 20. *fas* encodes for a transcript of 984 bp, consisting of 8 exons and encodes a protein of 293 amino acids which has the 30% of amino acid identity with the human protein. The transcript of *fasl* is 1314 bp long, consists of 4 exons and encodes for a protein of 268 amino acids which has the 35% of amino acid identity with human *FASL*. For both *fas* and *fasl* proteins, the functional domains (TNFR and TNF respectively) are conserved. Both genes are not duplicated in the zebrafish genome and are therefore present in a single copy.

Given this evidence, Fas and Fasl were involved in the regression of notochord cells in the nucleus pulposus of the adult rat and apoptosis has been demonstrated to be involved in the development of the *Xenopus laevis* notochord. But so far no functional studies have been performed in order to study the possible role directly played by *fas/fasl* in the notochord development and/or regression. Therefore, it should be useful to develop an *in vivo* model for the functional study of *fas/fasl* in this structure.

Rationale

Classical chordoma is characterized by differentiated physaliferous cells typical of notochord tissue. Both the origin and the histological features of chordoma lead to hypothesize that one or more notochord regression steps can be affected during development in a few cells that would give rise to the tumor. The notochord cells remnants, living in a non-physiological environment might be subject to anomalous cellular signalling that would lead to a deregulation of programmed cell death, and although chordoma cells show a differentiated phenotype, they could proliferate out of control. Recently the *T* gene has been implicated in the pathogenesis of chordoma and so far, its expression has an important significance as diagnostic hallmark of chordoma. However, the genetic basis of *T* expression in chordoma is largely unknown as only somatic copy-number changes of *T* gene have been observed in a minority of cases, including minor allelic gain in 4.5% of cases and amplification in 7% of cases. In addition no mutation of *T* have been detected. Therefore, the question of how Brachyury orchestrates chordoma development remained open. The finding of the *T* expression in this tumor might be due to its deregulated expression in notochord cells, alternatively the defects in notochord regression may maintain proliferating notochord cells which express the *T* gene, or both of these possibilities. Therefore, studies of *T* expression regulation are necessary to clarify chordoma tumorigenesis, but also parallel studies aimed at identifying further mechanisms involved in the biology of this tumor and in the notochord development/regression should be pursued, performing functional studies in suitable animal models.

Interestingly, it has been reported that the proper balance between notochord cell proliferation and apoptosis is fundamental for the development and regression of the notochord. Accordingly, the apoptotic process is involved in normal notochord development in *Xenopus laevis*, and in particular the extrinsic apoptotic pathway is necessary for notochord development in zebrafish. In

addition the expression of the tumor necrosis factor receptor (*TNFR*) Fas and its ligand (*TNF*) Fasl, activating the extrinsic apoptosis, leads to the notochordal cells regression in the intervertebral disks of the adult rat. The autocrine-paracrine interaction between Fas and Fasl, resulting in the trimerization and activation of the Fas receptor, leads to cell death. Besides their role in apoptosis, these factors have also been implicated in survival/proliferation and cell cycle progression showing a tumor suppressor activity. Multiple mechanisms regulate the sensitivity of Fas-expressing cells to Fas-induced apoptosis, including alternative splicing of *FAS* pre-mRNA: mRNAs lacking exon 6 encode soluble form of the receptor, which, sequestering Fasl, lead to a reduction of Fas signaling, inhibiting apoptosis.

On the basis of the above premises, the first aim of my PhD project was to investigate the *FAS/FASL* pathway activity in SBC specimens, obtained thanks to the collaboration with the Dipartimento di Neurochirurgia of the Ospedale San Raffaele, Milan. I studied *FAS* and *FASL* gene and protein expression in 34 SBCs and the presence of alternative-spliced forms of *FAS* in a subgroup of 12 SBC. To investigate the activation status of Fas/Fasl pathway in chordoma tumors we also verified the activation of downstream caspases 3 and 8.

Since failure of apoptosis is known to be a key mechanism for the induction and maintenance of the neoplastic phenotype, we hypothesized that apoptosis might be deregulated also in chordoma. In order to investigate whether apoptotic processes can be enhanced in chordoma cell lines inducing their regression, a further aim of my project was to administrate soluble Fasl to the chordoma cell line U-CH1 and then study the Fas apoptotic pathway activity. At this purpose, the U-CH1 cells were exposed to soluble Fasl at different doses and times. These experiments were performed in collaboration with Prof. Canti, Dip. Biotecnologie Mediche e Medicina Traslazionale. The increase of Fas/Fasl pathway activation would pinpoint Fasl as a potential therapeutical molecule to

be evaluated in further pharmacological studies and Fas as a pharmacological target.

With the aim of identifying the molecular mechanisms leading to chordoma, we carried out *in vivo* functional studies on notochord development interfering with *fas/fasl* expression in zebrafish animal model. These experiments were performed in collaboration with Prof. Franco Cotelli, Dip. Bioscienze, Università degli Studi di Milano.

Thus, we firstly evaluated the expression of *fas* and *fasl* in the zebrafish whole embryos and larvae and in the notochord. Then we performed the loss-of-function experiments by using morpholino technology, in order to analyze notochord defects in zebrafish embryos and larvae, which were characterized by both histological and molecular techniques, also considering the expression of *ntla* and *col2a1a* genes, which were found to be deregulated in chordoma. The purpose of this study, besides providing new insights on notochord biology, was to identify new pathogenetic mechanisms underlying chordoma tumorigenesis.

Zebrafish as a developmental model system

Zebrafish (*Danio rerio*) is a tropical fish native to Southeast Asia. It possesses a unique combination of features that makes it particularly well suited for experimental and genetic analysis of early vertebrate development. Zebrafish adults are small, so many fishes can be housed in a small space. They have a relatively short generation time, an adult female reaches the sexual maturity in about three months and it lays hundreds of eggs per mating every few weeks, generating many progeny for genetic or experimental analysis. The zebrafish eggs are fertilized and develop externally to the mother, providing ready access to the developing animal at all stages of its development. The fertilized

embryos develop rapidly, making it possible to observe the entire course of early development in a short time. Somitogenesis begins at about 9 hpf and at 24 hpf the zebrafish embryo has already formed all the major tissues and many organ precursors, such as a beating heart, circulating blood, nervous system, eyes and ears, all of which can be readily observed under a simple dissecting microscope. Larvae hatch by about 2.5 dpf and they are swimming and feeding by 5–6 dpf (Weinstein, 2002). A variety of tools and methodologies have been developed to exploit the advantages of the zebrafish system. Zebrafish embryos and early larvae are optically clear, allowing for direct, non-invasive observation or experimental manipulation at all stages of their development such as Whole-mount *In Situ* Hybridisation (WISH) analysis of gene expression patterns with extraordinarily high resolution (Vogel and Weinstein, 2000). The externally developing embryos are readily accessible to experimental manipulation by techniques such as microinjection of biologically active molecules (RNA, DNA or antisense oligonucleotides), cell transplantation, fate mapping and cell lineage tracing (Holder and Xu, 1999; Kozlowski and Weinberg, 2000; Mizuno et al., 1999; Reifers et al., 2000a; Reifers et al., 2000b). The genetic methods available in the fish have been complemented in the last few years by a full array of genomic and molecular genetic tools. Relatively dense meiotic and radiation hybrid maps now allow for the rapid genetic and physical localization of mutations and genes (http://zfish.uoregon.edu). Large-insert clones of genomic DNA are available from Yeast Artificial Chromosome (YAC), Bacterial Artificial Chromosome (BAC) and P1 Artificial Chromosome (PAC) libraries. Extensive Expressed Sequence Tag (EST) sequencing and mapping projects are underway (http://zfish.wustl.edu). Efforts have also been initiated to obtain the complete sequence of the zebrafish genome, a feat that will undoubtedly dramatically

increase the usefulness of the mutants and genetic tools available in the fish (Vogel and Weinstein, 2000).

Project aims

Starting from the reported rationale, my PhD project was outlined in two different principal objectives:

- to analyze the activity of Fas/Fasl pathway in skull base chordoma and study whether the apoptotic processes can be enhanced in the U-CH1 chordoma cell line by the exposure to soluble Fasl
- to study the functional role of *fas* and *fasl* in the *in vivo* zebrafish (*Danio rerio*) model in order to investigate their possible implication in notochord development, differentiation and regression and thus helping to unravel mechanisms possibly involved in chordoma onset

Results

Fas/Fasl pathway impairment in skull base chordoma addresses identification of potential pharmacological targets

The first aim of my PhD project was to investigate the *FAS/FASL* pathway activity in skull base chordomas. At this purpose, we studied *FAS* and *FASL* gene expression in tumors from a cohort of 34 SBC samples and in the U-CH1 chordoma cell line by RT-PCR. Most of the analyzed samples showed *FAS* expression, while in 62% of them *FASL* transcript was not detected. Otherwise the U-CH1 cell line expressed both genes, as well as in the control tissue Nucleus Pulposus (NP). To investigate the activation status of this pathway in chordoma tumors and U-CH1 cells, we checked for the expression of the pro-apoptotic and anti-apoptotic *FAS* isoforms. This latter study was performed in a sub-group of twelve tumors because of the paucity of the biological material. All the chordoma samples and the U-CH1 cell line showed the expression of both transmembrane and soluble *FAS*, while NP showed exclusively the expression of the pro-apoptotic transmembrane isoform.

In order to identify mechanisms possibly causing *FAS/FASL* expression deregulation, we genotyped our SBC patients for the presence of specific functional SNPs that have been reported to be correlated to differential allelic *FAS* and *FASL* expression in different tumors. The finding of the G/G *FAS* rs2234767 genotype in all chordoma patients, associated to high *FAS* expression levels, suggests that there would not be constitutional *FAS* expression reduction. Similarly, the C/C *FASL* rs763110 genotype has been associated to higher *FASL* expression level than T/T or T/C genotypes, thus these results did not allow to correlate *FASL* dysregulation in SBC to any of *FASL* rs763110 genotypes. Despite the low number of chordoma analyzed, this evidence let us to hypothesize that these functional SNPs are not directly associated to the observed expression dysregulation of *FAS/FASL* in SBCs, differently from what was previously reported for other type of tumors.

Therefore, other mechanisms could play a role in the control of *FAS* and *FASL* expression. We speculated that methylation and/or both post-transcriptional expression modulation by specific miRNAs might affect *FASL* expression regulation. Furthermore, the alternative splicing deregulation of *FAS*, enhancing the expression of anti-apoptotic isoform in chordoma, might be caused by the altered expression of one or more specific splicing factors known to be involved in *FAS* splicing.

This evidence led us to speculate that even when Fasl is expressed in SBCs, it poorly interacts with its transmembrane receptor for the presence of the soluble Fas which, acting as competitor, maintains inactivated the Fas/Fasl mediated pro-apoptotic signaling. All these results suggest that the activation status of Fas/Fasl pathway is impaired in chordoma.

In order to confirm our hypothesis on the impairment of Fas/Fasl pathway in SBC, we studied the presence of the activated downstream effectors Caspase 8 and Caspase 3 in the sub-group of 12 SBC samples by western blot. The inactive Caspase 8 was found to be expressed in all the samples analyzed, while the active form, a cleaved product derived from the Caspase 8 activation, was found to be weakly expressed only in three tumors. As far as the Caspase 3, the only inactive form was detected. These findings strongly support our hypothesis on the impairment of Fas/Fasl apoptotic pathway in chordoma. Therefore, this evidence led us to hypothesize that the exposure of chordoma cell line to soluble Fasl (SuperFAS Ligand) might strengthen the activation of apoptosis mediated by the transmembrane Fas, competing with the Fas anti-apoptotic soluble isoform.

At this purpose we studied whether the administration of soluble Fasl may increase the Fas apoptotic pathway activity in the U-CH1 chordoma cell line. The U-CH1 cells were exposed to soluble Fasl at different doses and times. We observed a significant induction of the apoptosis in the treated cells by means of

cytofluorimetric apoptotic assays, besides the significant increase of Pre caspase 8 together with the significant decrease of Pro caspase 8 levels in a dose and time exposure dependent manner. These data confirm our hypothesis and indicate that Fas pathway activity can be increased in this tumor.

The evidence obtained led us to speculate that Fas may be a potential therapeutic target and Fasl a potential pharmacological molecule, addressing studies aimed at identifying effective chemotherapeutical protocols for the treatment of chordoma.

fas/fasl downregulation impairs zebrafish notochord morphogenesis and regression affecting the expression of specific chordoma markers

Chordoma originates from notochord remnants that do not disappear during development of vertebral bodies. The apoptotic mechanisms are fundamental for notochord cells development and regression. Accordingly, the Fas/Fasl pathway was found to be involved in specific notochordal cells' regression step. Since we found that the *FAS/FASL* expression is dysregulated in chordoma and the pathway was found to be inactivated, we thus hypothesized that Fas/Fasl pathway dysregulation may have a role in chordoma onset. To unravel this issue we investigated the function of *fas* and *fasl* homologs in the zebrafish animal model notochord development. These genes are evolutionary conserved from fish to mammals. We firstly evaluated the expression of *fas* and *fasl* in the zebrafish whole embryos and larvae by RT-PCR. While *fas* was maternally and zigotycally expressed, *fasl* showed a maternal expression and a zygotic expression starting from 24 hpf. The expression pattern of *fas* and *fasl* in brain, eyes, gut, ovary of the adult fish is conserved in mammals, supporting the conservation of *FAS/FASL* function during evolution. The detection of *fas* and

fasl expression in zebrafish notochord sorted cells at the first stages of development, pinpoints for the first time the involvement of these two genes in the processes of notochord formation. Morpholino mediated knock-down of *fas* and *fasl* caused specific aberrant phenotypes such as bent tails and motility defects. Morphological and histological analyses of the *fas/fasl* morpholino-injected embryos and larvae showed notochord multi-cell-layer jumps instead of the typical "stack-of-coins" organization, larger notochord vacuolated cells, defects in the peri-notochordal sheath structure and in vertebral mineralization. It is known that these alterations are determined by notochord differentiation impairment. Interestingly, the defects in notochord differentiation following *fas/fasl* loss-of function, closely correlate with the phenotypes observed after the deregulation of other genes expressed in the notochord or in the perinotochord sheath, such as *col15a1, col27a1a* and *col27a1b*.

In addition, the loss-of-function of *fas/fasl* produced disorganized myofibrils and an aberrant primary motoneurons branching, resulting in a motility impairment. Indeed, both muscles and motoneurons formation require proper signaling from the notochord, and it has been demonstrated that also the integrity of the perinotochordal sheath is essential for the axon projections.

The knockdown of *fas* and *fasl* resulted later during development in vertebrae mineralization defects instead of the normal notochord ossification. Therefore, *fas/fasl* loss-of function might alter the proper notochord cells disappearance during notochord regression, similarly to what happens to the notochord cells in the nucleus pulposus of rat. This might cause the mechanical weakening of notochord sheath leading to defects in vertebrae formation.

To investigate whether the notochord aberrant phenotypes, observed in *fas/fasl* loss-of-function zebrafish, showed molecular alteration common to chordoma, we studied the expression of two chordoma markers' homologs, *ntla* (*T*) and

col2a1a (*COL2A1*), that are also finely regulated during notochord development and differentiation.

These two genes were found significantly upregulated and their expression was maintained in *fas/fasl*-MO-injected embryos in a developmental stage in which, in controls, they normally diminished and disappeared. These results are in accord with data on the reported hyper-expression of the homologs *T* and *COL2A1* genes in chordoma.

The obtained results allowed us to demonstrate that *fas/fasl* are involved in proper notochord development, differentiation and regression in zebrafish, and the effects detected by their deregulation are consistent with the implication of *FAS/FASL* pathway defects in chordoma onset.

Conclusions and Perspectives

Conclusions

- Dysregulaton of *FAS/FASL* in most SBCs analyzed, presence of both pro- and anti-apoptotic *FAS* isoforms and detection of the prevalent expression of inactive forms of both Caspase- 8 and Caspase- 3 SBCs analyzed

- *FAS/FASL* functional SNPs are not directly associated to the expression dysregulation of these genes in SBCs analyzed

- Significant induction of the apoptosis in the U-CH1 chordoma cells following treatment with soluble Fasl indicate that this pathway can be activated in chordoma

- *fas* and *fasl* zebrafish homologs were specifically expressed in the notochord

- Morpholino mediated knock-down of *fas* and *fasl* caused specific aberrant phenotypes such as bent tails and motility defects, notochord multi-cell-layer jumps instead of the typical "stack-of-coins" organization, larger notochord vacuolated cells, defects in the peri-notochordal sheath structure and in vertebral mineralization

- The two chordoma markers *ntla* (*T*) and *col2a1a* (*COL2A1*), were found to be deregulated in *fas/fasl* morpholino-injected embryos

- Fas/Fasl pathway activity can be enhanced in chordoma. Moreover, *fas* and *fasl* are involved in in notochord development, differentiation and regression in zebrafish suggesting the implication of this pathway in chordoma onset

Perspectives

- to investigate genetic/epigenetic mechanisms possibly involved in *FASL* silencing or down regulation
- to study the mechanisms leading to *FAS* antiapoptotic isoform overexpression in chordomas, in U-CH1 chordoma cell line
- to interfere with *FAS* different isoforms expression in U-CH1 cell line to study the possible different induction of apoptosis following soluble Fasl treatments
- to identify drugs that in combination with soluble Fasl treatment are able to induce apoptosis and inhibit growth in chordoma cell lines
- to generate *fas* and *fasl* zebrafish conditional mutants to better understand their implication in notochord development/regression at specific developmental stages and to investigate their potential causative role in tumorigenesis processes
- to generate xenotransplantation of human chordoma U-CH1 cells in zebrafish embryos to study the potential of tumor cells invasiveness and metastasis and to assess *in vivo* anticancer therapies

Bibliography

Adachi, M., Suematsu, S., Kondo, T., Ogasawara, J., Tanaka, T., Yoshida, N., and Nagata, S. (1995). Targeted mutation in the Fas gene causes hyperplasia in peripheral lymphoid organs and liver. Nat Genet *11*, 294-300.

Adachi, M., Watanabe-Fukunaga, R., and Nagata, S. (1993). Aberrant transcription caused by the insertion of an early transposable element in an intron of the Fas antigen gene of lpr mice. Proc Natl Acad Sci U S A *90*, 1756-1760.

Adams, D.S., Keller, R., and Koehl, M.A. (1990). The mechanics of notochord elongation, straightening and stiffening in the embryo of Xenopus laevis. Development *110*, 115-130.

Aguiar, D.J., Johnson, S.L., and Oegema, T.R. (1999). Notochordal cells interact with nucleus pulposus cells: regulation of proteoglycan synthesis. Exp Cell Res *246*, 129-137.

Amacher, S.L., and Kimmel, C.B. (1998). Promoting notochord fate and repressing muscle development in zebrafish axial mesoderm. Development *125*, 1397-1406.

Aszodi, A., Chan, D., Hunziker, E., Bateman, J.F., and Fassler, R. (1998). Collagen II is essential for the removal of the notochord and the formation of intervertebral discs. J Cell Biol *143*, 1399-1412.

Barbieri, O., Astigiano, S., Morini, M., Tavella, S., Schito, A., Corsi, A., Di Martino, D., Bianco, P., Cancedda, R., and Garofalo, S. (2003). Depletion of cartilage collagen fibrils in mice carrying a dominant negative Col2a1 transgene affects chondrocyte differentiation. Am J Physiol Cell Physiol *285*, C1504-1512.

Barresi, M.J., Stickney, H.L., and Devoto, S.H. (2000). The zebrafish slow-muscle-omitted gene product is required for Hedgehog signal transduction and the development of slow muscle identity. Development *127*, 2189-2199.

Beddington, R.S. (1994). Induction of a second neural axis by the mouse node. Development *120*, 613-620.

Bensimon-Brito, A., Cardeira, J., Cancela, M.L., Huysseune, A., and Witten, P.E. (2010). Distinct patterns of notochord mineralization in zebrafish coincide with the localization of Osteocalcin isoform 1 during early vertebral centra formation. BMC Dev Biol *12*, 28.

Boriani, S., Chevalley, F., Weinstein, J.N., Biagini, R., Campanacci, L., De Iure, F., and Piccill, P. (1996). Chordoma of the spine above the sacrum. Treatment and outcome in 21 cases. Spine (Phila Pa 1976) *21*, 1569-1577.

Brojatsch, J., Naughton, J., Adkins, H.B., and Young, J.A. (2000). TVB receptors for cytopathic and noncytopathic subgroups of avian leukosis viruses are functional death receptors. J Virol *74*, 11490-11494.

Bruderlein, S., Sommer, J.B., Meltzer, P.S., Li, S., Osada, T., Ng, D., Moller, P., Alcorta, D.A., and Kelley, M.J. (2010). Molecular characterization of putative chordoma cell lines. Sarcoma *2010*, 630129.

Buckwalter, J.A. (1995). Aging and degeneration of the human intervertebral disc. Spine (Phila Pa 1976) *20*, 1307-1314.

Bydon, M., Papadimitriou, K., Witham, T., Wolinsky, J.P., Bydon, A., Sciubba, D., and Gokaslan, Z. (2012). Novel therapeutic targets in chordoma. Expert Opin Ther Targets.

Casali, P.G., Messina, A., Stacchiotti, S., Tamborini, E., Crippa, F., Gronchi, A., Orlandi, R., Ripamonti, C., Spreafico, C., Bertieri, R., *et al.* (2004). Imatinib mesylate in chordoma. Cancer *101*, 2086-2097.

Casey, E.S., O'Reilly, M.A., Conlon, F.L., and Smith, J.C. (1998). The T-box transcription factor Brachyury regulates expression of eFGF through binding to a non-palindromic response element. Development *125*, 3887-3894.

Chambers, P.W., and Schwinn, C.P. (1979). Chordoma. A clinicopathologic study of metastasis. Am J Clin Pathol *72*, 765-776.

Christ, B., Huang, R., and Scaal, M. (2004). Formation and differentiation of the avian sclerotome. Anat Embryol (Berl) *208*, 333-350.

Cohen, P.L., and Eisenberg, R.A. (1991). Lpr and gld: single gene models of systemic autoimmunity and lymphoproliferative disease. Annu Rev Immunol *9*, 243-269.

Colli, B.O., and Al-Mefty, O. (2001). Chordomas of the skull base: follow-up review and prognostic factors. Neurosurg Focus *10*, E1.

Cretney, E., Takeda, K., Yagita, H., Glaccum, M., Peschon, J.J., and Smyth, M.J. (2002). Increased susceptibility to tumor initiation and metastasis in TNF-related apoptosis-inducing ligand-deficient mice. J Immunol *168*, 1356-1361.

Cunliffe, V.T., and Ingham, P.W. (1999). Switching on the notochord. Genes Dev *13*, 1643-1646.

Currie, P.D., and Ingham, P.W. (1996). Induction of a specific muscle cell type by a hedgehog-like protein in zebrafish. Nature *382*, 452-455.

Danial, N.N., and Korsmeyer, S.J. (2004). Cell death: critical control points. Cell *116*, 205-219.

Danos, M.C., and Yost, H.J. (1995). Linkage of cardiac left-right asymmetry and dorsal-anterior development in Xenopus. Development *121*, 1467-1474.

Deshpande, V., Nielsen, G.P., Rosenthal, D.I., and Rosenberg, A.E. (2007). Intraosseous benign notochord cell tumors (BNCT): further evidence supporting a relationship to chordoma. Am J Surg Pathol *31*, 1573-1577.

Dietzsch, E., Albrecht, C.F., and Parker, M.I. (1999). Effect of rooperol on collagen synthesis and cell growth. IUBMB Life *48*, 321-325.

Du, S.J., and Dienhart, M. (2001). Zebrafish tiggy-winkle hedgehog promoter directs notochord and floor plate green fluorescence protein expression in transgenic zebrafish embryos. Dev Dyn *222*, 655-666.

Eimon, P.M., Kratz, E., Varfolomeev, E., Hymowitz, S.G., Stern, H., Zha, J., and Ashkenazi, A. (2006). Delineation of the cell-extrinsic apoptosis pathway in the zebrafish. Cell Death Differ *13*, 1619-1630.

Erwin, W.M., and Inman, R.D. (2006). Notochord cells regulate intervertebral disc chondrocyte proteoglycan production and cell proliferation. Spine (Phila Pa 1976) *31*, 1094-1099.
Fekany, K., Yamanaka, Y., Leung, T., Sirotkin, H.I., Topczewski, J., Gates, M.A., Hibi, M., Renucci, A., Stemple, D., Radbill, A.*, et al.* (1999). The zebrafish bozozok locus encodes Dharma, a homeodomain protein essential for induction of gastrula organizer and dorsoanterior embryonic structures. Development *126*, 1427-1438.
Fernando, R.I., Litzinger, M., Trono, P., Hamilton, D.H., Schlom, J., and Palena, C. (2010). The T-box transcription factor Brachyury promotes epithelial-mesenchymal transition in human tumor cells. J Clin Invest *120*, 533-544.
Fouquet, B., Weinstein, B.M., Serluca, F.C., and Fishman, M.C. (1997). Vessel patterning in the embryo of the zebrafish: guidance by notochord. Dev Biol *183*, 37-48.
Fourney, D.R., and Gokaslan, Z.L. (2003). Current management of sacral chordoma. Neurosurg Focus *15*, E9.
Frezzetti, D., De Menna, M., Zoppoli, P., Guerra, C., Ferraro, A., Bello, A.M., De Luca, P., Calabrese, C., Fusco, A., Ceccarelli, M.*, et al.* (2010). Upregulation of miR-21 by Ras in vivo and its role in tumor growth. Oncogene *30*, 275-286.
Gagliardi, F., Boari, N., Riva, P., and Mortini, P. (2012). Current therapeutic options and novel molecular markers in skull base chordomas. Neurosurg Rev *35*, 1-13; discussion 13-14.
Girnita, D.M., Webber, S.A., Ferrell, R., Burckart, G.J., Brooks, M.M., McDade, K.K., Chinnock, R., Canter, C., Addonizio, L., Bernstein, D.*, et al.* (2006). Disparate distribution of 16 candidate single nucleotide polymorphisms among racial and ethnic groups of pediatric heart transplant patients. Transplantation *82*, 1774-1780.
Glickman, N.S., Kimmel, C.B., Jones, M.A., and Adams, R.J. (2003). Shaping the zebrafish notochord. Development *130*, 873-887.
Goldstein, A.M., and Fishman, M.C. (1998). Notochord regulates cardiac lineage in zebrafish embryos. Dev Biol *201*, 247-252.
Gritsman, K., Talbot, W.S., and Schier, A.F. (2000). Nodal signaling patterns the organizer. Development *127*, 921-932.
Grotmol, S., Kryvi, H., Keynes, R., Krossoy, C., Nordvik, K., and Totland, G.K. (2006). Stepwise enforcement of the notochord and its intersection with the myoseptum: an evolutionary path leading to development of the vertebra? J Anat *209*, 339-357.
Haga, Y., Dominique, V.J., 3rd, and Du, S.J. (2009). Analyzing notochord segmentation and intervertebral disc formation using the twhh:gfp transgenic zebrafish model. Transgenic Res *18*, 669-683.
Harland, R., and Gerhart, J. (1997). Formation and function of Spemann's organizer. Annu Rev Cell Dev Biol *13*, 611-667.
Hashemi, M., Fazaeli, A., Ghavami, S., Eskandari-Nasab, E., Arbabi, F., Mashhadi, M.A., Taheri, M., Chaabane, W., Jain, M.V., and Los, M.J. (2012). Functional polymorphisms of FAS and FASL gene and risk of breast cancer - pilot study of 134 cases. PLoS One *8*, e53075.
Henderson, S.R., Guiliano, D., Presneau, N., McLean, S., Frow, R., Vujovic, S., Anderson, J., Sebire, N., Whelan, J., Athanasou, N.*, et al.* (2005). A molecular map of mesenchymal tumors. Genome Biol *6*, R76.
Higinbotham, N.L., Phillips, R.F., Farr, H.W., and Hustu, H.O. (1967). Chordoma. Thirty-five-year study at Memorial Hospital. Cancer *20*, 1841-1850.
Holder, N., and Xu, Q. (1999). Microinjection of DNA, RNA, and protein into the fertilized zebrafish egg for analysis of gene function. Methods Mol Biol *97*, 487-490.
Huang, G., Nishimoto, K., Zhou, Z., Hughes, D., and Kleinerman, E.S. (2012). miR-20a encoded by the miR-17-92 cluster increases the metastatic potential of osteosarcoma cells by regulating Fas expression. Cancer Res *72*, 908-916.
Huang, Q.R., Morris, D., and Manolios, N. (1997). Identification and characterization of polymorphisms in the promoter region of the human Apo-1/Fas (CD95) gene. Mol Immunol *34*, 577-582.
Igaki, T., Kanda, H., Yamamoto-Goto, Y., Kanuka, H., Kuranaga, E., Aigaki, T., and Miura, M. (2002). Eiger, a TNF superfamily ligand that triggers the Drosophila JNK pathway. EMBO J *21*, 3009-3018.
Ingham, P.W. (1995). Signalling by hedgehog family proteins in Drosophila and vertebrate development. Curr Opin Genet Dev *5*, 492-498.
Izquierdo, J.M. (2011). Cell-specific regulation of Fas exon 6 splicing mediated by Hu antigen R. Biochem Biophys Res Commun *402*, 324-328.
Izquierdo, J.M., and Valcarcel, J. (2007). Fas-activated serine/threonine kinase (FAST K) synergizes with TIA-1/TIAR proteins to regulate Fas alternative splicing. J Biol Chem *282*, 1539-1543.
Jambhekar, N.A., Rekhi, B., Thorat, K., Dikshit, R., Agrawal, M., and Puri, A. (2010). Revisiting chordoma with brachyury, a "new age" marker: analysis of a validation study on 51 cases. Arch Pathol Lab Med *134*, 1181-1187.
Kanda, H., Igaki, T., Kanuka, H., Yagi, T., and Miura, M. (2002). Wengen, a member of the Drosophila tumor necrosis factor receptor superfamily, is required for Eiger signaling. J Biol Chem *277*, 28372-28375.
Karray, S., Kress, C., Cuvellier, S., Hue-Beauvais, C., Damotte, D., Babinet, C., and Levi-Strauss, M. (2004). Complete loss of Fas ligand gene causes massive lymphoproliferation and early death, indicating a residual activity of gld allele. J Immunol *172*, 2118-2125.
Kim, K.W., Kim, Y.S., Ha, K.Y., Woo, Y.K., Park, J.B., Park, W.S., and An, H.S. (2005). An autocrine or paracrine Fas-mediated counterattack: a potential mechanism for apoptosis of notochordal cells in intact rat nucleus pulposus. Spine (Phila Pa 1976) *30*, 1247-1251.

Kim, K.W., Lim, T.H., Kim, J.G., Jeong, S.T., Masuda, K., and An, H.S. (2003). The origin of chondrocytes in the nucleus pulposus and histologic findings associated with the transition of a notochordal nucleus pulposus to a fibrocartilaginous nucleus pulposus in intact rabbit intervertebral discs. Spine (Phila Pa 1976) *28*, 982-990.
Knopf, F., Hammond, C., Chekuru, A., Kurth, T., Hans, S., Weber, C.W., Mahatma, G., Fisher, S., Brand, M., Schulte-Merker, S.*, et al.* (2011). Bone regenerates via dedifferentiation of osteoblasts in the zebrafish fin. Dev Cell *20*, 713-724.
Knudson, W., Casey, B., Nishida, Y., Eger, W., Kuettner, K.E., and Knudson, C.B. (2000). Hyaluronan oligosaccharides perturb cartilage matrix homeostasis and induce chondrocytic chondrolysis. Arthritis Rheum *43*, 1165-1174.
Koehl, M.A. (1999). Ecological biomechanics of benthic organisms: life history, mechanical design and temporal patterns of mechanical stress. J Exp Biol *202*, 3469-3476.
Kozlowski, D.J., and Weinberg, E.S. (2000). Photoactivatable (caged) fluorescein as a cell tracer for fate mapping in the zebrafish embryo. Methods Mol Biol *135*, 349-355.
Li, F., He, Z., Shen, J., Huang, Q., Li, W., Liu, X., He, Y., Wolf, F., and Li, C.Y. (2010). Apoptotic caspases regulate induction of iPSCs from human fibroblasts. Cell Stem Cell *7*, 508-520.
Li, Y., Hao, Y.L., Kang, S., Zhou, R.M., Wang, N., and Qi, B.L. (2013). Genetic polymorphisms in the Fas and FasL genes are associated with epithelial ovarian cancer risk and clinical outcomes. Gynecol Oncol *128*, 584-589.
Li, Z., Huang, H., Chen, P., He, M., Li, Y., Arnovitz, S., Jiang, X., He, C., Hyjek, E., Zhang, J.*, et al.* (2012). miR-196b directly targets both HOXA9/MEIS1 oncogenes and FAS tumour suppressor in MLL-rearranged leukaemia. Nat Commun *3*, 688.
Linsenmayer, T.F., Gibney, E., and Schmid, T.M. (1986). Segmental appearance of type X collagen in the developing avian notochord. Dev Biol *113*, 467-473.
Locksley, R.M., Killeen, N., and Lenardo, M.J. (2001). The TNF and TNF receptor superfamilies: integrating mammalian biology. Cell *104*, 487-501.
Lohr, J.L., Danos, M.C., and Yost, H.J. (1997). Left-right asymmetry of a nodal-related gene is regulated by dorsoanterior midline structures during Xenopus development. Development *124*, 1465-1472.
Longoni, M., Orzan, F., Stroppi, M., Boari, N., Mortini, P., and Riva, P. (2008). Evaluation of 1p36 markers and clinical outcome in a skull base chordoma study. Neuro Oncol *10*, 52-60.
Malikova, M.A., Van Stry, M., and Symes, K. (2007). Apoptosis regulates notochord development in Xenopus. Dev Biol *311*, 434-448.
Matsuno, A., Sasaki, T., Nagashima, T., Matsuura, R., Tanaka, H., Hirakawa, M., Murakami, M., and Kirino, T. (1997). Immunohistochemical examination of proliferative potentials and the expression of cell cycle-related proteins of intracranial chordomas. Hum Pathol *28*, 714-719.
McMaster, M.L., Goldstein, A.M., Bromley, C.M., Ishibe, N., and Parry, D.M. (2001). Chordoma: incidence and survival patterns in the United States, 1973-1995. Cancer Causes Control *12*, 1-11.
Miozzo, M., Dalpra, L., Riva, P., Volonta, M., Macciardi, F., Pericotti, S., Tibiletti, M.G., Cerati, M., Rohde, K., Larizza, L.*, et al.* (2000). A tumor suppressor locus in familial and sporadic chordoma maps to 1p36. Int J Cancer *87*, 68-72.
Mizuno, T., Shinya, M., and Takeda, H. (1999). Cell and tissue transplantation in zebrafish embryos. Methods Mol Biol *127*, 15-28.
Munsterberg, A.E., and Lassar, A.B. (1995). Combinatorial signals from the neural tube, floor plate and notochord induce myogenic bHLH gene expression in the somite. Development *121*, 651-660.
Naka, T., Boltze, C., Kuester, D., Schulz, T.O., Schneider-Stock, R., Kellner, A., Samii, A., Herold, C., Ostertag, H., and Roessner, A. (2005). Alterations of G1-S checkpoint in chordoma: the prognostic impact of p53 overexpression. Cancer *104*, 1255-1263.
Naka, T., Boltze, C., Samii, A., Samii, M., Herold, C., Ostertag, H., Iwamoto, Y., Oda, Y., Tsuneyoshi, M., Kuester, D.*, et al.* (2009). Expression of c-MET, low-molecular-weight cytokeratin, matrix metalloproteinases-1 and -2 in spinal chordoma. Histopathology *54*, 607-613.
Naka, T., Kuester, D., Boltze, C., Schulz, T.O., Samii, A., Herold, C., Ostertag, H., and Roessner, A. (2008). Expression of matrix metalloproteinases-1, -2, and -9; tissue inhibitors of matrix metalloproteinases-1 and -2; cathepsin B; urokinase plasminogen activator; and plasminogen activator inhibitor, type I in skull base chordoma. Hum Pathol *39*, 217-223.
Nelson, A.C., Pillay, N., Henderson, S., Presneau, N., Tirabosco, R., Halai, D., Berisha, F., Flicek, P., Stemple, D.L., Stern, C.D.*, et al.* (2012). An integrated functional genomics approach identifies the regulatory network directed by brachyury (T) in chordoma. J Pathol.
Oakley, G.J., Fuhrer, K., and Seethala, R.R. (2008). Brachyury, SOX-9, and podoplanin, new markers in the skull base chordoma vs chondrosarcoma differential: a tissue microarray-based comparative analysis. Mod Pathol *21*, 1461-1469.
Odenthal, J., Haffter, P., Vogelsang, E., Brand, M., van Eeden, F.J., Furutani-Seiki, M., Granato, M., Hammerschmidt, M., Heisenberg, C.P., Jiang, Y.J.*, et al.* (1996). Mutations affecting the formation of the notochord in the zebrafish, Danio rerio. Development *123*, 103-115.
Oikawa, S., Kyoshima, K., Goto, T., Iwashita, T., Takizawa, T., Kobayashi, S., and Ito, M. (2001). Histological study on local invasiveness of clival chordoma. Case report of autopsy. Acta Neurochir (Wien) *143*, 1065-1069.

Pallini, R., Maira, G., Pierconti, F., Falchetti, M.L., Alvino, E., Cimino-Reale, G., Fernandez, E., D'Ambrosio, E., and Larocca, L.M. (2003). Chordoma of the skull base: predictors of tumor recurrence. J Neurosurg *98*, 812-822.
Park, J.Y., Lee, W.K., Jung, D.K., Choi, J.E., Park, T.I., Lee, E.B., Cho, S., Cha, S.I., Kim, C.H., Kam, S.*, et al.* (2009). Polymorphisms in the FAS and FASL genes and survival of early stage non-small cell lung cancer. Clin Cancer Res *15*, 1794-1800.
Parsons, M.J., Pollard, S.M., Saude, L., Feldman, B., Coutinho, P., Hirst, E.M., and Stemple, D.L. (2002). Zebrafish mutants identify an essential role for laminins in notochord formation. Development *129*, 3137-3146.
Placzek, M., Dodd, J., and Jessell, T.M. (2000). Discussion point. The case for floor plate induction by the notochord. Curr Opin Neurobiol *10*, 15-22.
Poulaki, V., Mitsiades, C.S., and Mitsiades, N. (2001). The role of Fas and FasL as mediators of anticancer chemotherapy. Drug Resist Updat *4*, 233-242.
Pourquie, O., Coltey, M., Teillet, M.A., Ordahl, C., and Le Douarin, N.M. (1993). Control of dorsoventral patterning of somitic derivatives by notochord and floor plate. Proc Natl Acad Sci U S A *90*, 5242-5246.
Presneau, N., Shalaby, A., Ye, H., Pillay, N., Halai, D., Idowu, B., Tirabosco, R., Whitwell, D., Jacques, T.S., Kindblom, L.G.*, et al.* (2011). Role of the transcription factor T (brachyury) in the pathogenesis of sporadic chordoma: a genetic and functional-based study. J Pathol *223*, 327-335.
Reifers, F., Adams, J., Mason, I.J., Schulte-Merker, S., and Brand, M. (2000a). Overlapping and distinct functions provided by fgf17, a new zebrafish member of the Fgf8/17/18 subgroup of Fgfs. Mech Dev *99*, 39-49.
Reifers, F., Walsh, E.C., Leger, S., Stainier, D.Y., and Brand, M. (2000b). Induction and differentiation of the zebrafish heart requires fibroblast growth factor 8 (fgf8/acerebellar). Development *127*, 225-235.
Riva, P., Crosti, F., Orzan, F., Dalpra, L., Mortini, P., Parafioriti, A., Pollo, B., Fuhrman Conti, A.M., Miozzo, M., and Larizza, L. (2003). Mapping of candidate region for chordoma development to 1p36.13 by LOH analysis. Int J Cancer *107*, 493-497.
Rufai, A., Benjamin, M., and Ralphs, J.R. (1995). The development of fibrocartilage in the rat intervertebral disc. Anat Embryol (Berl) *192*, 53-62.
Russell, J.H., and Wang, R. (1993). Autoimmune gld mutation uncouples suicide and cytokine/proliferation pathways in activated, mature T cells. Eur J Immunol *23*, 2379-2382.
Sachdev, S.W., Dietz, U.H., Oshima, Y., Lang, M.R., Knapik, E.W., Hiraki, Y., and Shukunami, C. (2001). Sequence analysis of zebrafish chondromodulin-1 and expression profile in the notochord and chondrogenic regions during cartilage morphogenesis. Mech Dev *105*, 157-162.
Salisbury, J.R. (2001). [Embryology and pathology of the human notochord]. Ann Pathol *21*, 479-488.
Salisbury, J.R., Deverell, M.H., Cookson, M.J., and Whimster, W.F. (1993). Three-dimensional reconstruction of human embryonic notochords: clue to the pathogenesis of chordoma. J Pathol *171*, 59-62.
Saude, L., Woolley, K., Martin, P., Driever, W., and Stemple, D.L. (2000). Axis-inducing activities and cell fates of the zebrafish organizer. Development *127*, 3407-3417.
Scaffidi, C., Fulda, S., Srinivasan, A., Friesen, C., Li, F., Tomaselli, K.J., Debatin, K.M., Krammer, P.H., and Peter, M.E. (1998). Two CD95 (APO-1/Fas) signaling pathways. EMBO J *17*, 1675-1687.
Scaffidi, C., Krammer, P.H., and Peter, M.E. (1999). Isolation and analysis of components of CD95 (APO-1/Fas) death-inducing signaling complex. Methods *17*, 287-291.
Schulte-Merker, S., van Eeden, F.J., Halpern, M.E., Kimmel, C.B., and Nusslein-Volhard, C. (1994). no tail (ntl) is the zebrafish homologue of the mouse T (Brachyury) gene. Development *120*, 1009-1015.
Senju, S., Negishi, I., Motoyama, N., Wang, F., Nakayama, K., Lucas, P.J., Hatakeyama, S., Zhang, Q., Yonehara, S., and Loh, D.Y. (1996). Functional significance of the Fas molecule in naive lymphocytes. Int Immunol *8*, 423-431.
Shalaby, A.A., Presneau, N., Idowu, B.D., Thompson, L., Briggs, T.R., Tirabosco, R., Diss, T.C., and Flanagan, A.M. (2009). Analysis of the fibroblastic growth factor receptor-RAS/RAF/MEK/ERK-ETS2/brachyury signalling pathway in chordomas. Mod Pathol *22*, 996-1005.
Sharma, K., Wang, R.X., Zhang, L.Y., Yin, D.L., Luo, X.Y., Solomon, J.C., Jiang, R.F., Markos, K., Davidson, W., Scott, D.W.*, et al.* (2000). Death the Fas way: regulation and pathophysiology of CD95 and its ligand. Pharmacol Ther *88*, 333-347.
Showell, C., Binder, O., and Conlon, F.L. (2004). T-box genes in early embryogenesis. Dev Dyn *229*, 201-218.
Sibley, K., Rollinson, S., Allan, J.M., Smith, A.G., Law, G.R., Roddam, P.L., Skibola, C.F., Smith, M.T., and Morgan, G.J. (2003). Functional FAS promoter polymorphisms are associated with increased risk of acute myeloid leukemia. Cancer Res *63*, 4327-4330.
Singhal, N., Kotasek, D., and Parnis, F.X. (2009). Response to erlotinib in a patient with treatment refractory chordoma. Anticancer Drugs *20*, 953-955.
Smith, J.C., Price, B.M., Green, J.B., Weigel, D., and Herrmann, B.G. (1991). Expression of a Xenopus homolog of Brachyury (T) is an immediate-early response to mesoderm induction. Cell *67*, 79-87.
Smits, P., and Lefebvre, V. (2003). Sox5 and Sox6 are required for notochord extracellular matrix sheath formation, notochord cell survival and development of the nucleus pulposus of intervertebral discs. Development *130*, 1135-1148.
Solnica-Krezel, L., Stemple, D.L., Mountcastle-Shah, E., Rangini, Z., Neuhauss, S.C., Malicki, J., Schier, A.F., Stainier, D.Y., Zwartkruis, F., Abdelilah, S.*, et al.* (1996). Mutations affecting cell fates and cellular rearrangements during gastrulation in zebrafish. Development *123*, 67-80.

Stacchiotti, S., Marrari, A., Tamborini, E., Palassini, E., Virdis, E., Messina, A., Crippa, F., Morosi, C., Gronchi, A., Pilotti, S., *et al.* (2009). Response to imatinib plus sirolimus in advanced chordoma. Ann Oncol *20*, 1886-1894.
Stacchiotti, S., Tamborini, E., Lo Vullo, S., Bozzi, F., Messina, A., Morosi, C., Casale, A., Crippa, F., Conca, E., Negri, T., *et al.* (2013). Phase II study on lapatinib in advanced EGFR-positive chordoma. Ann Oncol.
Stark, A.M., and Mehdorn, H.M. (2003). Images in clinical medicine. Chondroid clival chordoma. N Engl J Med *349*, e10.
Stemple, D.L. (2005). Structure and function of the notochord: an essential organ for chordate development. Development *132*, 2503-2512.
Stemple, D.L., Solnica-Krezel, L., Zwartkruis, F., Neuhauss, S.C., Schier, A.F., Malicki, J., Stainier, D.Y., Abdelilah, S., Rangini, Z., Mountcastle-Shah, E., *et al.* (1996). Mutations affecting development of the notochord in zebrafish. Development *123*, 117-128.
Szuhai, K., and Hogendoorn, P.C. (2012). 'The chicken or the egg?' dilemma strikes back for the controlling mechanism in chordoma(#). J Pathol *228*, 261-265.
Talbot, W.S., Trevarrow, B., Halpern, M.E., Melby, A.E., Farr, G., Postlethwait, J.H., Jowett, T., Kimmel, C.B., and Kimelman, D. (1995). A homeobox gene essential for zebrafish notochord development. Nature *378*, 150-157.
Theiler, K. (1988). Vertebral malformations. Adv Anat Embryol Cell Biol *112*, 1-99.
Tirabosco, R., Mangham, D.C., Rosenberg, A.E., Vujovic, S., Bousdras, K., Pizzolitto, S., De Maglio, G., den Bakker, M.A., Di Francesco, L., Kalil, R.K., *et al.* (2008). Brachyury expression in extra-axial skeletal and soft tissue chordomas: a marker that distinguishes chordoma from mixed tumor/myoepithelioma/parachordoma in soft tissue. Am J Surg Pathol *32*, 572-580.
Tsukita, S., and Yonemura, S. (1997). ERM (ezrin/radixin/moesin) family: from cytoskeleton to signal transduction. Curr Opin Cell Biol *9*, 70-75.
Urano, A., Suzuki, M.M., Zhang, P., Satoh, N., and Satoh, G. (2003). Expression of muscle-related genes and two MyoD genes during amphioxus notochord development. Evol Dev *5*, 447-458.
van Straaten, H.W., Hekking, J.W., Beursgens, J.P., Terwindt-Rouwenhorst, E., and Drukker, J. (1989). Effect of the notochord on proliferation and differentiation in the neural tube of the chick embryo. Development *107*, 793-803.
Varfolomeev, E.E., and Ashkenazi, A. (2004). Tumor necrosis factor: an apoptosis JuNKie? Cell *116*, 491-497.
Varfolomeev, E.E., Schuchmann, M., Luria, V., Chiannilkulchai, N., Beckmann, J.S., Mett, I.L., Rebrikov, D., Brodianski, V.M., Kemper, O.C., Kollet, O., *et al.* (1998). Targeted disruption of the mouse Caspase 8 gene ablates cell death induction by the TNF receptors, Fas/Apo1, and DR3 and is lethal prenatally. Immunity *9*, 267-276.
Villa-Morales, M., and Fernandez-Piqueras, J. (2012). Targeting the Fas/FasL signaling pathway in cancer therapy. Expert Opin Ther Targets *16*, 85-101.
Vogel, A.M., and Weinstein, B.M. (2000). Studying vascular development in the zebrafish. Trends Cardiovasc Med *10*, 352-360.
Walcott, B.P., Nahed, B.V., Mohyeldin, A., Coumans, J.V., Kahle, K.T., and Ferreira, M.J. (2012). Chordoma: current concepts, management, and future directions. Lancet Oncol *13*, e69-76.
Wang, J., Gao, J., Li, Y., Zhao, X., Gao, W., Peng, L., Yan, D., Liu, L., Li, D., Wei, L., *et al.* (2013). Functional polymorphisms in FAS and FASL contribute to risk of squamous cell carcinoma of the larynx and hypopharynx in a Chinese population. Gene.
Watanabe-Fukunaga, R., Brannan, C.I., Itoh, N., Yonehara, S., Copeland, N.G., Jenkins, N.A., and Nagata, S. (1992). The cDNA structure, expression, and chromosomal assignment of the mouse Fas antigen. J Immunol *148*, 1274-1279.
Weinstein, B.M. (2002). Plumbing the mysteries of vascular development using the zebrafish. Semin Cell Dev Biol *13*, 515-522.
Wold, L.E., and Laws, E.R., Jr. (1983). Cranial chordomas in children and young adults. J Neurosurg *59*, 1043-1047.
Wu, J., Metz, C., Xu, X., Abe, R., Gibson, A.W., Edberg, J.C., Cooke, J., Xie, F., Cooper, G.S., and Kimberly, R.P. (2003). A novel polymorphic CAAT/enhancer-binding protein beta element in the FasL gene promoter alters Fas ligand expression: a candidate background gene in African American systemic lupus erythematosus patients. J Immunol *170*, 132-138.
Wu, Z., Wang, H., Chu, X., Chen, J., and Fang, S. (2013). Association between FAS-1377 G/A polymorphism and susceptibility to gastric cancer: evidence from a meta-analysis. Tumour Biol.
Xiang, N., Li, X.M., Wang, G.S., Tao, J.H., and Li, X.P. (2012). Association of Fas gene polymorphisms with systemic lupus erythematosus: a meta-analysis. Mol Biol Rep *40*, 407-415.
Yamada, T., Pfaff, S.L., Edlund, T., and Jessell, T.M. (1993). Control of cell pattern in the neural tube: motor neuron induction by diffusible factors from notochord and floor plate. Cell *73*, 673-686.
Yamaguchi, T., Iwata, J., Sugihara, S., McCarthy, E.F., Jr., Karita, M., Murakami, H., Kawahara, N., Tsuchiya, H., and Tomita, K. (2008). Distinguishing benign notochordal cell tumors from vertebral chordoma. Skeletal Radiol *37*, 291-299.
Yang, C., Schwab, J.H., Schoenfeld, A.J., Hornicek, F.J., Wood, K.B., Nielsen, G.P., Choy, E., Mankin, H., and Duan, Z. (2009a). A novel target for treatment of chordoma: signal transducers and activators of transcription 3. Mol Cancer Ther *8*, 2597-2605.
Yang, X.R., Ng, D., Alcorta, D.A., Liebsch, N.J., Sheridan, E., Li, S., Goldstein, A.M., Parry, D.M., and Kelley, M.J. (2009b). T (brachyury) gene duplication confers major susceptibility to familial chordoma. Nat Genet *41*, 1176-1178.

Yeh, W.C., Itie, A., Elia, A.J., Ng, M., Shu, H.B., Wakeham, A., Mirtsos, C., Suzuki, N., Bonnard, M., Goeddel, D.V., *et al.* (2000). Requirement for Casper (c-FLIP) in regulation of death receptor-induced apoptosis and embryonic development. Immunity *12*, 633-642.
Yeh, W.C., Pompa, J.L., McCurrach, M.E., Shu, H.B., Elia, A.J., Shahinian, A., Ng, M., Wakeham, A., Khoo, W., Mitchell, K., *et al.* (1998). FADD: essential for embryo development and signaling from some, but not all, inducers of apoptosis. Science *279*, 1954-1958.
Zhao, Q., Eberspaecher, H., Lefebvre, V., and De Crombrugghe, B. (1997). Parallel expression of Sox9 and Col2a1 in cells undergoing chondrogenesis. Dev Dyn *209*, 377-386.
Zhu, Q., Wang, Z., Hu, Y., Li, J., Li, X., Zhou, L., and Huang, Y. (2012). miR-21 promotes migration and invasion by the miR-21-PDCD4-AP-1 feedback loop in human hepatocellular carcinoma. Oncol Rep *27*, 1660-1668.

Manuscripts

Cancer Investigation

Fas/Fasl pathway impairment in skull base chordoma addresses identification of potential pharmacological targets

Journal:	*Cancer Investigation*
Manuscript ID:	LCNV-2013-0113
Manuscript Type:	Original Article
Date Submitted by the Author:	17-Apr-2013
Complete List of Authors:	Ferrari, Luca; Università Degli Studi di Milano, Biotecnologie Mediche e Medicina Traslazionale Calastretti, Angela; Università Degli Studi di Milano, Biotecnologie Mediche e Medicina Traslazionale Boari, Nicola; Università Vita-Salute IRCCS Ospedale San Raffaele, Neurochirurgia Canti, Gianfranco; Università Degli Studi di Milano, Biotecnologie Mediche e Medicina Traslazionale Mortini, Pietro; Università Vita-Salute IRCCS Ospedale San Raffaele, Neurochirurgia Riva, Paola; Università Degli Studi di Milano, Biotecnologie Mediche e Medicina Traslazionale
Keywords:	Cancer Genetics, Chordoma, Fas/Fasl pathway, apoptosis, soluble Fasl

Fas/Fasl pathway impairment in skull base chordoma addresses identification of potential pharmacological targets

Luca Ferrari[1], Angela Calastretti[2], Nicola Boari[3], Gianfranco Canti[2], Pietro Mortini[3] and Paola Riva[1]

[1]Dipartimento di Biotecnologie Mediche e Medicina Traslazionale, Università Degli Studi di Milano, Via Viotti 3/5 20133 Milan, Italy

[2]Dipartimento di Biotecnologie Mediche e Medicina Traslazionale, Università Degli Studi di Milano, Via Vanvitelli 32 20133 Milan, Italy

[3]Dipartimento di Neurochirurgia, Università Vita-Salute IRCCS Ospedale San Raffaele, Via Olgettina 60, 20132 Milan, Italy

KEYWORDS: cancer genetics, chordoma, Fas/Fasl pathway, apoptosis, soluble Fasl

RUNNING TITLE: Fas/Fasl pathway impairment in skull base chordoma

Corresponding author:
Paola Riva
Department of Medical Biotechnology and Translational Medicine
Via Viotti 3/5
20133 Milano, ITALY
tel. +390250315862, fax +390250315864
e-mail: paola.riva@unimi.it

ABSTRACT

Chordoma, originating from notochord remnants, is characterized by chemoresistance. Since the apoptotic Fas/FasI pathway is involved in notochordal cell apoptosis, we investigated its possible role in chordoma. We detected *FASL* expression absence and the presence of both *FAS* anti- and pro-apoptotic isoforms in most tumors analyzed and in U-CH1 cells. These findings, besides the prevalent expression of inactive Caspases 8 and 3, suggest the inactivity of Fas/FasI pathway in chordoma. The enhancement of apoptosis in U-CH1 cells by treatment with soluble FasI indicates that this pathway can be activated in chordoma. The obtained results indicate Fas/FasI as potential pharmacological targets.

INTRODUCTION

Chordoma is a malignant tumor arising from embryonic remnants of the notochord that do not disappear during development of vertebral bodies. This tumor is characterized by local invasiveness and variable tendency for recurrences. Metastases are rare and are more likely to be confined to terminal stages of disease. Chordomas, localizing at skull base (SBC), at sacral or spinal axis level, account for approximately 0.1-0.25% of intracranial tumors and 1-4% of all malignant bone tumors (1, 2). The treatment of choice for these tumors is en-bloc resection followed by postoperative radiation therapy. To date chordoma is considered unresponsive to chemotherapy (3) and no validated molecular markers are available to monitor the tumor progression, nevertheless the occurrence of 1p36 loss of heterozygosity (LOH) has been frequently observed in skull base chordomas (75%) and the absence of LOH has been associated with a mild prognosis, indicating 1p36 LOH as a potential prognostic marker to be validated in a larger casuistry (4, 5).

Chordoma recapitulates the differentiation repertoire of notochordal cells. The maintenance of the notochordal tissue characteristics in chordoma is confirmed also by the expression of the transcription factor *T* (coding for the protein Brachyury) in this tumor. The factor *T*, the founding member of the T-Box family of transcription factors, is required for notochord development, and was recently appointed as the pathognomonic marker for chordoma (6, 7). The evidence of duplication of the 6q27 region, including the *T* gene, indicates the involvement of this transcription factor or of its specific target genes in the tumor onset (8). Moreover, apoptosis seems to be a fundamental process leading to normal notochord development, being required for the formation of the anterior-posterior axis in *Xenopus laevis* embryo (9). The evidence of the involvement of Fas/Fasl pathway in the regression of the notochordal cells during nucleus pulposus (NP) formation in rat (10), pinpoints the pro-apoptotic processes as key mechanisms leading to the shaping of notochord structure. *FAS* and *FASL*, mapping respectively at 10q24.1 and 1q23 regions,

are type I and type II members of the tumour necrosis factor (*TNF*) and receptor superfamily (*TNFR*). The autocrine–paracrine interaction between Fas and FasI results in the trimerization and activation of the Fas receptor, which leads to cell death (11, 12). Besides their role in apoptosis, these factors have also been implicated in survival/proliferation and cell cycle progression showing a tumor suppressor activity (13). Multiple mechanisms regulate the sensitivity of Fas-expressing cells to Fas-induced apoptosis, including alternative splicing of *FAS* pre-mRNA: mRNAs lacking exon 6 encode soluble form of the receptor, which, sequestering FasI, lead to a reduction of Fas signaling, inhibiting apoptosis (14). FasI is an important effector of cell-mediated cytotoxicity against transformed cells. Therefore, resistance to Fas-mediated apoptosis could provide a malignant cell with a selective advantage in its attempt to evade immune surveillance (13). Taking in account the notochordal derivation of chordoma together with the implication of Fas pro-apoptotic pathway in the notochord regression, we hypothesized that Fas/FasI pathway may be affected in chordoma. This study, demonstrating for the first time the alteration of Fas/FasI pathway in SBCs and the possibility of activating apoptosis following administration of soluble *FASL* in a chordoma cell line, contributed to elucidate the role of apoptosis in chordoma tumorigenesis, and addressed the identification of new potential pharmacological targets.

MATERIALS AND METHODS

Patients

The cohort includes fourteen SBC patients described for the first time in this study and seventeen patients previously reported (5), for a total of 31 patients with SBC (Table 1), each of whom underwent surgery at the Department of Neurosurgery of the San Raffaele Scientific Institute in Milan between August 1997 and December 2011. Twenty three patients were male (71.9%), and 6 were female (28.1%); ages ranged from 19 to 71 years

(average 47,7 years; SD = 15.24). Six patients (19%) had been treated previously. The histological specimens were reviewed in each case by the same pathologist for the presence of specific immunohistochemical markers diagnostic of chordoma (S-100, vimentin, EMA, cytokeratine), allowing to classify all the tumors as classic or chondroid chordoma. The genetic study carried out on the surgical specimens didn't impact neither the course of surgical operations nor the decision about post-operative adjuvant therapies. An informed consent, regarding the possibility of doing genetic researches on the surgical specimens were signed by all the patients before operations.

FAS/FASL expression analysis

Total RNA was extracted from frozen samples by using Trizol reagent (Life Technologies, Carlsbad, CA, USA) according to the producer's instructions. Reverse transcription was carried out on 1 µg of total RNA using the iScript™ cDNA Synthesis kit (Bio-Rad Laboratories Inc. Barkeley, CA, USA). The gene specific PCR primers and PCR conditions for *FAS* isoforms were already reported. *FASL* specific primers FW 5'-GGCCTGTGTCTCCTTGTGAT-3' and REV 5'-GCAGGTTGTTGCAAGATTGA-3' were designed on different exons for each amplimer, thus making it possible to distinguish the cDNA-specific band from genomic PCR products (14). The *FASL* PCR conditions were 95°C for 4 min, 1 cycle; 95°C for 30 sec, 54 for 30 sec, and 72°C for 30 sec, 40 cycles.

SNPs analysis

rs1800682 and rs2234767 *FAS* SNPs regions were amplified from constitutional DNA by PCR with the following cycling profile: 4 min initial denaturation at 95°C, 95°C for 4 min, 1

cycle; 95°C for 30 sec, 59 for 35 sec, and 72°C for 30 sec, 32 cycles. Specific primers for rs1800682 FW 5'-TGTTCACCAGAGCACGAAAG-3' REV 5'-AGGAAGGAGTCAGGGTTCGT-3'; specific primers for rs2234767 FW 5'-TCCCTCCTTCCATTCCTTCT-3' REV 5'ACCAAGCTCTGCACCTCACT-3'. rs763110 *FASL* SNP region was amplified by PCR with the following cycling profile: 4 min initial denaturation at 95°C, 95°C for 4 min, 1 cycle; 95°C for 30 sec, 63 for 35 sec, and 72°C for 30 sec, 32 cycles. Specific primers for rs763110 FW 5'-CTGGGCAACATAGCAAGTCC-3' REV 5'-GAGAATGGTCAGTGGGGCTA-3'; PCR products were directly sequenced in both directions using the Big Dye Terminator kit (Applied Biosystem) and resolved on a 3100 ABI Prism Genetic Analyzer (Applied Biosystem, Foster City, CA).

Western blot analysis

The whole proteins extraction was performed on fresh/frozen specimens from the new enrolled patients, which were disaggregated into a SDS-PAGE sample buffer containing protease inhibitors. Protein samples were separated by 12% SDS-PAGE, Western blotted onto nitrocellulose membrane (Whatman protran BA 85, 0.45 µm) (ImmobilonTM-P, Millipore, Billerica, MA, USA). Following a blocking with 5% BSA in Tris-buffered saline, the membranes have been probed with the following antibodies (Ab): diluted 1:1000 p53 (Bp53-12) human anti-mouse monoclonal IgG (Santa Cruz Biotechnology, Santa Cruz, CA, USA); diluted 1:1000 Brachyury (H-210) rabbit polyclonal IgG (Santa Cruz Biotechnology); diluted 1:1000 Fas (C18C12) human anti-rabbit monoclonal IgG (Cell Signaling Technology, Beverly, MA, USA), diluted 1:1000 Fasl rabbit policlonal IgG (Cell Signaling Technology); diluted 1:1000 Caspase 8 (1C12) human anti-mouse monoclonal IgG (Cell Signaling Technology); diluted 1:1000 Caspase 3 (8G10) human anti-rabbit monoclonal IgG (Cell Signaling Technology); diluted 1:2000 αβ Tubulin anti-rabbit policlonal IgG (Cell Signaling Technology), diluted 1:15000 Gapdh anti-goat policlonal IgG

(Novus Biologicals, Littelton, CO, USA) . The incubation with secondary antibodies for 1 h at room temperature have been performed using the following antibodies: diluted 1:2000 ECL-rabbit IgG, HRP (horseradish peroxidise)-linked whole Ab from donkey (Amersham, Piscataway, NJ, USA) or 1:1000 or goat anti-mouse IgG-HRP (Santa Cruz Biotechnology); diluted 1:40000 HRP goat anti-rabbit IgG (Pierce, Rockford, IL, USA) or diluted 1:20000 HRP goat anti-mouse IgG (Sigma-Aldrich).

Cell lines and reagent

Chordoma cell line U-CH1 was obtained from the Chordoma Foundation and it was maintained in IMDM (Invitrogen 12440) / RPMI1640 (Sigma-Aldrich Milan, Italy) four to one ratio (4:1), supplemented with 10% FBS (EuroClone, Milan, Italy) and 100 u/mL penicillin/streptomycin (Sigma-Aldrich) at 37°C and 5% CO_2 (15). The cells were seeded in coated plates or flasks (Collagen Cellware Becton DickinsonSan Jose, CA) and treated with SuperFAS Ligand (soluble Fasl, Enzo Life Science, Farmingdale, NY) at different time.

SuperFAS Ligand was reconstituted with 50 µL sterile water to 0.1 mg/mL and stored at -20° C, according to the manufacturer's instructions.

Treatment with SuperFAS Ligand

U-CH1 cells were seeded 1x 10^5/well in 6-wells coated plate or 4x10^5 in 25 cm^3 coated flasks. After 24 hours they were treated with 30-100 ng/mL SuperFAS Ligand for different times. Cells viability was measured by Trypan blue dye exclusion assay and by Propidium Iodide exclusion assay.

Cell viability assays

Trypan Blue dye exclusion assay. Treated cells were stained with 0.1% trypan blue and counted in a hemocytometer chamber.

Propidium iodide exclusion assay. Cell viability was determined by PI staining exclusion test by flow cytometry. Cytotoxicity was defined as the cellular damage identified by PI staining which evidences the loss of structural integrity of the plasma membrane. Treated cells were washed, resuspended in PBS and stained with the supravital PI (10 µg/ml) for 1 min. Cells were run on a FACSCalibur flow cytometer (Becton Dickinson) and analyzed using CellQuest Pro software (Becton Dikinson). Viable cells were distinguished from dead cells based on their ability to exclude propidium iodide.

Annexin-V Assay

Treated cells U-CH1 were simultaneously stained with Alexa Fluor 488-conjugated Annexin V and Propidium Iodide, used the Vybrant Apoptosis Assay kit #2 (Molecular Probes, USA), according to the manufacturer's instructions and the samples were counted by FACScalibur flow cytometer using CellQuest Pro software (Becton Dickinson) (16).

RESULTS

Fas/FasI pathway is inactivated in SBCs

All the SBC samples included in this study were preliminarily found to express the *T* gene by RT-PCR, while a pull of three NP did not express it, as previously reported (15) (Figure S1(a)). Brachyury expression was investigated by western blot analysis only in a sub-group of twelve tumors because of the paucity of the biological material. All of the twelve samples analyzed expressed brachyury, confirming the RT-PCR results (Figure S1(b)).

The data confirm the previous chordoma diagnosis obtained by immunohistochemistry (data not shown).

Both the involvement of Fas/Fasl apoptotic pathway in notochordal cells regression, together with the histological origin of chordoma, prompted us to investigate the activation status of this pathway in chordoma. At this purpose, we studied *FAS* and *FASL* expression in tumors from a cohort of 31 SBC patients and in the U-CH1 chordoma cell line. We also investigated the downstream Caspase 8 and Caspase 3 activation status. The transcription of both *FAS* and *FASL* was detected by means of RT-PCR in the control tissue from the pull of three NP, in the U-CH1 cell line and in 34 SBC samples, including the recurrence of patient 22 and the first and second recurrences of patient 51. Most of the analyzed samples (82%) showed *FAS* expression, while in 62% of them *FASL* transcript was not detected. Otherwise the U-CH1 cell line expressed both genes, as well as the NP (Figure 1 (a)). These data indicate that *FAS*/*FASL* expression is dysregulated in most SBCs. To investigate the status of activation of Fas/Fasl mediated pathway in chordoma, we then checked for the expression of both the pro-apoptotic and anti-apoptotic *FAS* isoforms by means of RT-PCR, together with the presence of Fas, Fasl and the downstream effectors, Caspase 8 and Caspase 3, by western blot analysis. This latter study was performed in the sub-group of twelve tumors (Figure 1 (b-c)). All the chordoma samples and the U-CH1 cell line showed the expression of both transmembrane and soluble *FAS*, while NP showed exclusively the expression of the pro-apoptotic transmembrane isoform (Figure 1 (b)). After incubation with specific antibodies, we detected the expression of the Fas protein in all the tumor samples and in the U-CH1 cell line, while Fasl was expressed only by the two samples CH23 and CH54 and by the U-CH1 cells, according to the RT-PCR results. We also studied the expression of both the inactive and active forms of Caspase 8. The inactive Caspase 8 (pro Caspase 8) was found to expressed in all the samples analyzed, while the active form (pre Caspase 8), a

cleaved product derived from the Caspase 8 activation, was found to be weakly expressed only in three tumors (Figure 1 (c)). As far as the Caspase 3, the only inactive form was detected in ten samples and in U-CH1, while patients 54 and 71 did not show any Caspase 3 expression (Figure 1 (c)). These findings indicate that Fas/Fasl apoptotic pathway is affected in chordoma.

Frequency distribution of *FAS* and *FASL* functional SNPs in chordoma samples

Recently *FAS* (rs1800682 and rs2234767) and *FASL* (rs763110) functional SNPs have been identified and specific alleles were demonstrated to be associated with *FAS* and *FASL* dysregulation in different tumour (17-20). We established the frequency of each genotype of rs1800682, rs2234767 and rs763110 in the subgroup of chordoma samples that was previously investigated for the activity of Fas/Fasl pathway. We did not find any statistically significant difference in the genotype distribution frequency for the rs1800682 *FAS* SNP (Table 2), in respect to the frequencies reported for the same genotypes in Caucasian populations, taken as controls (20, 21). The rs1800682 *FAS* SNP is situated within the signal transducers and activators of transcription 1 (*STAT1*) binding element, and the G/G genotype reduces the promoter activity. Instead, the genotypes of *FAS* rs2234767 and *FASL* rs763110 show a different frequency distribution in SBC patients in comparison to the control population. Only the G/G *FAS* rs2234767 genotype was found in SBCs analyzed and the frequency of the C/T and C/C *FASL* rs763110 genotypes were respectively higher and lower than in the control. Notably, the rs2234767 *FAS* SNP is located within the stimulatory protein 1 (Sp1) transcription factor binding site of the *FAS* gene, and the A/A genotype, not present in our SBC patients, diminishes the promoter activity. While the *FASL* C/C genotype, located within the binding motif for the transcription factor CAAT/ enhancer binding protein β, is associated with a higher *FASL* expression

then the C/T and T/T genotypes. Nevertheless, the only SBC patient detected with C/C genotype, does not express *FASL* (Table 2).

Soluble Fas ligand induces cell death in the U-CH1 chordoma cell line

Most of the SBCs, as well as the U-CH1 cell line, show the expression of *FAS* pro-apoptotic isoform, but also of the anti-apoptotic one that reduces the apoptotic pathway activity. This evidence let us to hypothesize that the exposure of chordoma cell line to soluble Fasl (SuperFAS Ligand) may strengthen the activation of apoptosis mediated by the transmembrane Fas, competing with the Fas anti-apoptotic soluble isoform. At this purpose, the U-CH1 cells were exposed for 24, 48 and 72 hours to different doses of soluble Fasl. After soluble Fasl treatment, viable cells were counted by using the trypan blue exclusion assay allowing to appreciate a reduction of cell growth (Figure 2 (a)). Precisely, after 24 hours of 30 ng/mL soluble Fasl treatment cell number was reduced over the 60% and after 72 hours UCH1 cells treated with 100 ng/mL showed only a 10% of living cells. In order to confirm these data we measured the cell death index by FACS analysis using propidium Iodide (PI) staining (Figure 2 (b)). Following both treatments, we observed a relevant increase in the number of dead cells. It is worth to be noticed that after the exposure to 100 ng/mL of soluble Fasl, the dead cells number was increased 3 to 4 folds compared to those of the untreated control cells. In order to establish the amount of apoptotic cells in comparison to the necrotic ones, we carried out the Annexin-V assay. Accordingly, the percentage of the apoptotic cells, identified by the positivity for Annexin-V, was dose responsive (Figure 3). Notably, the U-CH1 cells treated with 100ng/mL showed a relevant increase of apoptotic cells: 38%, 48% and 60% at 24, 48 and 72 hours respectively. These results are consistent with the findings obtained following the viability assays and indicate that the exposure to soluble Fasl is able to induce apoptosis in U-CH1 chordoma cell line. To confirm the higher activity of Fas apoptotic mediated pathway

following soluble Fasl treatments, we evaluated the amount of Pro caspase 8 and of Pre Caspase 8 by means of western blot analysis, in U-CH1 treated cell line. The levels of Pre caspase 8 significantly increased together with the significant decrease of Pro caspase 8 levels in a dose and time exposure dependent manner (Figure 4 (a-e)). Moreover, as a matter of fact, the ratio between Pre caspase 8 and Pro caspase 8 increased in a dose and time dependent manner (Figure 4 (b-e)). These results, confirming that the treatment with soluble Fasl drives apoptosis in U-CH1 chordoma cell line, suggest that Fas pathway can be reactivated in this tumor.

DISCUSSION

Chordoma is a tumor characterized by chemoresistance, so that the identification of pharmacological targets represents a challenge for the research in this field, aimed at setting up an effective chemotherapy. We here report the evidence of impairment of Fas/Fasl apoptotic pathway in SBC and of the possibility of inducing apoptosis in U-CH1 chordoma cell line through the exposure to soluble Fasl.

We found that most of the SBCs analyzed do not express *FASL*. *FAS* and *FASL* RNA analysis evidenced a heterogeneous expression of *FASL*, indicating that in most of the samples *FAS* receptor could not be activated by its natural ligand. Differently, the NP, the only tissue of notochordal origin, showed the expression of both genes. Furthermore, all SBC specimens, also those expressing *FASL*, showed the *FAS* anti-apoptotic isoform, not detected in the NP. This evidence led us to speculate that even when Fasl is expressed in SBCs, it poorly interacts with its transmembrane receptor for the presence of the soluble Fas which, acting as competitor, maintains inactivated the Fas/Fasl mediated pro-apoptotic signaling. All these results suggest that Fas/Fasl pathway is impaired in chordoma.

In order to identify mechanisms possibly causing *FAS/FASL* expression deregulation, we genotyped our SBC patients for the presence of specific functional SNPs associated to differential allelic *FAS* and *FASL* expression. The finding of the G/G *FAS* rs2234767 genotype in all chordoma patients, correlated to high *FAS* expression levels, suggests that there would not be constitutional *FAS* expression reduction. Similarly, the C/C *FASL* rs763110 genotype has been associated to higher *FASL* expression level than T/T or T/C genotypes, thus these results did not allow to correlate *FASL* dysregulation in SBC to any of *FASL* rs763110 genotypes. Despite the low number of chordoma analyzed, this evidence let us to hypothesize that these functional SNPs are not directly associated to the observed expression dysregulation of *FAS/FASL* in SBCs, differently from what was previously reported for other type of tumors.

Other mechanisms could play a role in the control of *FAS* and *FASL* expression. We speculated that methylation and/or both post-transcriptional expression modulation by specific miRNAs might affect *FASL* expression regulation. Interestingly, *FASL* is known to be targeted by miR-21, which has been shown to be involved in tumor progression and its up-regulation was correlated with a lower cancer survival rate in different tumors (22-24). miR-21 has been shown to be a biomarker for chemoresistance and clinical outcome following adjuvant therapy (25), and it could be a potential pharmacological target to be evaluated in chordoma. The alternative splicing deregulation of *FAS*, enhancing the expression of anti-apoptotic isoform in chordoma, might be caused by the expression alteration of one or more specific splicing factors such as the RNA-Binding Motif protein 5 (Rbm5) and the Hu protein antigen R (HuR), both known to regulate *FAS* exon 6 alternative splicing. Interestingly, they were both found to be dysregulated in several tumours (26-28).

A further evidence supporting the impairment of Fas/Fasl in chordoma is the prevalence of the inactive form of the downstream effectors Caspase 3 and Caspase 8. Furthermore

Caspase 3, when expressed, did not show any detectable activated peptide form. Knowing that Caspase 3 is the most downstream caspase of the apoptotic cascade and that it can be regulated by means of different apoptotic pathways, these results strongly suggest that apoptosis is generally affected this tumor. Interestingly, genomic losses or unbalances affecting 1q24.1 and 10q23 regions, where *FAS* and *FASL* are located, and 1p36 region, dense in pro-apoptotic genes, have been reported (5, 29, 30).

The implication of apoptosis impairment among the tumorigenic mechanisms leading to chordoma is consistent with its embryogenetic origin from notochord remnants, which did not correctly regress during development. As a matter of fact in *Xenopus laevis* animal model the apoptosis has been demonstrated to be necessary for normal notochord development, morphogenesis, and regression during axis elongation (9), and the Fas/FasI apoptotic pathway was found to be involved in the regression of the notochordal cells in rat model (31). Interestingly, the expression of the *T* gene in the notochord (32), as well as in chordoma cells, prompted us to speculate that this tumor originated from notochordal cells that did not regress because of the impairment of specific mechanisms controlling notochord development/regression. One of them might be the apoptosis involving Fas/FasI pathway (9, 10). In accord to this hypothesis the expression of Brachyury, a chordoma diagnostic marker, indicates that this is a differentiated tumor maintaining not only the cytological, but also the molecular features of notochordal cells (6).

The evidence that the exposure of U-CH1 cells to soluble FasI leads to apoptosis by the activation of Caspase 8 in a dose and time dependent manner, supports the hypothesis that Fas/FasI pathway can be reactivated in chordoma. Thus, the expression of the transmembrane *FAS* in chordoma makes this factor a key molecule through which it is possible to increase apoptosis, addressing the identification of new pharmacological targets. So far, this tumor shows a multidrug resistance to chemotherapy and there are no approved pharmacological protocols for its treatment (33), even if several studies for the

evaluation of the efficacy of different drugs have been reported. For instance, patients harboring SBCs chordomas were found to express Pdgfrb at stromal cells level (34, 35), and chemotherapy with imatinib mesylate (IM), a Pdgfr inhibitor, might represent a therapeutic option in patients with recurrent chordoma not even eligible for surgery or radiotherapy (33). The anti-tumor activity of IM was documented by the detection of a decrease in the size of the tumor and/or tumor stabilization with altered tumor density (35), notwithstanding the complete remission of the mass tumor was never observed. Furthermore the association of IM with other chemotherapeutic agents, such as mTOR inhibitor molecules, showed to be effective in the treatment of IM-resistant chordomas (36). Interestingly, the pharmacological potentiality of Fas receptors, never investigated for chordoma treatments, has been studied in gastrointestinal stromal tumors (GIST). The exposure of a panel of GIST cell lines to the soluble Fasl seems to potentiate the apoptotic effects of IM (37).

The study of mechanisms regulating *FAS* alternative splicing or *FASL* expression might identify further pharmacological targets that should be investigated. The evidence here provided prompted us to propose Fas, and/or related regulatory factors, as potential therapeutic targets and Fasl as a pharmacological molecule to be evaluated for the treatment of this tumor, in particular when it, localizing in skull base, often cannot be completely surgically removed, or when it is resistant to radiotherapy.

This study, providing new insights on mechanisms potentially involved in chordoma tumorigenesis, contributes to address pharmacological studies with a relapse in the development of new strategies for the setting up of a chemotherapeutic treatment.

Acknowledgements: The authors thank Dr. Samantha Milanesi, Dr. Laura Libera and Dr. Giuliana Gatti for their technical contribution, Dr. Filippo Gagliardi for his clinical support

and the Italian Association for Cancer Research, AIRC (Associazione Italiana per la Ricerca sul Cancro) that funded this study (grant number IG 10525 to PR).

Conflicts of Interest: The authors declare that they have no conflicts of interest.

REFERENCES

1. Bydon M, Papadimitriou K, Witham T, Wolinsky JP, Bydon A, Sciubba D, et al. Novel therapeutic targets in chordoma. Expert Opin Ther Targets. 2012 Aug 4.
2. Walcott BP, Nahed BV, Mohyeldin A, Coumans JV, Kahle KT, Ferreira MJ. Chordoma: current concepts, management, and future directions. Lancet Oncol. Feb;13(2):e69-76.
3. York JE, Kaczaraj A, Abi-Said D, Fuller GN, Skibber JM, Janjan NA, et al. Sacral chordoma: 40-year experience at a major cancer center. Neurosurgery. 1999 Jan;44(1):74-9; discussion 9-80.
4. Riva P, Crosti F, Orzan F, Dalpra L, Mortini P, Parafioriti A, et al. Mapping of candidate region for chordoma development to 1p36.13 by LOH analysis. Int J Cancer. 2003 Nov 10;107(3):493-7.
5. Longoni M, Orzan F, Stroppi M, Boari N, Mortini P, Riva P. Evaluation of 1p36 markers and clinical outcome in a skull base chordoma study. Neuro Oncol. 2008 Feb;10(1):52-60.
6. Presneau N, Shalaby A, Ye H, Pillay N, Halai D, Idowu B, et al. Role of the transcription factor T (brachyury) in the pathogenesis of sporadic chordoma: a genetic and functional-based study. J Pathol. 2011 Feb;223(3):327-35.
7. Nelson AC, Pillay N, Henderson S, Presneau N, Tirabosco R, Halai D, et al. An integrated functional genomics approach identifies the regulatory network directed by brachyury (T) in chordoma. J Pathol. 2012 Jul 30.
8. Yang XR, Ng D, Alcorta DA, Liebsch NJ, Sheridan E, Li S, et al. T (brachyury) gene duplication confers major susceptibility to familial chordoma. Nat Genet. 2009 Nov;41(11):1176-8.
9. Malikova MA, Van Stry M, Symes K. Apoptosis regulates notochord development in Xenopus. Dev Biol. 2007 Nov 15;311(2):434-48.
10. Kim KW, Kim YS, Ha KY, Woo YK, Park JB, Park WS, et al. An autocrine or paracrine Fas-mediated counterattack: a potential mechanism for apoptosis of notochordal cells in intact rat nucleus pulposus. Spine (Phila Pa 1976). 2005 Jun 1;30(11):1247-51.
11. Kaufmann T, Strasser A, Jost PJ. Fas death receptor signalling: roles of Bid and XIAP. Cell Death Differ. 2012 Jan;19(1):42-50.
12. Lavrik IN, Krammer PH. Regulation of CD95/Fas signaling at the DISC. Cell Death Differ. 2012 Jan;19(1):36-41.
13. Sharma K, Wang RX, Zhang LY, Yin DL, Luo XY, Solomon JC, et al. Death the Fas way: regulation and pathophysiology of CD95 and its ligand. Pharmacol Ther. 2000 Dec;88(3):333-47.
14. Izquierdo JM, Valcarcel J. Fas-activated serine/threonine kinase (FAST K) synergizes with TIA-1/TIAR proteins to regulate Fas alternative splicing. J Biol Chem. 2007 Jan 19;282(3):1539-43.
15. Bruderlein S, Sommer JB, Meltzer PS, Li S, Osada T, Ng D, et al. Molecular characterization of putative chordoma cell lines. Sarcoma.2010:630129.
16. van Engeland M, Nieland LJ, Ramaekers FC, Schutte B, Reutelingsperger CP. Annexin V-affinity assay: a review on an apoptosis detection system based on phosphatidylserine exposure. Cytometry. 1998 Jan 1;31(1):1-9.

17. Li Y, Hao YL, Kang S, Zhou RM, Wang N, Qi BL. Genetic polymorphisms in the Fas and FasL genes are associated with epithelial ovarian cancer risk and clinical outcomes. Gynecol Oncol. 2013 Mar;128(3):584-9.
18. Liu F, Bardhan K, Yang D, Thangaraju M, Ganapathy V, Waller JL, et al. NF-kappaB directly regulates Fas transcription to modulate Fas-mediated apoptosis and tumor suppression. J Biol Chem. 2012 Jul 20;287(30):25530-40.
19. Park JY, Lee WK, Jung DK, Choi JE, Park TI, Lee EB, et al. Polymorphisms in the FAS and FASL genes and survival of early stage non-small cell lung cancer. Clin Cancer Res. 2009 Mar 1;15(5):1794-800.
20. Hashemi M, Fazaeli A, Ghavami S, Eskandari-Nasab E, Arbabi F, Mashhadi MA, et al. Functional polymorphisms of FAS and FASL gene and risk of breast cancer - pilot study of 134 cases. PLoS One.8(1):e53075.
21. Girnita DM, Webber SA, Ferrell R, Burckart GJ, Brooks MM, McDade KK, et al. Disparate distribution of 16 candidate single nucleotide polymorphisms among racial and ethnic groups of pediatric heart transplant patients. Transplantation. 2006 Dec 27;82(12):1774-80.
22. Kilic T, Topkaya SN, Ozkan Ariksoysal D, Ozsoz M, Ballar P, Erac Y, et al. Electrochemical based detection of microRNA, mir21 in breast cancer cells. Biosens Bioelectron. Oct-Dec;38(1):195-201.
23. Pinto R, Pilato B, Ottini L, Lambo R, Simone G, Paradiso A, et al. Different methylation and microRNA expression pattern in male and female familial breast cancer. J Cell Physiol. 2012 Jun;228(6):1264-9.
24. Zhu M, Wang N, Tsao SW, Yuen MF, Feng Y, Wan TS, et al. Up-regulation of microRNAs, miR21 and miR23a in human liver cancer cells treated with Coptidis rhizoma aqueous extract. Exp Ther Med. Jan;2(1):27-32.
25. Frezzetti D, De Menna M, Zoppoli P, Guerra C, Ferraro A, Bello AM, et al. Upregulation of miR-21 by Ras in vivo and its role in tumor growth. Oncogene. Jan 20;30(3):275-86.
26. Bonnal S, Martinez C, Forch P, Bachi A, Wilm M, Valcarcel J. RBM5/Luca-15/H37 regulates Fas alternative splice site pairing after exon definition. Mol Cell. 2008 Oct 10;32(1):81-95.
27. Izquierdo JM. Cell-specific regulation of Fas exon 6 splicing mediated by Hu antigen R. Biochem Biophys Res Commun. 2011 Nov 12;402(2):324-8.
28. Izquierdo JM. Hu antigen R (HuR) functions as an alternative pre-mRNA splicing regulator of Fas apoptosis-promoting receptor on exon definition. J Biol Chem. 2008 Jul 4;283(27):19077-84.
29. Dalpra L, Malgara R, Miozzo M, Riva P, Volonte M, Larizza L, et al. First cytogenetic study of a recurrent familial chordoma of the clivus. Int J Cancer. 1999 Mar 31;81(1):24-30.
30. Larizza L, Mortini P, Riva P. Update on the cytogenetics and molecular genetics of chordoma. Hered Cancer Clin Pract. 2005;3(1):29-41.
31. Salisbury JR. [Embryology and pathology of the human notochord]. Ann Pathol. 2001 Dec;21(6):479-88.
32. Evans AL, Faial T, Gilchrist MJ, Down T, Vallier L, Pedersen RA, et al. Genomic targets of Brachyury (T) in differentiating mouse embryonic stem cells. PLoS One. 2012;7(3):e33346.
33. Gagliardi F, Boari N, Riva P, Mortini P. Current therapeutic options and novel molecular markers in skull base chordomas. Neurosurg Rev. 2012 Jan;35(1):1-13; discussion -4.
34. Orzan F, Terreni MR, Longoni M, Boari N, Mortini P, Doglioni C, et al. Expression study of the target receptor tyrosine kinase of Imatinib mesylate in skull base chordomas. Oncol Rep. 2007 Jul;18(1):249-52.
35. Casali PG, Messina A, Stacchiotti S, Tamborini E, Crippa F, Gronchi A, et al. Imatinib mesylate in chordoma. Cancer. 2004 Nov 1;101(9):2086-97.
36. Stacchiotti S, Marrari A, Tamborini E, Palassini E, Virdis E, Messina A, et al. Response to imatinib plus sirolimus in advanced chordoma. Ann Oncol. 2009 Nov;20(11):1886-94.

37. Rikhof B, van der Graaf WT, Meijer C, Le PT, Meersma GJ, de Jong S, et al. Abundant Fas expression by gastrointestinal stromal tumours may serve as a therapeutic target for MegaFasL. Br J Cancer. 2008 Nov 18;99(10):1600-6.

Casuistry of patients

Patient	Sex	Age	Histology	Recurrence*	Death*	Description
12	M	67	chondroid	-	-	Riva et al. 2003
13	M	55	classic	-	-	Riva et al. 2003
20	M	55	classic	41	47	Riva et al. 2003
21	M	46	classic	-	-	Riva et al. 2003
22	M	40	classic	22	30	Riva et al. 2003
23	M	56	-	-	-	Riva et al. 2003
24	F	29	chondroid	-	-	Riva et al. 2003
25	M	27	chondroid	24	53	Riva et al. 2003
26	M	52	classic	-	-	Longoni et al. 2008
28	F	69	-	-	-	Longoni et al. 2008
35	F	25	classic	-	-	Longoni et al. 2008
37	F	41	classic	-	-	Longoni et al. 2008
38	M	31	classic	-	-	Longoni et al. 2008
39	F	32	chondroid	-	-	Longoni et al. 2008
40	F	30	chondroid	16	-	Longoni et al. 2008
45	M	52	chondroid	5	7	Longoni et al. 2008
47	M	66	-	-	-	This work
49	M	46	classic	-	-	Longoni et al. 2008
51	M	55	classic	36	-	This work
53	M	47	chondroid	-	-	This work
54	M	nd	-	-	-	This work
59	F	69	chondroid	-	-	This work
60	F	61	classica	-	0	This work
61	M	65	classica	-	-	This work
62	M	71	classic	-	-	This work
64	M	46	classic	-	-	This work
65	M	49	classic	-	-	This work
66	M	45	-	-	-	This work
68	M	20	-	-	-	This work
69	M	62	-	-	-	This work
71	M	19	classic	-	-	This work

Abbreviations: M, male; F, female; * months afetr surgery

Genotype distribution of *FAS* and *FASL* functional SNPs in 10 SBC patients

	genotypes				*FAS/FASL* expr. for each genotype	
			patients %	controls %	*FAS* %	*FASL* %
FAS	rs1800682	A/A	30	42	3/3	-
		A/G	70	51	7/7	-
		G/G	0	7	-	-
	rs2234767	A/A	0	7	-	-
		A/G	0	76	-	-
		G/G	100	17	10/10	-
FASL	rs763110	C/C	10	41	-	0/1
		C/T	80	42	-	1/8
		T/T	10	17	-	0/1

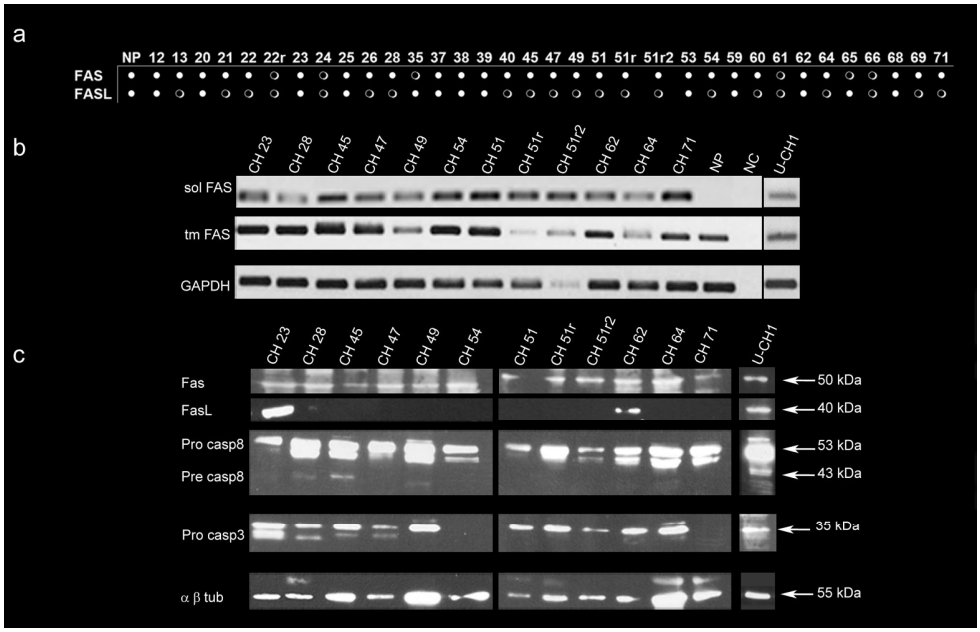

Figure 1: FAS,FASL and downstream Caspase 8 and Caspase 3 expression in SBCs. a) RT-PCR results of FAS and FASL in 34 SBCs, in the U-CH1 cell line and in nucleus pulposus (NP), black dots indicate gene expression; white dots indicate no gene expression; b) RT-PCR of anti-apoptotic soluble FAS (sol FAS) and proapototic transmembrane F AS (tm FAS) in 12 SBCs samples, in U-CH1 cell line and in nucleus pulposus (NP), NC indicates the RT-PCR negative control; c) western blots of Fas, Fasl, Pro caspase 8 (Pro casp8) and Pre caspase 8 (Pre casp8), Pro caspase 3 (Pro casp3) in 12 SBCs and in the U-CH1 cell line, the αβ tubulin (αβ tub) was included as a housekeeping protein expression.
169x108mm (300 x 300 DPI)

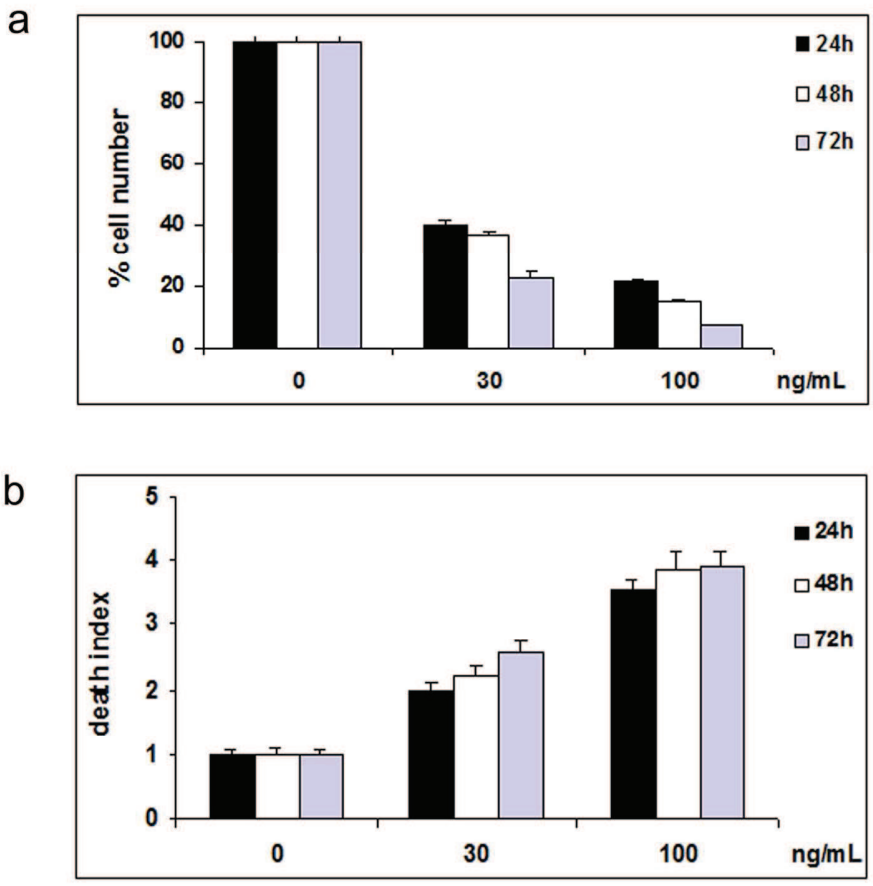

Figure 2: Evaluation of effects of Soluble FasI treatments on U-CH1 chordoma cell line by viability and PI assays. U-CH1 cells were treated with 30-100 ng/mL soluble FasI for 24, 48 and 72 hours. Cell viability was evaluated under the microscope by trypan blue dye exclusion assay (a) or analyzed by flow cytometry with Propidium Iodide staining (b). Data are means ± SE of 3 experiments in triplicate.
139x138mm (300 x 300 DPI)

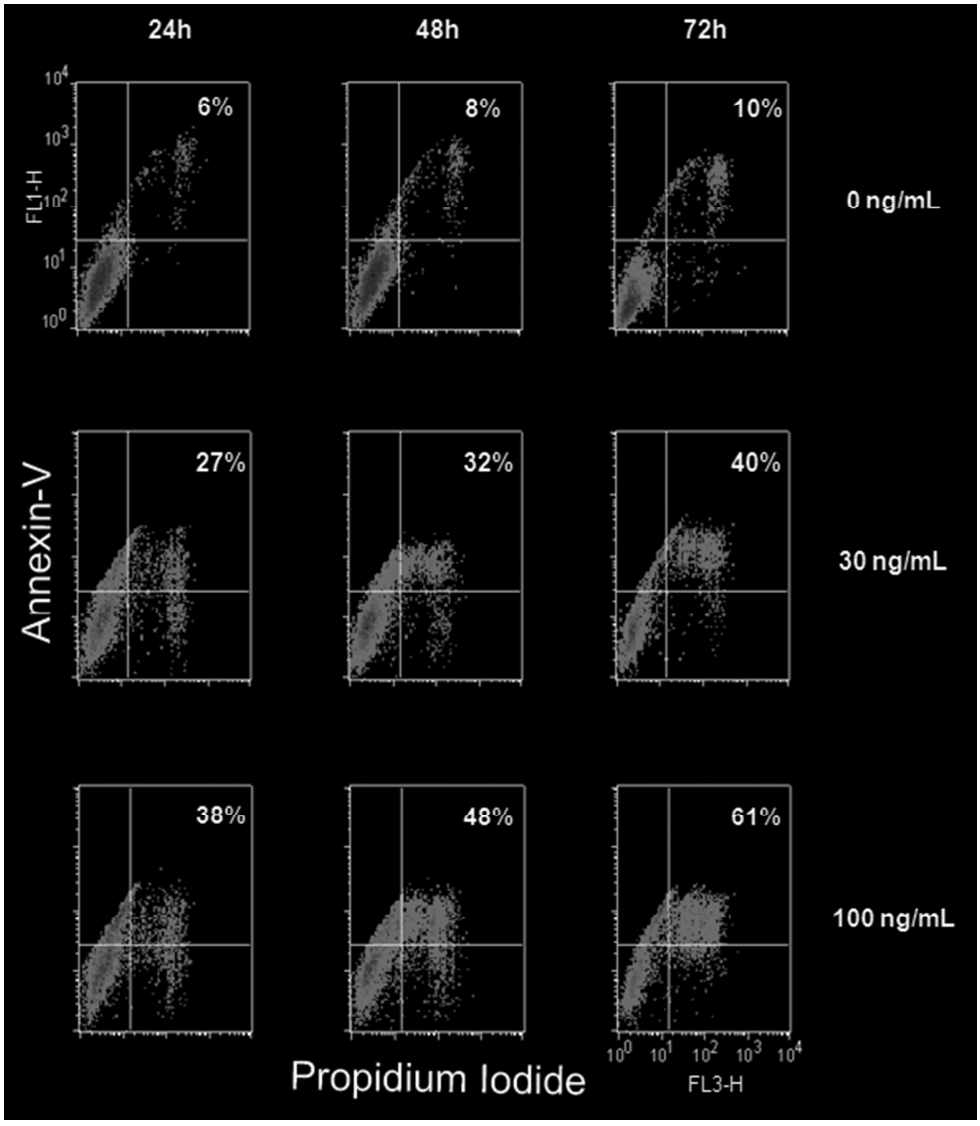

Figure 3: Apoptotic cells determination. UCH1 cells, treated with 30-100 ng/mL FASL for 24, 48 and 72 hours, were simultaneously stained with Alexa Fluor 488-Annexin V and Propidium Iodide and analyzed by flow cytometry to determine the early and late apoptotic fraction (Annexin-V+/PI- and Annexin-V+/PI+). The percentages of Annexin-V-positive cells are indicated in the pictograms. Data are representative of three independent experiments.
52x59mm (300 x 300 DPI)

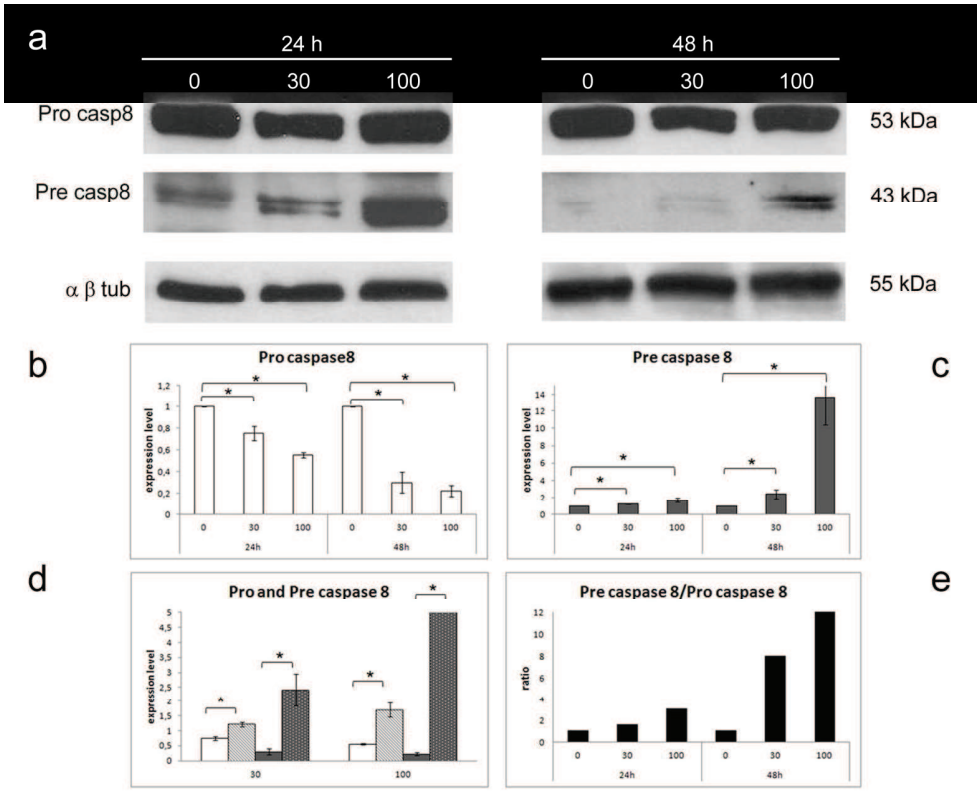

Figure 4: Caspase 8 activation following soluble Fasl treatment. U-CH1 cell line were treated with soluble Fasl at the doses of 0 ng/mL (untreated control), 30 and 100 ng/mL for 24 and 48 hours, left and right western blot panels respectively. a) Representative Western blot analysis of Pro caspase 8 (Pro casp8), Pre caspase 8 (Pre casp 8) and αβ tubulin (αβ tub); b) Quantification of relative Pro casp 8 expression levels after normalization to a/b tub, the white bars represent expression level of Pro casp 8; c) Quantification of relative Pre casp 8 expression levels after normalization to a/b tub, gray bars indicate the level of Pre casp 8; d) Representation of the quantification of relative Pro casp 8 and of Pre casp 8 expression levels after normalization to a/b tub divided for each concentration, white bars indicate Pro casp 8 in U-CH1 cells treated with soluble Fasl for 24hours, white-dithered bars indicate Pre casp 8 treated with soluble Fasl for 24 hours, gray bars indicate Pro casp 8 of soluble Fasl for 48 hours, gray-dithered bars indicate Pre casp 8 treated with soluble Fasl for 48 hours; e) Ratios between Pre casp 8 and Pro casp 8 after treatments, the black bars represent the ratio for each treatment concentration at each time of exposure; b-d) The data are expressed as fold increase over the untreated control (0 ng/mL); *p<0,05.
156x127mm (300 x 300 DPI)

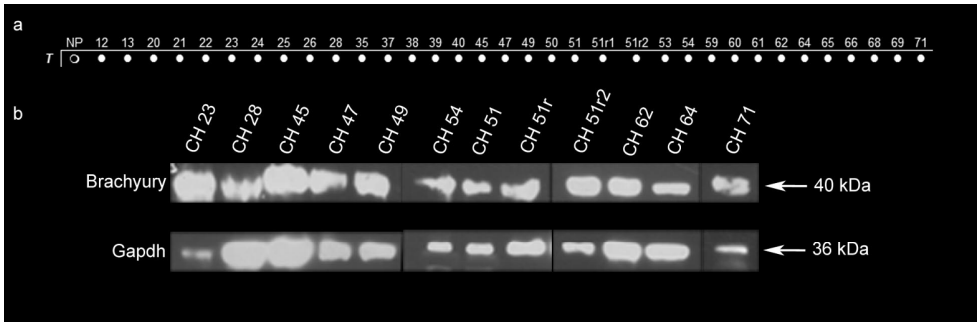

Figure S1: T/Brachyury expression in SBCs. a) RT-PCR results of T gene expression in 34 SBCs, and in nucleus pulposus (NP), black dots indicate gene expression; white dots indicate no gene expression; b) western blots of Brachyury in 12 SBCs, the Gapdh was included as a housekeeping protein expression.
163x53mm (300 x 300 DPI)

fas/fasl downregulation impairs zebrafish notochord formation affecting the expression of specific chordoma markers

Luca Ferrari[1,*], Anna Pistocchi[1, 2,*], Laura Libera[1], Franco Cotelli[2,#] and Paola Riva[1,#]

[1]Dipartimento di Biotecnologie Mediche e Medicina Traslazionale, Università Degli Studi di Milano, Via Viotti, 3/5 20133 Milan, Italy

[2]Dipartimento di Bioscienze, Università Degli Studi di Milano, Via Celoria, 26 20133 Milan, Italy

[*,#] these authors contributed equally to this paper.

KEYWORDS: zebrafish, notochord, *fas/fasl*, chordoma

RUNNING TITLE: critical role for *fas/fasl* in zebrafish notochord formation

Corresponding author:

Paola Riva

Department of Medical Biotechnology and Translational Medicine

Via Viotti 3/5

20133 Milano, ITALY

tel. +390250315862, fax +390250315864

e-mail: paola.riva@unimi.it

Abstract

The chordoma is a malignant tumor characterized by chemoresistance and unforeseeable prognosis. This tumor originates from notochord remnants that do not disappear during development of vertebral bodies. The apoptotic mechanisms are fundamental for notochord cells development and regression. accordingly the Fas/Fasl pathway was found to be involved in specific notochordal cells' regression steps. Interestingly *FAS/FASL* expression is dysregulated in chordoma and the pathway was found to be inactivated. We thus hypothesized that Fas/Fasl pathway dysregulation may have a role in chordoma onset. To unravel this issue we investigated the function of *fas* and *fasl* homologs in the zebrafish notochord development. We found that these genes were evolutionary conserved from fish to mammals and were specifically expressed in notochord cells. Morpholino mediated knock-down of *fas* and *fasl* resulted in abnormal phenotypes mainly showing curved tail and altered motility. Notochord multi-cell-layer jumps instead of the typical "stack-of-coins" organization, larger vacuolated cells, defects in the peri-notochordal sheath structure and in vertebral mineralization have been detected in most morphants. In addition, we observed the persistent expression of *ntla* and *col2a1a*, the zebrafish homologs of the human *T* gene and *COL2A1*, which were found to be specifically upregulated in chordoma. These data demonstrate the role of *fas* and *fasl* in notochord development, differentiation and regression in zebrafish suggesting the implication of this pathway in chordoma onset.

Introduction

Chordoma is a rare slow-growing malignant bone tumour arising from embryonic remnants of the notochord that do not disappear during development of vertebral bodies. This tumour is characterized by local invasiveness and variable tendency for recurrences. Metastases are rare and are more likely to be confined to terminal stages of disease. Chordomas can localize at skull base, sacral or spinal axis level, and account for approximately 0.1%– 0.25% of intracranial tumors and 1% - 4% of all malignant bone tumors (1, 2). The treatment of choice for these tumors is en-bloc

resection followed by postoperative radiation therapy (3). To date chordoma is considered unresponsive to chemotherapy and no validated molecular markers are available to monitor the tumor progression (3).

The maintenance of the notochordal tissue characteristics in chordoma is confirmed by microscopic features, the localization of the tumor along the axial skeleton, and the expression of similar transcription factors. Among them, the most significant is the transcription factor *T* (encoding for Brachyury), the founder member of the T-box family involved in notochord development (4-6) and recently identified as the pathognomonic marker for chordoma. Brachyury is predicted to be a master regulator of an elaborate oncogenic transcriptional network encompassing diverse signalling pathways including components of the cell cycle and extracellular matrix components. The evidence of duplication of the 6q27 region, including the *T* gene, indicates the involvement of this transcription factor or its specific target genes in the tumor onset. At a functional level, the silencing of Brachyury induced growth arrest in a chordoma cell line (7, 8), while its overexpression, observed in the human pancreatic cell line PANC-1 which does not express it, resulted in enhanced proliferation, motility and invasiveness (9). In a recent characterization of chordoma tumors and cell lines, other genes were found differentially expressed; among them the α1 collagen type II (*COL2A1*) was significantly overexpressed (10).

The proper balance between notochordal cell proliferation and apoptosis seems to be fundamental for the development and regression of the notochord. The apoptotic process is involved in normal notochord development in *Xenopus laevis* (11), and in particular the extrinsic apoptotic pathway is necessary for notochord development in zebrafish (12). In addition the expression of tumor necrosis factors (TNFs) *FAS* and its ligand *FASL*, activating the extrinsic apoptosis, leads to the notochordal cells regression in the adult rat intervertebral disks (13, 14).

Our recent findings demonstrated that *FAS* and *FASL* expression is dysregulated in skull base chordoma and in the U-CH1 chordoma cell line mainly for the coexpression of the anti-apoptotic

and pro-apoptotic FAS isoforms and the lack of *FASL* transcript that leads to apoptosis impairment (Ferrari et al., 2013 under revision).

In view of the chordoma arise from notochordal remnants that could remain following misleading apoptotic events, we sought to turn to the zebrafish (*Danio rerio*) model to study the functional role of *fas* and *fasl* in the notochord development, differentiation and regression.

The zebrafish notochord starts to form during gastrulation (15) when the antecedent of the notochord, the chordamesoderm, expresses *brachyury* (*ntl)* (16) sonic-hedgehog *shh*, and later *α1-collagen Type II* (*col2a1*) (17). During the segmentation period of development, central cells of the notochord differentiate and acquire a large vacuole and the notochord becomes surrounded by a sheath of tissue, which in combination with the turgor pressure, generated by the vacuolated cells, imparts to the notochord its stiffness (18). The differentiation correlates to apoptotic events that in the zebrafish notochord and peri-notochoral sheath happen between 14 and 24 hours post fertilization (hpf) of development (19). As notochord cells become vacuolated, the expression of *ntl*, *shh* and *col2a1* are each extinguished in the notochord (16) while expression of *shh* is maintained in the floor plate and *col2a1* in the floor plate and the hypochord (17, 20).

Members of the extrinsic apoptotic pathway have been identified in teleosts and they closely resemble their mammalian counterpart (21): studies with the Apo2 ligand/tumor necrosis factor related apoptosis-inducing ligand (*Apo2L/TRAIL*) homologs demonstrated that they induced apoptosis in erythroblasts and notochord cells and *fas* and *fasl* homologs have been identified on chromosome 17 and 20 respectively with conserved synteny between fish and mammals (12). In the present study, we found that *fas*/*fasl* are expressed in notochord cells and are required for notochord differentiation and regression. Indeed, simultaneous knock-down of *fas* and *fasl* resulted in notochord multi-cell-layer jumps instead of the typical “stack-of-coins” organization, larger vacuolated cells, defects in the peri-notochordal sheath structure and in vertebral mineralization. Interestingly, we also observed the maintenance of the oxpression of *ntla* and *col2a1a*, the zebrafish

homologs of the human *T* gene and *COL2A1*, which were found to be specifically upregulated in chordoma (10). This data suggest the implication of *fas/fasl* pathway in chordoma tumorigenesis.

Material and methods

Animals

Breeding wild type fish of the AB strain were maintained at 28°C on a 14 h light/10 h dark cycle. Embryos were collected by natural spawning, staged according to Kimmel and colleagues (15) and raised at 28°C in fish water (Instant Ocean, 0,1% Methylene Blue) in Petri dishes, according to established techniques, approved by the veterinarian (OVSAC) and the animal use committee (IACUC) at the University of Oregon, in agreement with local and national sanitary regulations. We express the embryonic ages in somites (s), hours post fertilization (hpf) and days post fertilization (dpf).

The *twhh-GFP* construct was kindly provided by J. Du (22) and injected at a concentration of 200 pg/embryo.

The following line were used: AB obtained from the Wilson lab, University College London, London, United Kingdom, the ET30:Et(kita:GalTA4,UAS:mCherry)hzm line was kindly provided by R. W. Koster and M. Mione (23, 24), IFOM, Milan Italy, and Tg(*flk1*:EGFP) obtained from the Lawson lab, University of Massachusetts Medical School, Boston, USA.

In situ hybridization, histological analysis and immunohistochemistry Whole mount *in situ* hybridization (WISH) experiments, were carried out as described by Thisse and colleagues (25). Antisense riboprobes were previously *in vitro* labelled with modified nucleotides (*i.e.* digoxigenin, fluorescein, Roche).

For histological sections, stained embryos/larvae were re-fixed in 4% PFA, dehydrated and stored in methanol, wax embedded and sectioned (5-8 μm). *col2a1a* probe has been kindly provided by Topczewski laboratory and *ntla* probe was cloned already reported (26).

RT-PCR

Total RNA from 17 samples (an average of 30 embryos/larvae per sample) was extracted with the TOTALLY RNA isolation kit (Ambion, Life Technologies, Paisley UK), treated with RQ1 RNase-Free DNase (Promega, Madison, WI) and oligo(dT)-reverse transcribed using SuperScript II RT (Life Technologies), according to manufacturers' instructions. Following primers have been used:

fas sense 5'-GTGACGCTAATGCAAAAATGAAG-3'

fas antisense 5'-CGATGTCCTGCAGAGTGGTG-3'

fasl sense 5'-CACTCGTCCCAACCAGTGGTTC-3'

fasl antisense 5'-AAGCTGGCAGATTGCATTG-3'

beta-actin sense 5'-TGTTTTCCCCTCCATTGTTGG-3';

beta-actin antisense 5'-TTCTCCTTGATGTCACGGAC-3';

Quantitative real time RT-PCR

Reverse transcriptions (RTs) were performed using 2 µg of DNase treated (DNA-*free*™, Ambion) total RNA in presence of random hexamers (Life Technologies) and SuperScript II reverse transcriptase (Life Technologies). Real-time PCRs were carried out in a total volume of 15 µl containing 1X iQ SYBR Green Super Mix (BioRad, Barckley, CA), using 1 µl of the RT reaction. PCRs were performed using the BioRad iCycler iQ Real Time Detection System (BioRad). For normalization purposes, *ef1-alpha* RNA level was tested in parallel with the gene of interest. The following primers were used:

*ntla*_sense 5'-CCTCGGGTTCGTACTGTGAG-3'

*ntla*_antisense 5'-TCCGGAAGAGTTGTCCATGT-3'

*col2a1a*_sense 5'-ATCCCATCATTTCACCTGGA-3'

*col2a1a*_antisense 5'-TCTGTCCCTTTGCACCAAGT-3'

*ef1alpha*_sense 5'-GGTACTTCTCAGGCTGACTGT-3';

*ef1alpha*_antisense 5'-CAGACTTGACCTCAGTGGTTA-3'.

Injections Injections were carried out on 1- to 2-cell stage embryos; the dye tracer rhodamine dextran was also co-injected. To repress *fasl* and *fas* mRNA translation, an ATG-targeting morpholino (*fas*-MO, *fasl*-MO) and a splice-MO were synthesized (splice-*fas*-MO, splice-*fasl*-MO) (Gene Tools LLC, Philomath, OR):

fas i1e2 5'-TCCTGTAATACACAAACACATGCAG-3'

fasl e1i1 5'-TACATTCTGTAGGTCTTACCTGTGT-3'

fas ATG 5'-TCGAGGAGGTCACCCGAATTAGA-3'

fasl ATG 5'-GGCCGAAGTTAGCACTCATGTTTGC-3'

and used at the concentration of 0,5 pmol/embryo in 1x Danieau buffer (pH 7,6) as previously reported (27). As control we injected a standard control morpholino oligonucleotide (ctrl-MO). The *in-vivo* test of the specificity was carried out as described in Brusegan and colleagues (28). In brief: 200 pg/embryo of the pCS2+-*fasl*-MO-EGFP sensor plasmid have been injected alone or co-injected with 0,5 pmol/embryo of *fasl*-MO. The presence/absence of the GFP signal has been monitored under a fluorescent microscope from 24 to 48 hpf. *fasl*-MO cDNA fragments inserted in the *BamHI* site were obtained using the following complementary oligos:

sense 5'-gatcGATCGCAAAACATGAGTGCTAACTTCGGCC-3';

antisense 5'-gatcGGCCGAAGTTAGCACTCATGTTTGC-3';

Same results were obtained with the pCS2+-*fas*-MO-EGFP. *fas*-MO cDNA fragments inserted in the *BamHI* site were obtained using the following complementary oligos:

sense 5'-gatcTCTAATTCGGGTGACCTCCTCGA- 3'

antisense 5'-gatcTCGAGGAGGTCACCCGAAT-3'

For the specificity of phenotype, 0,7 pmol of *fasl*-MO was injected together with 200 pg/embryo of endogenous *fasl* full length mRNA. Synthetic capped *fasl* mRNA was obtained using the following primers:

*fasl*_sense 5'-TTTGAATTCCGCCACCATGAGTGCTAACTT-3';

*fasl*_antisense 5'-TTTGCTCTAGAGATCAGTGGATCTTAAAGA-3';

cloned into the PCS2+-expression-vector and transcribed with the mMessage kit (Ambion).

To validate splice-site-MO (splice-*fas*-MO and splice-*fasl*-MO) and verify intron retention or exon skipping respectively, following primers were used:

*fas exon 1*_sense 5'-ATGCCCACTTTGACTTATAGC-3';

*fas exon 7*_antisense 5'-GATGAAGCCTCGACAATGTTC-3';

*fasl exon 1*_sense 5'-ATGAGTGCTAACTTCGGCCAC-3';

fas exon 4 reverse 5'-AAGCTGGCAGATTGCATTG-3'.

Sorting

50-100 *twhh*-GFP transgenic embryos at 24 and 48 hpf were incubated in trypsin solution (0.5% trypsin and 1mM EDTA) for 2 h with gentle pipetting to dissociate the cells. Cells were resuspended in PBS (Gibco, Life Technologies)-20% fetal calf serum (FCS; Euroclone, Milan, Italy)-20 mM HEPES and 2 mM EDTA and filtered through 40-µm cell strainers (Euroclone) before sorting using a Vantage Sorter SE (Becton-Dickinson, San Jose, CA) at a flow rate of 3000 cells per second. GFP was exited at 488 nm using an argon laser. Cells dissociated from wild-type embryos were used to set the gating to exclude green autofluorescence. After sorting, the *GFP*+ cells were collected and RNA was extracted with the micro-RNAeasy kit (Qiagenm, Venlo, Netherlands). RNA was directly retro-transcribed with the iSCRIPTtm cDNA synthesis kit (Biorad) and the obtained cDNA was used for RT-PCR reactions.

Confocal images

Live ET30 transgenic fish were anesthetized in a 0,5% tricaine solution in fish water, then mounted in a 1% low melt agarose. Embryos were imaged on a Leica TCS NT confocal microscope.

Calcein staining

Calcein (Sigma-Aldrich, Italy) staining was done according to Du and colleagues (22, 29).

Results

Zebrafish fas and fasl are expressed in notochordal cells

The zebrafish orthologs of human *FAS* and *FASL* were identified in previous works (12, 21); they are present in a single copy in the genome and they conserve the architecture of the functional domains (12).

We performed RT-PCR analyses of *fas* and *fasl* in the developing embryo, larva and in adult tissues (Fig. 1A). Interestingly, while *fas* is expressed in all the analyzed developmental stages, *fasl* expression is modulated during development. In fact, as shown in figure 1A, *fasl* presented a maternal expression while the zygotic expression started from 24 hpf. To specifically analyze the expression of *fas* and *fasl* in the notochord, we took advantage from the microinjection of the GFP-construct twhh:GFP-pCS2+, in which the *twhh* promoter directs the GFP expression in notochord cells (29). We then FACS-sorted GFP positive cells from embryos at 24 and 48 hpf and analyzed *fas* and *fasl* expression by RT-PCR. As shown in figure 1B, *fas* is detected in the notochord cells at both 24 and 48 hpf while *fasl* only at 48 hpf. Studies previously reported, *fas* and *fasl* expression were not seen by whole-mount *in situ* hybridization (WISH) during the first stages of development (12).

fas and fasl loss-of-function phenotypes

To investigate the function of *fas* and *fasl* in zebrafish development, we employed the knock-down strategy using oligonucleotide-antisense morpholinos targeting the ATG start codon (*fas*-MO and *fasl*-MO respectively). Both morpholinos were injected at a concentration of 0,7 pmol/embryo or co-injected (*fas/fasl*-MO) at a concentration of 0,5 pmol/embryo each. The knock-down embryos were compared to embryos injected with the same amount of a non-specific control MO (ctrl-MO) at the same developmental stage.

The embryos injected with the *fas*-MO showed a phenotype from 24 hpf while embryos injected with the *fasl*-MO showed no overt phenotype prior to 48 hpf, consistently with the temporal expression of zygotic *fasl* mRNA from 48 hpf (Fig.2A). Moreover, embryos co-injected with *fas*/*fasl*-MO at a dosage that did not individually cause morphological defects (0,5 pmol/embryo of *fas*-MO and 0,5 pmol/embryo of *fasl*-MO) presented the same phenotypical defects of the single *fas*- or *fasl*-MO injection. Therefore, for all the following results, we decided to show the double knock-down. The *fas/fasl*-loss of function phenotype was charactherized by bent notochord, curved tail and cephalic and cardiac edema (Fig. 2 B-D') and was worsening during later stages of development. In addition, from 3 dpf, the most evident defect in *fas*/*fasl*-MO injected embryos was a high reduction in motility. The ctrl-MO injected larvae escaped in the opposite direction when stimulated (100% N=50, Movie 1), *fas*/f*asl*-MO injected larvae were characterized by an altered motility, swimming in circle (80% N=80, Movie 2). As explained above, the single or concurrent injection of *fas* and *fasl* morpholinos gave rise to the same phenotype. Following the injection of *fasl* mRNA and, we were able to rescue the phenotype, confirming the specificity of the downregulation (80% N=65 Movie 3). Moreover, we designed splice-site morpholinos (splice-*fas*-MO and splice-*fasl*-MO) that presented consistent phenotypes with the ATG morpholinos, confirming the specificity of the loss-of-function.

We tested the *in-vivo* efficiency of the ATG morpholinos, sensor plasmids containing the sequence targeted by *fas* (pCS2/*fas*-MO1-EGFP) and *fasl* morpholinos (pCS2/*fasl*-MO1-EGFP) in frame with

the EGFP sequence, were co-injected with *fas*-MO, *fasl*-MO or ctrl-MO respectively (Suppl. Fig. S1). The presence/absence of the EGFP was monitored at 24 hpf. Most (80%, N=25) of the embryos injected with the sensor plasmid and the ctrl-MO were positive for the EGFP (Suppl. Fig. S1 A-A'). This percentage decreased to 15% (N=50) when the plasmids were co-injected with *fas*-MO (Suppl. Fig. S1 B-B') or *fasl*-MO (Suppl. Fig. S1 C-C'), indicating that morpholinos specifically bind to their target regions. Moreover, RT-PCR performed on the splice-site-morpholinos targeted regions (splice-*fas*-MO and splice-*fasl*-MO), showed abnormal splicing in embryos injected with *fas* (Suppl. Fig. S1 D) and *fasl* respectively (Suppl. Fig. S1 E), and normal splicing in control-MO injected embryos.

Notochord architecture and surrounding tissues are affected in fas/fasl-MO injected larvae

Because *fas* and *fasl* are expressed in the notochord, we analyzed possible defects caused by *fas/fasl*-loss-of-function in this structure and in the surrounding tissues. Taking advantage of the ET30:Et(kita:GalTA4,UAS:mCherry)hzm (ET30) transgenic line, where the fluorescent protein mcherry is expressed in notochord cells (23, 24), we were able to analyze the morphology of the notochord. Notwithstanding the curved tails and the notochord bents observed in *fas/fasl*-MO injected embryos starting from 24 hpf, no evident morphological defects in the notochord cells were shown before 48 hpf (data not shown). However, later during development (*i.e.* 4 dpf) the *fas/fasl*-MO injected larvae presented notochord undulations and multi-cell-layer jumps (Fig. 3B) instead of the single "stack-of-coins" structure which is characteristic of ctrl-MO injected larvae (Fig. 3A) .

Moreover, longitudinal sections of *fas/fasl*-MO injected larvae at 4 dpf showed that the notochord cells and the entire notochord structure were bigger in comparison to ctrl-MO injected larvae and the lager vacuolated cells were not properly connected to the peri-notochordal sheath, indicative of a failure of the cells to differentiate (Fig. 3C-D). Indeed, the peri-notochordal basement membrane of *fas/fasl*-MO injected larvae at 4 dpf, was abnormally undulated and thicker than the ctrl-MO injected larvae, in particular in areas where the profile of the notochord is bent (Fig. 3C-D).

We considered the possibility that the defects in notochord morphology might have resulted from a general developmental delay, although *fas/fasl*-loss-of-function embryos did not differ noticeably in overall development from control-MO. We then checked the vessels formation that was comparable in control and *fas/fasl*-MO *flk1:*EGFP-trangenic injected larvae (30) as shown in the Suppl. Fig. S2, indicating that they were at the same developmental stage.

Muscle organization and primary motoneuron axonal projections are altered in fas/fasl-MO injected larvae

The lack of motility of *fas/fasl*-MO injected larvae from 3 dpf, prompted us to analyze the muscle structure by means of histological sections: at 4 dpf *fas*/f*asl*-MO injected larvae showed muscles with a disorganized alignment of myofibrils that appeared undulated and oriented in unusual directions (Fig. 4A-B). To exclude that motility impairment could be due to motoneuron defects, we analyze primary motoneurons (visualized by the znp1 antibody). Primary motoneurons and their axon were formed in a proper number and position in *fas/fasl*-MO injected embryos at 24 hpf. However, the disorganization in muscle and myosepta caused a disorganized branching of axonal projections (Fig. 4C-D).

Notochord defects in fas/fasl-MO injected larvae leads to abnormal vertebral development

Several evidences suggest that the notochord has been directly implicated in the formation of vertebrae and intervertebral discs (22, 31). Therefore, we verified whether defects in notochord differentiation and in *fas/fasl*-MO injected larvae could influence subsequent vertebral formation. We calcein stained *fas/fasl*-MO injected larvae at early (13 dpf, around 5 mm, Fig. 5A-B') and complete vertebral mineralization (18 dpf, around 7-9 mm, Fig. 5C-D) and we showed that there were significant defects in vertebrae formation with extensive vertebrae fusion (15% N=30, Fig. 5B,B',D) in comparison to ctrl-MO injected larvae (0% N=30 Fig. 5A,A',C).

Expression of ntla and col2a1a in fas/fasl-MO-injected embryos is upregulated as in chordoma tumors.

fas/fasl-loss-of-function resulted in alterations in notochord development, differentiation and regression and might model the morphological and molecular defects underlying the chordoma onset. Hence, we south to analyze the expression profile of the genes that have been found altered in the chordoma tumors, such as the *T* gene and *COL2A1*. Both the zebrafish homologs *ntla* and *col2a1a* were found to be significantly upregulated in *fas/fasl*-MO-injected-embryos by Q-PCR (Fig. 6A-B). These results were confirmed by WISH analyses. The expression of *ntla,* that normally progressively decays 20 hpf (around 20 somite stage), was maintained at high levels in *fas/fasl*-MO injected embryos (50% of *fas/fasl*-MO-injected, total N= 30) (Fig. 6C-D). The expression of *col2a1a*, that normally diminished from 30 hpf and disappeared at 48 hpf (Yan et al., 1995; Dale and Topczewski, 2011), persisted in the peri-notochordal sheath in *fas/fasl*-MO injected embryos at 48 hpf (70% of *fas/fasl*-MO-injected, total N= 60) (Fig. 6E-F).

Discussion

Chordoma is a rare malignant bone tumor arising from embryonic remnants of the notochord that do not correctly disappear during development of vertebral bodies. The notochord regression is regulated by several mechanisms, and among them, the apoptotic process was demonstrated to play a relevant role (11, 32, 33). In particular, the *FAS/FASL* pathway is implicated in the regression of the notochordal cells during adult nucleus pulposus formation in rat (13). Starting from this hypothesis, we previously demonstrated that this pathway was deregulated in chordomas and in the U-CH1 chordoma cell line, mainly for the lack of *FASL* expression and for the presence of the anti-apoptotic isoform of *FAS* (Ferrari et al., 2013 under revision). However, the unrevealing of Fas/Fasl role in chordoma onset made it necessary to develop a suitable animal model, therefore we moved to the zebrafish.

We firstly evaluated the expression of *fas* and *fasl* in the zebrafish whole embryos and larvae. While *fas* was maternally and zigotycally expressed, *fasl* showed a maternal expression and a zygotic expression starting from 24 hpf. The expression pattern of *fas* and *fasl* in brain, eyes, gut, ovary of the adult fish is conserved in mammals, supporting the conservation of *FAS/FASL* function during evolution(14, 34-37). The detection of *fas* and *fasl* expression in zebrafish notochord sorted cells at the first stages of development, pinpoints for the first time the involvement of these two genes in the processes of notochord formation. By using morpholino technology, we performed the loss-of-function experiments to analyze notochord defects in zebrafish embryos and larvae. The single or concurrent knock-down of *fas* and *fasl* resulted in the same phenotypes characterized by curved bodies and bent tails. The *fasl*-MO injected embryos showed aberrant phenotypes from 48 hpf, while the *fas*-MO and the *fas/fasl* co-injected embryos showed aberrant phenotypes from 24 hpf. It is known that Fasl is expressed in a limited number of cell types such as the notochord, the central nervous system or the skeletal muscle (38, 39) and its expression is finely regulated during development; conversely, Fas is expressed in a variety of cell types (14). Therefore, the finding that *fas*-MO-injected embryos showed aberrant phenotypes at a stage of development where we observed *fasl* expression in the whole embryo, but we did not detect its expression in the sorted notochord cells, led us to hypothesize that the receptor might be activated by paracrine interaction with *fasl*. In addition, in human, the Epstein-Barr Virus Latent Membrane Protein 1 (*LMP1*) drives the autoactivation of Fas in absence of Fasl expression (40). So far, no similar mechanisms have been described in zebrafish but, eventually, *fas* might undergo to autoactivation even in the absence of *fasl*.

Following *fas/fasl* loss-of-funtion in zebrafish, severe alterations of the notochord morphology were observed, with various degrees of packed cells that were larger and not properly connected to the perinotochordal sheath, which presented structural defects. It is known that these alterations are determined by notochord differentiation impairment (41). Indeed, in the normal development in zebrafish, at around 20 hpf chordamesoderm cells start to differentiate into mature notochord cells

and begin to secrete the components driving to the correct formation of perinotochordal base membrane. This structure is crucial for the mechanical support of the notochord against its own hydrostatic pressure and for the maintenance of its classic rod-like structure (42-44). Interestingly, the defects in notochord differentiation following *fas/fasl* loss-of function, closely correlate with the phenotypes observed after the deregulation of other genes expressed in the notochord or in the perinotochord sheath, such as *col15a1, col27a1a* and *col27a1b* (42, 43).

In addition, the loss-of-function of *fas/fasl* produced disorganized myofibrils and an aberrant primary motoneurons branching, resulting in a motility impairment. Indeed, both muscle and motoneuron formation require proper signaling from the notochord, and it has been demonstrated that also the integrity of the perinotochordal sheath is essential for the axon projections (43, 45-47).

Early depletion of *fas* and *fasl,* later resulted in vertebrae mineralization defects instead of the normal notochord ossification (26). *fas/fasl* loss-of function might alter the proper notochord cells disappearance during notochord regression, similarly to what happens to the notochord cells in the nucleus pulposus of rat (13). This might cause the mechanical weakening of notochord sheath leading to defects in vertebrae formation (43).

To investigate whether the notochord aberrant phenotypes, observed in *fas/fasl* loss-of-function zebrafish, showed molecular alteration common to chordoma, we studied the expression of two chordoma markers' homologs, *ntla* (*T*) and *col2a1a* (*COL2A1*) (10), that are also finely regulated during notochord development and differentiation. These two genes were found significantly upregulated and their expression was maintained in *fas/fasl*-MO-injected embryos in a developmental stage in which, in controls, they normally diminished and disappeared, suggesting a role for *fas/fasl* in notochord development and differentiation. Conversely, $Ntl^{-/-}$ mice show the disorganisation of the notochord, and the *ntla* zebrafish mutants do not develop notochord and tail (48, 49). The expression of the human homologs of *ntla*, the *T* gene, terminates with notochord maturation even if it may be kept in a focal fashion during early childhood and sometimes throughout life. It is of interest that Brachyury (encoded by *T* gene), is expressed in a reduced

number of low-grade malignant differentiated embryogenetic tumors, such as the chordoma tumor, so that it has been recently proposed as the ultimate solution to the differential diagnosis between chordoma and other tumors with similar characteristics (1, 2, 50). However, the genetic basis of *T* expression in chordoma is largely unknown as only somatic copy-number changes of *T* gene have been observed in a minority of cases (51), including minor allelic gain in 4.5% of cases and amplification in 7% of cases (7). In addition no mutations of *T* have been detected (52, 53). Therefore, the question of how brachyury orchestrates chordoma development remained open (50). On the other hand, *COL2A1* is another gene previously found overexpressed in chordoma tumours compared with non-chordoma mesenchymal tumors, normal tissues, and intervertebral disks (10). Moreover, the upregulation of the *col2a1a* is linked to defects of the notochord sheath and of proteins' aggregation in zebrafish notochord cells, as demonstrated in previous works (54, 55). The role of *col2a1* in notochord remodelling is confirmed also in other models, such as in mouse, but its function is controversial in fact, *Col2a1*-null mice are enable to dismantle the notochord (56).

Taking in account the above evidence, the results here provided, and considering that *FAS/FASL* pathway was recently found to be impaired in chordoma tumours and in UCH1 chordoma cell lines (Ferrari et al. 2013, under revision) we propose that the deregulated expression of *FAS* and/or *FASL* might alter the maturation, differentiation and regression of notochord cells. Thus, the remnant notochordal cells might be exposed to anomalous cellular signalling, leading to a deregulation of programmed cell death and a proliferation out of control. As a matter of fact, the upregulation of *T* gene leads to notochord cells proliferation (5, 9); alternatively the defects in notochord regression may maintain proliferating notochord cells expressing the *T* gene, or both these possibilities (50).

This study, besides providing new insights on notochord biology, allowed us to infer new pathogenetic models underlying chordoma tumorigenesis, addressing future investigations.

Acknowledgements: The authors thank Dr. M. Venturin and Dr. G. Gaudenzi for their bioinformatics support, Dr. V. Melzi for her technical contribution, Prof. J. Topczewski for providing *col2a1a* and *col2a1b* probes, Prof. J. Du for providing *twhh*-GFP construct, Prof. R. W. Koster and Dr. M. Mione for providing the ET30 transgenic line, and the Italian Association for Cancer Research, AIRC (Associazione Italiana per la Ricerca sul Cancro) that funded this study (grant number IG 10525 to PR).

Conflicts of Interest: The authors declare that they have no conflicts of interest.

References

1. Bydon M, Papadimitriou K, Witham T, et al. Novel therapeutic targets in chordoma. Expert Opin Ther Targets 2012.
2. Walcott BP, Nahed BV, Mohyeldin A, Coumans JV, Kahle KT, Ferreira MJ. Chordoma: current concepts, management, and future directions. Lancet Oncol;13:e69-76.
3. Gagliardi F, Boari N, Riva P, Mortini P. Current therapeutic options and novel molecular markers in skull base chordomas. Neurosurg Rev 2012;35:1-13; discussion -4.
4. Salisbury JR. [Embryology and pathology of the human notochord]. Ann Pathol 2001;21:479-88.
5. Nelson AC, Pillay N, Henderson S, et al. An integrated functional genomics approach identifies the regulatory network directed by brachyury (T) in chordoma. J Pathol 2012.
6. O'Donnell P, Tirabosco R, Vujovic S, et al. Diagnosing an extra-axial chordoma of the proximal tibia with the help of brachyury, a molecule required for notochordal differentiation. Skeletal Radiol 2007;36:59-65.
7. Presneau N, Shalaby A, Ye H, et al. Role of the transcription factor T (brachyury) in the pathogenesis of sporadic chordoma: a genetic and functional-based study. J Pathol 2011;223:327-35.
8. Hsu W, Mohyeldin A, Shah SR, et al. Generation of chordoma cell line JHC7 and the identification of Brachyury as a novel molecular target. J Neurosurg;115:760-9.
9. Fernando RI, Litzinger M, Trono P, Hamilton DH, Schlom J, Palena C. The T-box transcription factor Brachyury promotes epithelial-mesenchymal transition in human tumor cells. J Clin Invest;120:533-44.
10. Bruderlein S, Sommer JB, Meltzer PS, et al. Molecular characterization of putative chordoma cell lines. Sarcoma;2010:630129.
11. Malikova MA, Van Stry M, Symes K. Apoptosis regulates notochord development in Xenopus. Dev Biol 2007;311:434-48.
12. Eimon PM, Kratz E, Varfolomeev E, et al. Delineation of the cell-extrinsic apoptosis pathway in the zebrafish. Cell Death Differ 2006;13:1619-30.
13. Kim KW, Kim YS, Ha KY, et al. An autocrine or paracrine Fas-mediated counterattack: a potential mechanism for apoptosis of notochordal cells in intact rat nucleus pulposus. Spine (Phila Pa 1976) 2005;30:1247-51.
14. Inui Y, Nishida K, Doita M, et al. Fas-ligand expression on nucleus pulposus begins in developing embryo. Spine (Phila Pa 1976) 2004;29:2365-9.
15. Kimmel CB, Ballard WW, Kimmel SR, Ullmann B, Schilling TF. Stages of embryonic development of the zebrafish. Developmental dynamics : an official publication of the American Association of Anatomists 1995;203:253-310.

16. Schulte-Merker S, Ho RK, Herrmann BG, Nusslein-Volhard C. The protein product of the zebrafish homologue of the mouse T gene is expressed in nuclei of the germ ring and the notochord of the early embryo. Development 1992;116:1021-32.
17. Yan YL, Hatta K, Riggleman B, Postlethwait JH. Expression of a type II collagen gene in the zebrafish embryonic axis. Dev Dyn 1995;203:363-76.
18. Glickman NS, Kimmel CB, Jones MA, Adams RJ. Shaping the zebrafish notochord. Development 2003;130:873-87.
19. Cole LK, Ross LS. Apoptosis in the developing zebrafish embryo. Dev Biol 2001;240:123-42.
20. Krauss S, Concordet JP, Ingham PW. A functionally conserved homolog of the Drosophila segment polarity gene hh is expressed in tissues with polarizing activity in zebrafish embryos. Cell 1993;75:1431-44.
21. Glenney GW, Wiens GD. Early diversification of the TNF superfamily in teleosts: genomic characterization and expression analysis. J Immunol 2007;178:7955-73.
22. Haga Y, Dominique VJ, 3rd, Du SJ. Analyzing notochord segmentation and intervertebral disc formation using the twhh:gfp transgenic zebrafish model. Transgenic Res 2009;18:669-83.
23. Santoriello C, Gennaro E, Anelli V, et al. Kita driven expression of oncogenic HRAS leads to early onset and highly penetrant melanoma in zebrafish. PLoS One;5:e15170.
24. Distel M, Wullimann MF, Koster RW. Optimized Gal4 genetics for permanent gene expression mapping in zebrafish. Proc Natl Acad Sci U S A 2009;106:13365-70.
25. Thisse C, Thisse B, Schilling TF, Postlethwait JH. Structure of the zebrafish snail1 gene and its expression in wild-type, spadetail and no tail mutant embryos. Development 1993;119:1203-15.
26. Dale RM, Topczewski J. Identification of an evolutionarily conserved regulatory element of the zebrafish col2a1a gene. Dev Biol;357:518-31.
27. Nasevicius A, Ekker SC. Effective targeted gene 'knockdown' in zebrafish. Nature genetics 2000;26:216-20.
28. Brusegan C, Pistocchi A, Frassine A, Della Noce I, Schepis F, Cotelli F. Ccdc80-l1 Is involved in axon pathfinding of zebrafish motoneurons. PLoS One;7:e31851.
29. Du SJ, Dienhart M. Zebrafish tiggy-winkle hedgehog promoter directs notochord and floor plate green fluorescence protein expression in transgenic zebrafish embryos. Dev Dyn 2001;222:655-66.
30. Thompson MA, Ransom DG, Pratt SJ, et al. The cloche and spadetail genes differentially affect hematopoiesis and vasculogenesis. Developmental biology 1998;197:248-69.
31. Hunter CJ, Matyas JR, Duncan NA. The notochordal cell in the nucleus pulposus: a review in the context of tissue engineering. Tissue Eng 2003;9:667-77.
32. Erwin WM, Islam D, Inman RD, Fehlings MG, Tsui FW. Notochordal cells protect nucleus pulposus cells from degradation and apoptosis: implications for the mechanisms of intervertebral disc degeneration. Arthritis Res Ther;13:R215.
33. Yamashita M, Mizusawa N, Hojo M, Yabu T. Extensive apoptosis and abnormal morphogenesis in pro-caspase-3 transgenic zebrafish during development. J Exp Biol 2008;211:1874-81.
34. Takada T, Nishida K, Doita M, Kurosaka M. Fas ligand exists on intervertebral disc cells: a potential molecular mechanism for immune privilege of the disc. Spine (Phila Pa 1976) 2002;27:1526-30.
35. Ferguson TA, Green DR. Fas-ligand and immune privilege: the eyes have it. Cell Death Differ 2001;8:771-2.
36. Xerri L, Devilard E, Hassoun J, Mawas C, Birg F. Fas ligand is not only expressed in immune privileged human organs but is also coexpressed with Fas in various epithelial tissues. Mol Pathol 1997;50:87-91.
37. Green DR, Ferguson TA. The role of Fas ligand in immune privilege. Nat Rev Mol Cell Biol 2001;2:917-24.
38. Sandri M, Sandri C, Brun B, et al. Inhibition of fasL sustains phagocytic cells and delays myogenesis in regenerating muscle fibers. J Leukoc Biol 2001;69:482-9.
39. Shin SW, Park JW, Suh MH, Suh SI, Choe BK. Persistent expression of Fas/FasL mRNA in the mouse hippocampus after a single NMDA injection. J Neurochem 1998;71:1773-6.
40. Le Clorennec C, Youlyouz-Marfak I, Adriaenssens E, Coll J, Bornkamm GW, Feuillard J. EBV latency III immortalization program sensitizes B cells to induction of CD95-mediated apoptosis via LMP1: role of NF-kappaB, STAT1, and p53. Blood 2006;107:2070-8.

41. Odenthal J, Haffter P, Vogelsang E, et al. Mutations affecting the formation of the notochord in the zebrafish, Danio rerio. Development 1996;123:103-15.
42. Christiansen HE, Lang MR, Pace JM, Parichy DM. Critical early roles for col27a1a and col27a1b in zebrafish notochord morphogenesis, vertebral mineralization and post-embryonic axial growth. PLoS One 2009;4:e8481.
43. Pagnon-Minot A, Malbouyres M, Haftek-Terreau Z, et al. Collagen XV, a novel factor in zebrafish notochord differentiation and muscle development. Dev Biol 2008;316:21-35.
44. Hawkins TA, Cavodeassi F, Erdelyi F, Szabo G, Lele Z. The small molecule Mek1/2 inhibitor U0126 disrupts the chordamesoderm to notochord transition in zebrafish. BMC Dev Biol 2008;8:42.
45. Brennan C, Mangoli M, Dyer CE, Ashworth R. Acetylcholine and calcium signalling regulates muscle fibre formation in the zebrafish embryo. J Cell Sci 2005;118:5181-90.
46. Chan J, Mably JD, Serluca FC, et al. Morphogenesis of prechordal plate and notochord requires intact Eph/ephrin B signaling. Dev Biol 2001;234:470-82.
47. Beattie CE, Eisen JS. Notochord alters the permissiveness of myotome for pathfinding by an identified motoneuron in embryonic zebrafish. Development 1997;124:713-20.
48. Schulte-Merker S, van Eeden FJ, Halpern ME, Kimmel CB, Nusslein-Volhard C. no tail (ntl) is the zebrafish homologue of the mouse T (Brachyury) gene. Development 1994;120:1009-15.
49. Beddington RS, Rashbass P, Wilson V. Brachyury--a gene affecting mouse gastrulation and early organogenesis. Dev Suppl 1992:157-65.
50. Szuhai K, Hogendoorn PC. 'The chicken or the egg?' dilemma strikes back for the controlling mechanism in chordoma(#). J Pathol 2012;228:261-5.
51. Yang XR, Ng D, Alcorta DA, et al. T (brachyury) gene duplication confers major susceptibility to familial chordoma. Nat Genet 2009;41:1176-8.
52. Shalaby A, Presneau N, Ye H, et al. The role of epidermal growth factor receptor in chordoma pathogenesis: a potential therapeutic target. J Pathol;223:336-46.
53. Le LP, Nielsen GP, Rosenberg AE, et al. Recurrent chromosomal copy number alterations in sporadic chordomas. PLoS One;6:e18846.
54. Topczewski J, Sepich DS, Myers DC, et al. The zebrafish glypican knypek controls cell polarity during gastrulation movements of convergent extension. Dev Cell 2001;1:251-64.
55. Stemple DL, Solnica-Krezel L, Zwartkruis F, et al. Mutations affecting development of the notochord in zebrafish. Development 1996;123:117-28.
56. Aszodi A, Chan D, Hunziker E, Bateman JF, Fassler R. Collagen II is essential for the removal of the notochord and the formation of intervertebral discs. J Cell Biol 1998;143:1399-412.

Figures

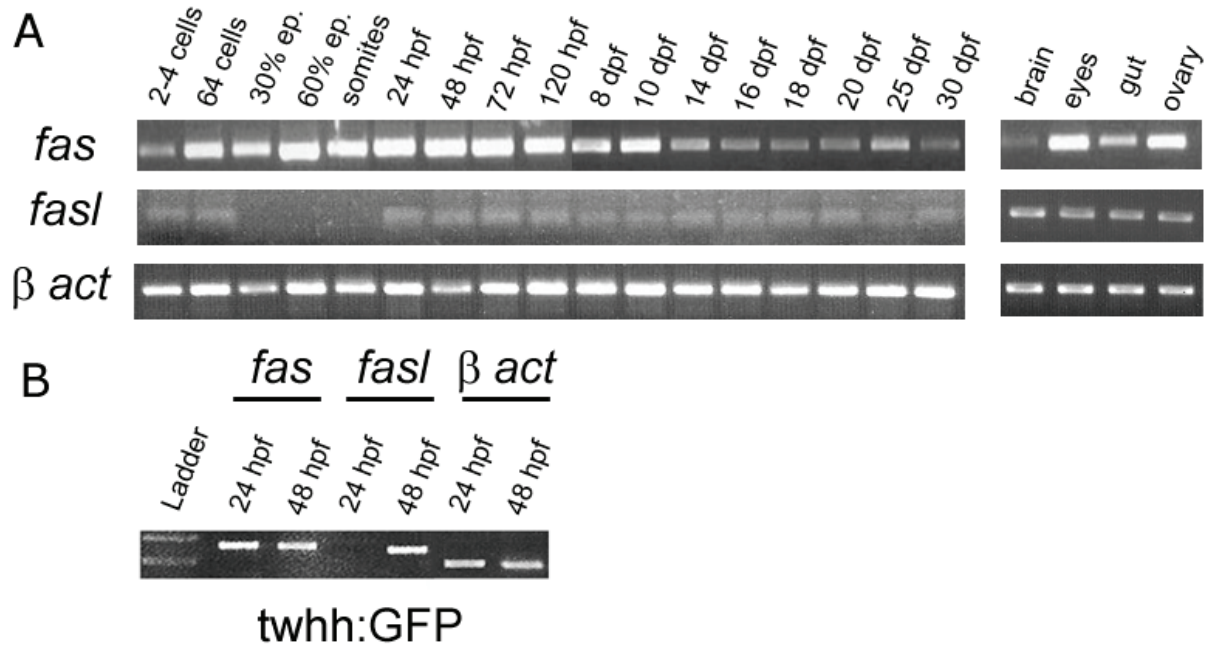

Fig. 1 Expression analysis of *fas* and *fasl.* *(A)* RT-PCR performed on different developmental stages and adult tissues. *fas* is expressed in all the analyzed developmental stages, *fasl* presents a maternal expression, while the zygotic expression starts from 24 hpf. Both genes are expressed in all the adult tissues analyzed. *(B)* RT-PCR performed on cDNA of the notochord cells sorted from embryos at 24 and 48 hpf injected with the *twhh*:*gfp* plasmid. *fas* is expressed in the notochord cells at both 24 and 48 hpf while *fasl* only at 48 hpf.

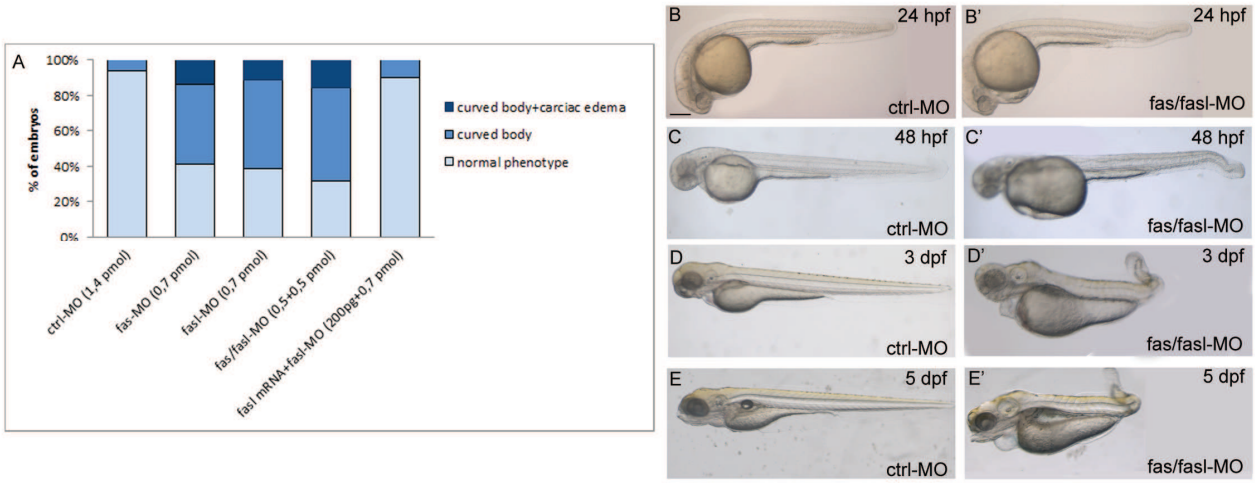

Fig. 2 *fas/fasl*-loss-of-function phenotypes. *(A)* MO-injected embryos were analyzed by scoring the presence/absence of curved bodies and subdivided into phenotypic classes. *(B-E)* Embryos and larvae injected with ctrl-MO exhibit normal development at 24 hpf *(B)*, 48 hpf *(C)*, 3 dpf *(D)* and 5 dpf *(E)*. (*A'-E'*) Embryos and larvae co-injected with *fas*/*fasl*-MO develop defects in the tail curvature due to notochord distortion and cardiac edema. This phenotype is worsening during development.

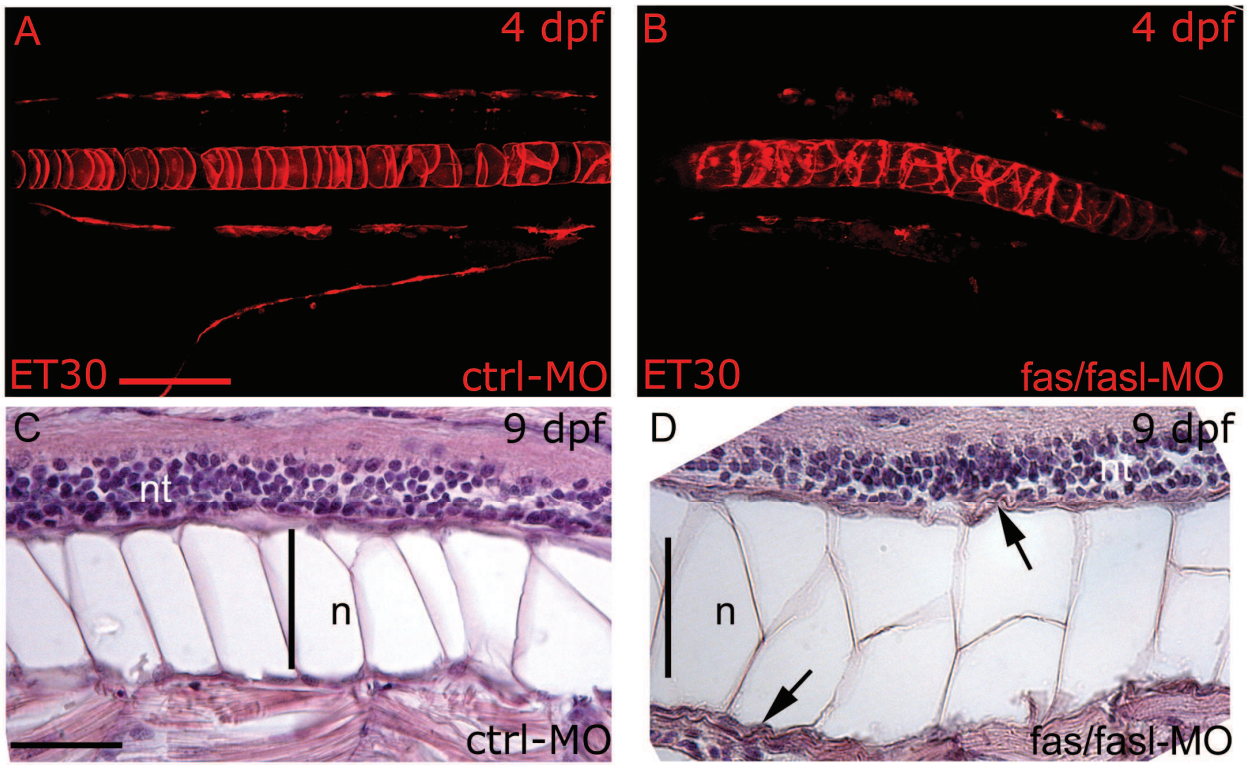

Fig. 3 The lack of *fas* and *fasl* affects notochord differentiation and peri-notochordal sheath integrity. *(A-B)* Confocal images of the mcherry-positive-notochord cells of the ET30 transgenic line at 4 dpf. In ctrl-MO injected larvae *(A),* the notochord shows its characteristic "stack-of-coins" structure while *fas/fasl*-MO injected larvae *(B)* present notochord undulations and form multi-cell-layer jumps. *(C-D)* Longitudinal sections hematoxilin-eosin (HE) stained of ctrl-MO and *fas/fasl*-MO injected larvae at 4 dpf. The notochord (n) of morphants is thicker, and vacuolated cells are not properly connected to the peri-notochordal sheat that is abnormally undulated (arrowheads, *D),* in comparison to ctrl-MO injected larvae *(C)*. (*A-D)* lateral views, anterior to the left, dorsal up. Scale bars: 100 μm.

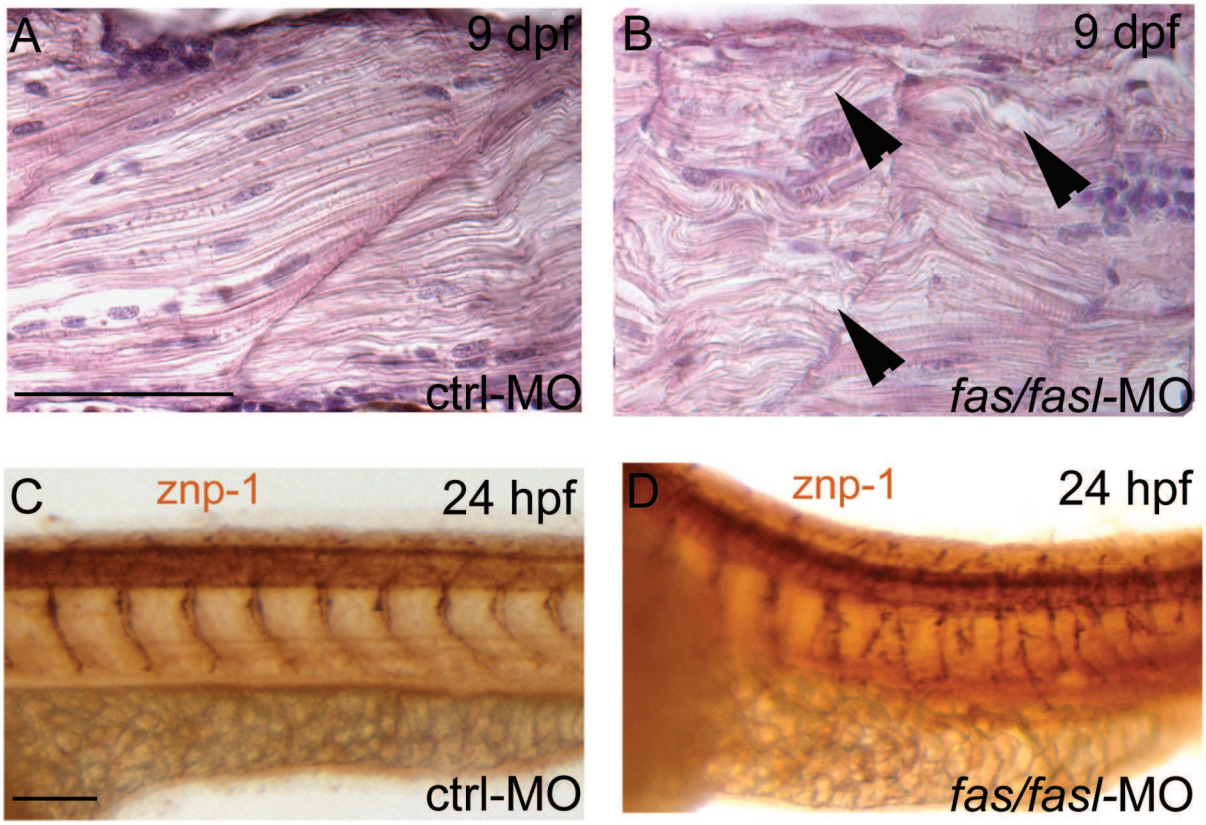

Fig. 4 Defects in notochord differentiation prevent normal muscle structure and primary motoneuron axon projections. *(A-B)* Longitudinal histological sections, HE stained. At 4 dpf, muscle fibres in *fas/fasl*-MO injected larvae are disorganized, undulated and oriented in opposite directions (*B*, arrowheads) in comparison to ctrl-MO injected larvae (*A*). *(C-D)* Axonal projections of primary motoneurons visualized by znp1 antibody present branching defects in *fas/fasl*-MO injected embryos at 24 hpf. *(A-D)* lateral views, anterior to the left, dorsal up. Scale bar: 100 μm.

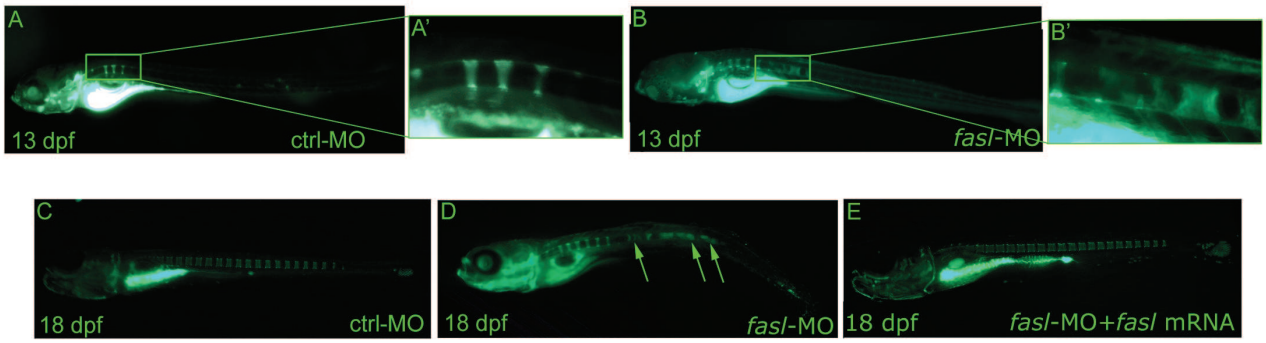

Fig. 5 Analyses of notochord segmentation and vertebral formation following *fas/fasl* loss of function. *(A-D)* Calcein staining shows notochord segmentation by formation of calcified chordacentra in an antero-posterior fashion. The process of vertebrae formation starts at around 11 dpf (3 mm) and is completed at around 18-21 dpf (7-9 mm). *fas/fasl*-MO-injected larvae at early *(B-B'* higher magnification*)* and complete vertebral mineralization *(*arrows, *D)* show significant defects in vertebrae formation with extensive vertebrae fusion in comparison to ctrl-MO injected larvae *(A,A'* higher magnification*, C*). Scale bar: 100 µm.

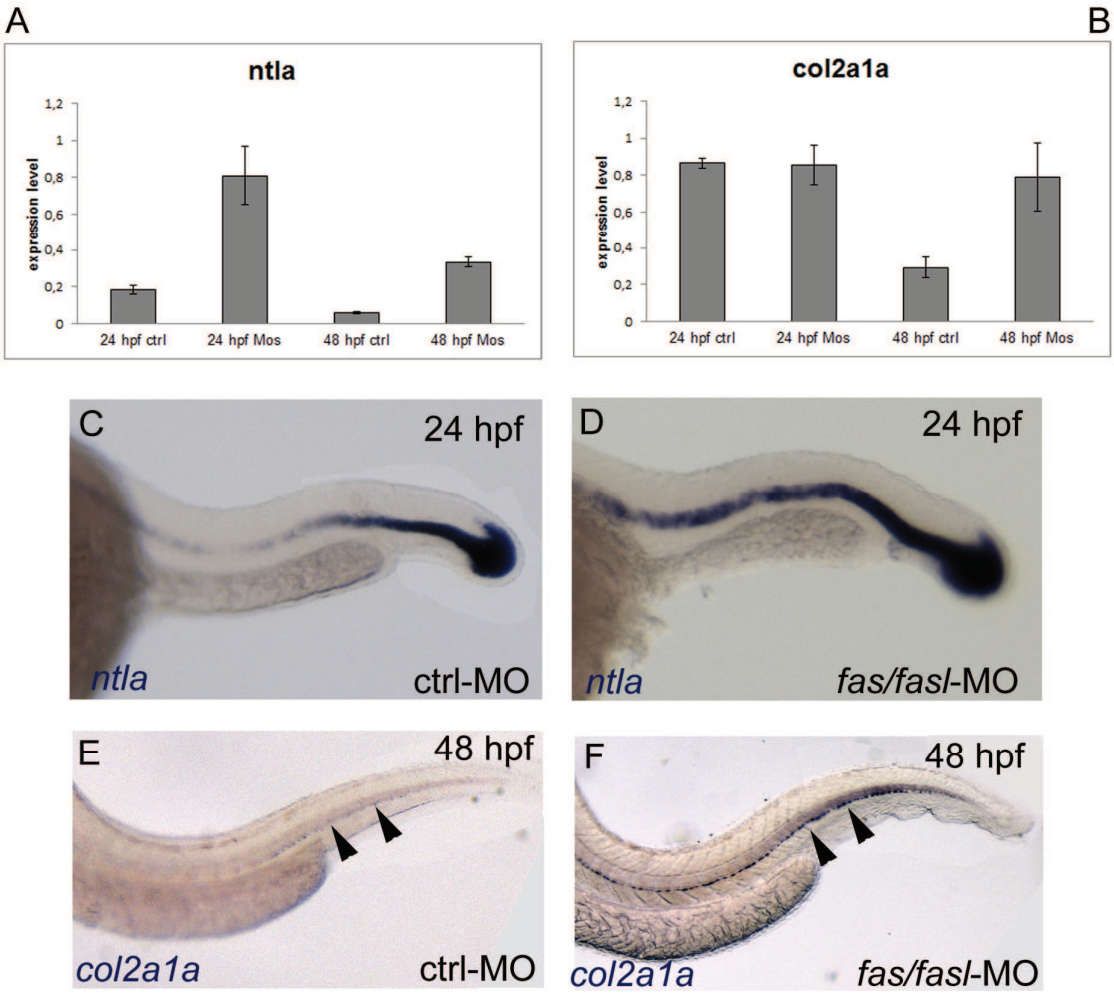

Fig. 6 *ntla* and *col2a1a* are upregulated in *fas/fasl*-MO injected embryos. *(A-B) Q-PCR* analysis of *ntla (A)* and *col2a1a (B)* showing an upregulation.of the expression in *fas/fasl*-MO injected embryos for both genes. *(C-D)* WISH analysis showing persistent expression of the notochord marker *ntla* in the notochord of *fas/fasl*-MO injected embryos at 24 hpf *(D)* compared to control embryos *(C)*. *(E-F)* WISH analysis showing persistent expression of the chordamesoderm marker *col2a1a* in the peri-norochordal sheath of *fas/fasl*-MO injected embryos *(F*, arrowheads*)* compared to control embryos in which *col2a1a* expression normally decreases at 48 hpf (*E*, arrowheads).

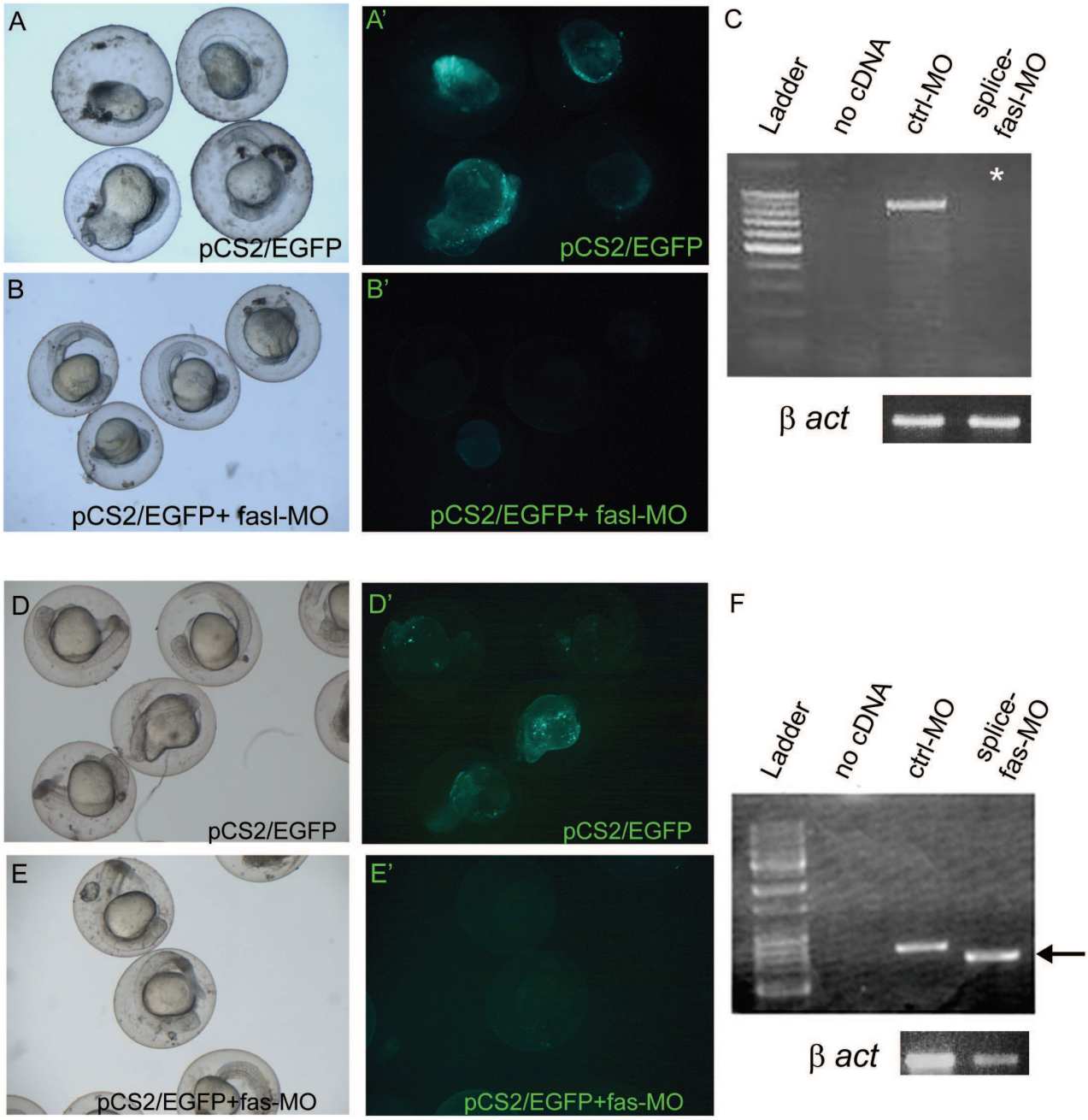

Suppl. Fig. S1 Validation and specificity of *fas*- and *fasl*-MOs. For the *in-vivo* test of the specificity of *fasl*-MO, a *fasl*-EGFP sensor has been generated. The pCS2+ construct containing the sequence recognized by the *fasl*-MO fused with the EGFP open reading frame is used for injection experiments with ctrl-MO or with the *fasl*-MO. *(A-A')* Embryos at 24 hpf: EGFP-positive cells in the trunk and in the yolk epithelium following co-injection of the sensor and the control-MO. *(B-B')* The complete absence of GFP expression when the sensor is co-injected with *fasl*-MO confirms the specificity of the ATG targeting morpholino action. *(D-E')* Same experiments have been performed

to *in-vivo* test the specificity of the *fas*-MO1. In *A,B,D,E* embryos are visualized under normal light, in *A',B',D',E'* under fluorescent light. *(C)* RT-PCR on control and splice-*fasl*-MO injected embryos at 24 hpf. RT-PCR primers are designed in exon 1 and exon 2 respectively; the amplification product is present in ctrl-MO injected embryos, while it is too large to be amplified in splice-*fasl*-MO injected embryos, confirming the intron retention. *(F)* RT-PCR performed on control and splice-*fas*-MO injected embryos at 24 hpf. RT-PCR primers are designed in exon 1 and exon 3 respectively. The amplification product, that comprehends the second exon, is 326 bp in ctrl-MO injected embryos, while a band at 174 bp (arrowhead) is detected in splice-*fas*-MO injected embryos, confirming the skipping of the second exon (150 bp).

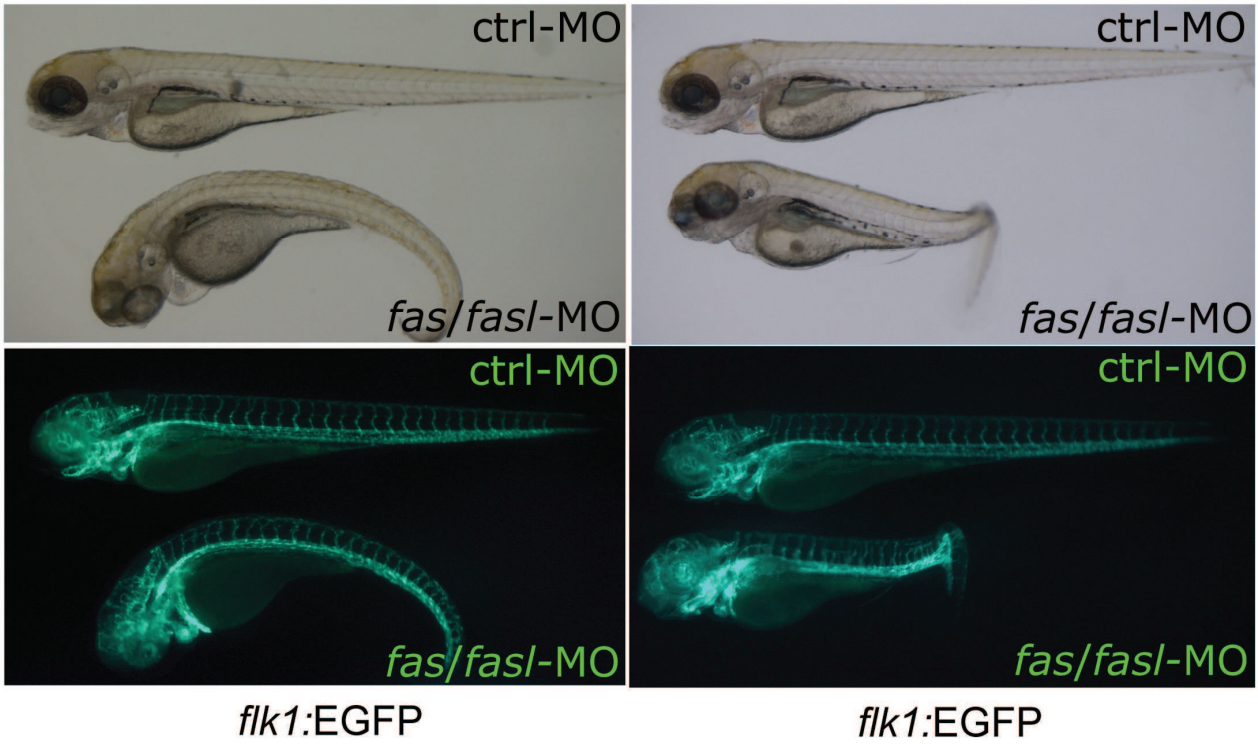

Suppl. Fig. S2 Vessel formation is comparable in control and *fas/fasl*-MO *fliI:*EGFP-trangenic injected embryos. Visible *(A-B)* and fluorescent images *(A'-B')* of EGFP-vessels visualized in control *(A-A')* and *fas/fasl*-MO *(B-B')* injected embryos at 3 dpf .

Movie 1-Movie 2 *fas/fasl*-MO injected larvae present reduced motility after 48 hpf. Larvae at 6 dpf have been tested with a tactile stimulus response assay. *fas/fasl*-MO injected larvae (Movie 2) are less sensitive to tactile stimuli than controls (Movie 1) and do not swim away when touched.

Movie 3 Partial rescue of the motility of *fas/fasl*-MO injected larvae by means of the *fasl* mRNA injection. Larvae at 6 dpf have been tested with a tactile stimulus response assay. *fas/fasl*-MO larvae have been injected with *fasl* full lenght mRNA. 55% (N=70) of the co-injected larvae partially rescued the immotile phenotype and swim away when stimulated.